

สภาพภูมิศาสตร์บรรพกาลและสภาพแวดล้อมบรรพกาลของหนองหานกุมภวาปี จังหวัดอุดรธานี



นางสาววิฑูราตรี กลับแสง

ศูนย์วิทยพัทยากร
จุฬาลงกรณ์มหาวิทยาลัย

วิทยานิพนธ์นี้เป็นส่วนหนึ่งของการศึกษาตามหลักสูตรปริญญาวิทยาศาสตรมหาบัณฑิต

สาขาวิชาโลกศาสตร์ ภาควิชาธรณีวิทยา

คณะวิทยาศาสตร์ จุฬาลงกรณ์มหาวิทยาลัย

ปีการศึกษา 2553

ลิขสิทธิ์ของจุฬาลงกรณ์มหาวิทยาลัย



PALEOGEOGRAPHY AND PALEOENVIRONMENT OF NONG HAN KUMPHAWAPI,
CHANGWAT UDON THANI



Miss Wichuratree Klubseang

ศูนย์วิทยทรัพยากร
จุฬาลงกรณ์มหาวิทยาลัย
A Thesis Submitted in Partial Fulfillment of the Requirements
for the Degree of Master of Science Program in Earth Sciences

Department of Geology

Faculty of Science


Chulalongkorn University

Academic Year 2010

Copyright of Chulalongkorn University

Thesis Title PALEOGEOGRAPHY AND PALEOENVIRONMENT OF NONG
HAN KUMPHAWAPI, CHANGWAT UDON THANI
By Miss Wichuratree Klubseang
Field of Study Earth Sciences
Thesis Advisor Professor Thanawat Jarupongsakul, Ph.D.


Accepted by the Faculty of Science, Chulalongkorn University in Partial
Fulfillment of the Requirements for the Master's Degree


..... Dean of the Faculty of Science
(Professor Supot Hannongbua, Dr.rer.nat)

THESIS COMMITTEE


..... Chairman
(Assistant Professor Somchai Nakapadungrat, Ph.D.)


..... Thesis Advisor
(Professor Thanawat Jarupongsakul, Ph.D.)


..... External Examiner
(M.r. Niran Chaimanee)

วิทยุราตรี กลับแสง: สภาพภูมิศาสตร์บรรพกาลและสิ่งแวดล้อมบรรพกาลของหนองหาน
กุมภวาปี จังหวัดอุดรธานี. (PALEOGEOGRAPHY AND PALEOENVIRONMENT OF
NONG HAN KUMPHAWAPI, CHANGWAT UDON THANI) อ.ที่ปรึกษาวิทยานิพนธ์
หลัก : ศ.ดร. ธนวัฒน์ จารุพงษ์สกุล, 121 หน้า.

ลมมรสุมตะวันตกเฉียงใต้ และลมมรสุมตะวันออกเฉียงเหนือ เป็นตัวการหลักที่ควบคุม
สภาพภูมิอากาศ การหมุนเวียนของลมมรสุมมีความสัมพันธ์ต่อการเปลี่ยนแปลงของรูปแบบลม
และฝนเหนือประเทศไทย ซึ่งส่งผลให้เกิดภาวะแห้งแล้ง และน้ำท่วมเป็นบริเวณกว้าง ตะกอน
ทะเลสาบเป็นหนึ่งในหลักฐานทางธรณีวิทยาที่แสดงถึงความรุนแรงของลมมรสุมในอดีต

งานวิจัยนี้มีวัตถุประสงค์เพื่อ ศึกษาความสัมพันธ์ระหว่างลมมรสุมแถบเอเชีย, ลักษณะ
ทางภูมิศาสตร์, ลักษณะทางภูมิศาสตร์บรรพกาล และสภาพแวดล้อมบรรพกาล ของหนองหาน
กุมภวาปี โดยตรวจสอบคุณสมบัติทางกายภาพ เคมีและการตรวจวัดหาอายุของตะกอนโดยใช้วิธี
AMS ^{14}C เรดิโอคาร์บอน ในหนองหานกุมภวาปี จังหวัดอุดรธานี เก็บตะกอนโดยใช้ Russian
corer (เส้นผ่านศูนย์กลาง 10 เซนติเมตร และ 7.5 เซนติเมตร ยาว 1 เมตร โดยเก็บตัวอย่างให้มี
ระยะซ้อนกัน 0.5 เมตร)บริเวณที่ทำการเจาะแท่งตะกอนจะใช้ GPS เพื่อบันทึกตำแหน่งที่แน่นอน
ของตะกอน แท่งตะกอน CP3A เป็นแท่งตะกอนที่ความต่อเนื่องและสมบูรณ์ที่สุดจึงถูกเลือกไป
วิเคราะห์ด้วยวิธีที่มีความละเอียดและแม่นยำสูง สำหรับการวิเคราะห์แท่งตะกอนจะใช้เครื่องมือ
Magnetic Susceptibility (MS), X-ray fluorescence (XRF), Loss-on-ignition method (LOI)
และ หาอายุ โดยใช้วิธี AMS ^{14}C เรดิโอคาร์บอน นอกจากนี้ได้รวบรวมภาพถ่ายทางอากาศ และ
แผนที่ GIS เพื่อใช้ตรวจสอบ ลักษณะทางภูมิศาสตร์ และลักษณะทางภูมิศาสตร์บรรพกาลอีก
ด้วย

ผลการศึกษาแสดงให้เห็นว่าตัวอย่างตะกอนเก่ามีอายุอยู่ในช่วง 7,763 yr B.P. และ
อายุก่อนสุดอยู่ในช่วง 436 yr B.P. สรุปได้ว่าตะกอน และผลที่ได้จากการตรวจวัด บ่งชี้ว่าหนอง
หานกุมภวาปี มีการเปลี่ยนแปลงระดับน้ำขึ้น-ลง ซึ่งมีความสัมพันธ์กับความรุนแรงของลมมรสุม

ภาควิชา.....ธรณีวิทยา.....
สาขาวิชา.....โลกศาสตร์.....
ปีการศึกษา.....2553.....

ลายมือชื่อนิสิต.....
ลายมือชื่อ อ.ที่ปรึกษาวิทยานิพนธ์หลัก.....

5072463123 : MAJOR EARTH SCIENCES

KEYWORDS : PALEOGEOGRPHY / PALEOENVIRONMENT / NONG HAN KUMPHAWAPI
/ UDON THANI

WICHURATREE KLUBSEANG : PALEOGEOGRAPHY AND
PALEOENVIRONMENT OF NONG HAN KUMPHAWAPI, CHANGWAT UDON
THANI. ADVISOR : PROF. THANAWAT JARUPONGSAKUL, Ph.D.,121 pp.

The Southwest monsoon and the Northeast monsoon mainly controls climate and its circulation related with change in wind and precipitation pattern over Thailand. Changes in this convectively active region can result in severe drought or flood over large regions. Lake sediment is one of geological archives which have potential to reconstruct past monsoon intensity.

Then, this research aims to study the relationship between Asian Monsoon, geographical feature, paleogeographical and paleoenvironment of Nong Han Kumphawapi. The investigate of physical and chemical properties of lake sediment, and the measurement of AMS ¹⁴C radiocarbon dating were made at Nong Han Kumphawapi, Udon Thani Province. Sediment cores were collected by a Russian corer (chamber Ø: 10 cm and 7.5 cm, chamber length: 1 m) and with 0.5 m overlap. The coring point's co-ordinates were identified by GPS to improve the accuracy of sediment cores' position. The most complete sequence (CP3A) was selected for high-resolution multi-proxy sub-sampling in the laboratory. Magnetic Susceptibility (MS), X-ray fluorescence (XRF), Loss-on-ignition method (LOI) and AMS ¹⁴C dating were use in the sediment cores analysis. In addition, we combine the data from aerial photos interpretation and GIS based map in order to investigate geographical feature and paleogeographical.

The results show that the oldest sediment sample is around 7,763 cal years B.P. and the youngest sample dates to around 436 cal years B.P. In conclusion, the sediment and the combined proxy data indicate that Nong Han Kumphawapi underwent several phases with higher/lower lake levels, which potentially could be related to changes in monsoon intensity.

Department : Geology Student's Signature
Field of Study : Earth Sciences Advisor's Signature
Academic Year : 2010

ACKNOWLEDGEMENTS

I gratefully acknowledge the continuous support and co-operation with the Department of Geological Sciences, Stockholm University, the Swedish Research Council for financial support and the Nong Han Kumphawapi wire project officer for support during fieldwork. Geo-Informatics and Space Technology Development Agency (Public Organization) provided a partial funding and data for this study.

I sincerely thank my Advisor, Professor Dr. Thanawat Jarupongsakul, Department of Geology, Faculty of Science, Chulalongkorn University and Co-advisor, Professor Dr. Barbara Wohlfarth, Department of Geosciences, Faculty of Science, Stockholm University for their supports, encouragements, critically advises and reviews of this thesis.

Appreciation is also done to thank Assistant Professor Dr. Somchai Nakapadungrat, Department of Geology, Faculty of Sciences and Mr. Niran Chaimanee, Thesis Evaluation Committee members who contributed to this thesis by providing useful suggestions and practical advices.

I would like to thank Miss Boossarasiri Thana, and Mr. Akkaneewut Chabangbon, Department of Geology, Faculty of Sciences, Chulalongkorn University, and Assoc. Professor Dr. Ludvig Lowemark, Department of Geosciences, Faculty of Science, Stockholm University especially for their valuable suggestion and support. Furthermore, I sincerely gratify the Land Development Department of the Ministry of Agriculture and Cooperation, and Royal Thai Survey Department, for their permission to use essential data for this research.

I thank to Mr. Puttinun Sukumonjan, Miss Chanita Duangyiwa, Miss Jinchula Chotipitayasunon, Mr. Weerapong Kamduang, Miss Wirongrong Suka, Miss Witchuda Ponsai, Miss Sakonvan Chaochai, Miss Suda Inthongkaew, Miss Barbara Kline and all of my friends for their support throughout my thesis with their valuable suggestions.

Finally, I would like to thank my parents and my family for their support and encouragement throughout my study at the university.

CONTENTS

	Page
ABSTRACT IN THAI.....	iv
ABSTRACT IN ENGLISH	v
ACKNOWLEDGEMENTS.....	vi
CONTENTS.....	vii
LIST OF TABLES.....	x
LIST OF FIGURES.....	xi
CHAPTER I INTRODUCTION	1
1.1 Rationale.....	1
1.2 Objectives	3
1.3 Scope and limitation.....	3
1.4 Location of the study area	3
1.5 Expected outputs	5
1.6 Research methodology	5
1.6.1 Preparation.....	5
1.6.2 Map reconstruction.....	5
1.6.3 Field investigation	6
1.6.4 Laboratorial analyses.....	6
1.7 Components of the thesis	7
CHAPTER II LITERATURE REVIEW.....	8
2.1 Past Asian monsoon variability.....	8
2.2 The previous studies for Paleogeography, Paleoenvironment and Paleoclimatic change of Nong Han Kumphawapi, Udon Thani Province.	11
CHAPTER III SITE DESCRIPTION	15

	Page
3.1 Location and Topography	15
3.2 Geology.....	21
3.2.1 Khorat Plateau	21
3.2.2 The Sakon Nakhon Basin	26
3.3 Climate.....	29
3.3.1 Monsoon characteristics and season.....	29
3.3.2 Temperature	30
3.3.3 Precipitation.....	31
3.3.4 Tropical Cyclone	31
3.3.5 Climate of Northeastern Region and Udon Thani.....	31
3.4 Vegetation	34
3.4.1 Plant communities of Nong Han Kumphawapi	35
3.5 Archaeology	38
CHAPTER IV METHODOLOGY	44
4.1 Map reconstruction	44
4.2 Field investigation	45
4.3 Laboratory analyses	47
4.3.1 Lithostratigraphy	47
4.3.2 Magnetic susceptibility.....	48
4.3.3 X-ray fluorescence (XRF) analysis	55
4.3.4 Loss on ignition (LOI)	59
4.3.5 Radiocarbon Dating	62
CHAPTER V RESULTS AND ANALYSIS.....	71
5.1 Map reconstruction.	71
5.1.1 Aerial photos interpretation.	71

	Page
5.1.2 Correlation of Landuse/Land cover.	71
5.1.3 Combined thematic map with old geomorphic map.	78
5.1.4 Geomorphic map and lake flooded model.	82
5.2 Lithostratigraphy of the sediment sequences	84
5.2.1 Kumphawapi CP3A	85
5.2.2 Kumphawapi CP3B	86
5.2.3 Correlation between CP3A and CP3B	89
5.3 Loss-on ignition (LOI), mineral magnetic- susceptibility (MS) and X-ray fluorescence (XRF) of Kumphawapi CP3A.....	89
5.4 Chronology.	92
CHAPTER VI DISCUSSION AND CONCLUSIONS	95
6.1 Geographical feature, Land-use and cover change, and Paleogeography of Nong Han Kumphawapi.....	95
6.2 Lithostratigraphy correlation with previous work	96
6.3 Paleoenvironment and paleoclimatic reconstruction	99
6.4 Relationship between archaeological sites and paleogeography	101
REFERENCES.....	107
APPENDIX	115
BIOGRAPHY	121

ศูนย์วิจัยทรัพยากร
จุฬาลงกรณ์มหาวิทยาลัย

LIST OF TABLES

Table		Page
3-1	The properties of Nong Han Kumphawapi after the dam were built.....	19
3-2	Mean monthly temperature and rainfall data for Udon Thani Province, for the years 1951-2008.....	34
3-3	The Ban Chiang cultural sequences.	39
4-1	Data collection.	44
4-2	Susceptibility values of common minerals and rocks.	50
4-3	The standard ITRAX procedure.	58
4-4	Selected sample for ¹⁴ C dating.	66
5-1	Lithostratigraphy of Core CP3A, 2.15-6.00 m.....	85
5-2	Lithostratigraphy of Core CP3B, 2.00-6.00 m.	87
5-3	Results of ¹⁴ C AMS dating of core CP3A.	93
6-1	Paleoenvironment and paleoclimate of Nong Han Kumphawapi	103

ศูนย์วิจัยทรัพยากร
จุฬาลงกรณ์มหาวิทยาลัย

LIST OF FIGURES

Figure		Page
1-1	The location of Nong Han Kumphawapi.	4
3-1	Physiographic regions of Thailand.	16
3-2	Location and major topographic features of the Khorat Basin and the Sakon Nakhon Basin.	17
3-3	Arial photos from 1996 of Nong Han Kumphawapi (after the dam was built). Data from The Royal-Thai Survey.	20
3-4	The general tectonic elements of the region and the location of the Khorat and the Sakon Nakhon basins.	21
3-5	Mesozoic and Cenozoic stratigraphy of the Khorat Basin in NE Thailand and summary of the geological history of the Indochina microplate during the Mesozoic and the Cenozoic.	24
3-6	Geologic map of Khorat Plateau, including Sakon Nakhon Basin and Khorat Basin.	25
3-7	Profile of the Quaternary deposit of the Northeastern region of Thailand.	27
3-8	Geological map of Udon Thani Province.	28
3-9	The present Monsoon Season and Tropical Strom in Thailand.	30
3-10	Average monthly rainfall and temperature of northeastern Thailand for 1951-2004.	33
3-11	Average monthly rainfall and temperature for Udon Thani Province, for 1951-2008.	33
3-12	Vegetation map of the Ban Chiang/Hong Han Kumphawapi region, prepared by White (2004) based on interpretation of aerial photographs from the 1950s in conjunction with the ethnoecological field research undertaken in 1979 – 1981 and 1994.	36
3-13	Photos of Nong Han Kumphawapi and its surroundings.	37
3-14	Photos of Nong Han Kumphawapi and its surroundings.	37

Figure	Page
3-15	Historic and prehistoric sites around Nong Han Kumphawapi 41
4-1	The zodiac boat with special platform. 46
4-2	Russian corer with lake sediment 46
4-3	Fieldwork and laboratory analyses diagram. 47
4-4	Process of describing stratigraphies in the laboratory 48
4-5	Schematic representation of the distribution of magnetization vectors in ferromagnetic materials, (a) ferromagnetic, (b) antiferromagnetic, (c) canted-antiferromagnetic (d) ferromagnetic. 49
4-6	The multi-sensor core logger device used in this study. Only the magnetic susceptibility point sensor (after Zolitschka et al., 2001) for logging of split cores was used. 53
4-7	The Compton Scattering process. 55
4-8	The Itrax core scanner. 58
4-9	The different preparation steps. 60
4-10	A muffle furnace. 61
4-11	Production of ^{14}C and its cycle. 63
4-12	The decay curve of radiocarbon. 64
4-13	Plant macrofossils for AMS ^{14}C dating. 66
4-14	Example of a tandem accelerator. 69
4-15	The AMS systems. 70
5-1	Lake surface area based on interpretation of aerial photos from the 1954 and 1996 72
5-2	Lake surface and lake boundary based on interpretation of aerial photos from the 1954 and 1996..... 73
5-3	Vegetation map of the Nong Han Kumphawapi region, prepared by White (2004). 74

Figure	Page
5-4 Landuse map based on data of Land and Land development Department from the year 1985.	75
5-5 Landuse map based on data of Land and land development Department from the year 2001.	76
5-6 Landuse map based on data of Land and land development Department from the year 2009.	77
5-7 Soil map based on the classification of Land and Land development Department.	79
5-8 Landform map based on classification of land and Land development Department.	80
5-9 Digital Elevation Model (DEM) generated from the database of Land and land development department.	81
5-10 The old geomorphic map.	82
5-11 Geomorphic map with the model of lake flooded level.	83
5-12 Location of Nong Han Kumphawapi and of coring points CP1, CP2, CP3, CP3A and CP3B.	84
5-13 Lithostratigraphy of sediment sequences, Kumphawapi (a) CP3A and (b) CP3B	88
5-14 Lithostratigraphy ,MS, LOI, XRF, results and selected sample for ¹⁴ C AMS dating.	91
5-15 Results of ¹⁴ C AMS dating from Nong Han Kumphawapi are presented at the 2σ calibrated range.	92
5-16 Age depth curve for CP3A.	94
6-1 Cross section of CP3A coring point and three of Penny's cores.....	97
6-2 Lithostratigraphy correlation of CP1, CP2, CP3, CP3A and CP3B.....	98
6-3 a-e Conception model suggests five stages of lake level and its paleoenvironment.....	104
6-4 Paleogeographic map with archaeological sites of Nong Han Kumphawapi..	106

CHAPTER I

INTRODUCTION

1.1 Rationale

The Asian monsoon system is one of the most important components of the Earth's modern climate system. It largely controls climate in Asia and the Indo-Pacific realm where people depend on mainly agriculture. Changes in this convectively active region can result in severe drought or flood over large, densely populated regions (Webster et al., 1998, cited in Wang, 2005). Thus, precipitation is the important factor to population's livelihood. The Asian monsoon system is composed of two major sub-systems roughly divided at 105°E: the Indian (or Southwest Asian) monsoon (IOM) is a single tropical monsoon system; and the Southeast (or East) Asian monsoon (EAM) is a coupled tropical-subtropical monsoon system. These are linked in that they both respond to the strength of the continental high- and low- pressure cells, which grow and decay seasonally over the Asian landmass (Wang et al., 2005). Monsoon circulation is defined on the basis of seasonal change (cold, dry winters and warm, wet summers) in regional patterns of wind and precipitation. These meteorological parameters are not directly preserved in geological records, but they can indirectly influence the physics, chemistry and biology of the surrounding ocean, and of land surface processes, and can be preserved as distinct signals in geological archives such as marine records (Sirocko et al., 1996; Rashid et al., 2007 and Slott et al., 2007), lakes and bogs (Penny, 1998; Dam et al., 2001; Herzschuh et al., 2005; Hong et al., 2003; Morill et al., 2006; Wang et al., 2007 and Liew et al., 2004), speleothems (Wang, 2008, Shakun et al., 2007; Partin et al., 2007 and Fleitman et al., 2007), tree rings (Hu et al., 2004; Buckley et al., 2007) and ice cores (Thompson et al., 2000). These geological archives therefore preserve indirect, or proxy, measures of past monsoon variability (O'Sullivan and

Reynolds, 2004).

Thailand occupies an area between 5° – 20° N and 97° – 105° E and is situated at the boundary between two monsoon sub-systems and in close proximity to the Western Pacific Ocean. Thus, Thailand is a key region for a better understanding of the dynamics and impact of the Asian monsoon system. The Inter Tropical Convergence Zone (ITCZ) moves over Thailand in a northerly direction during May and in a southerly direction during September. The climate of Thailand is therefore influenced by two major air streams, the northeast and the southwest monsoon (Khedari et al., 2002). The Southwest monsoon brings high humidity air masses from the Indian Ocean to Thailand during mid May to mid October and coincides with the tropical cyclone which contributes with additional precipitation. The northeast monsoon brings cool and dry air masses from the Siberian anti-cyclone over the major part of Thailand between November and February. Moreover, tropical cyclones influence Thailand from August through December. Thailand's climate situation is therefore special, because there are two sources of precipitation, exist during in almost the same period derived from the southwest monsoon and the tropical cyclones.

This thesis uses lake sediments from Nong Han Kumphawapi, Udon Thani Province, Thailand as an archive to investigate the relationship between past changes in Asian monsoon, and paleoenvironmental changes in the lake itself. Detailed analyses of the fossils, chemistry and physical characters present within the lake sediments allow us to reconstruct past lake and catchment processes. Lake sediments can therefore be extremely important archives for reconstructing past climatic and environmental changes (O'Sullivan and Reynolds, 2004). Previous work by Penny (1999) indicated that the oldest sediments in Nong Han Kumphawapi are around 14350 year B.P. old and that they can be used to reconstruct the paleoenvironment and human environment interactions since the

late Pleistocene. This thesis also presents aerial photo interpretations, as well as topographic, land use, soil and geology maps to reconstruct paleogeography of the area. These give a better understanding of the changing geographical feature and of the paleogeography of the area.

1.2 Objectives

The purpose of this study is to investigate the relationship between past changes in Asian monsoon, geographical features, paleogeography and paleoenvironment of Nong Han Kumphawapi.

1.3 Scope and limitation

The scope and limitation of this thesis are:

- The study area is at Nong Han Kumphawapi in Udonthani Province.
- Field investigations and lake sediment coring
- Analyses of the sediments in the laboratory
- Aerial photo interpretation and geomorphologic map reconstruction

1.4 Location of the study area

Nong Han Kumphawapi ($17^{\circ}11'N$ and $103^{\circ}02'E$) is a natural lake located in the southwestern part of the Sakon Nakorn basin (Figure 1.1), approximately 36 km southeast of Udon Thani. The lake occupies an area of approximately 32 km^2 and is situated at approximately 160 – 170 m a.s.l. It occupies a broad alluvial floodplain with a low local relief and is surrounded by hills rising to over 200 m a.s.l. Kumphawapi is a shallow lake with a water depth of $< 4 \text{ m}$. It is about 13 km long from north to south and about 5 km wide from

east to west. Altogether 11 small streams drain the surrounding low hills, including Huai Phai Chan Yai, a primary inflow which originates in the northwestern part of the Phu Phan mountain range and flows into the northeastern side of the lake. Runoff from Huai Phai Chan Yai and numerous streams drain south into Lam Pao River.

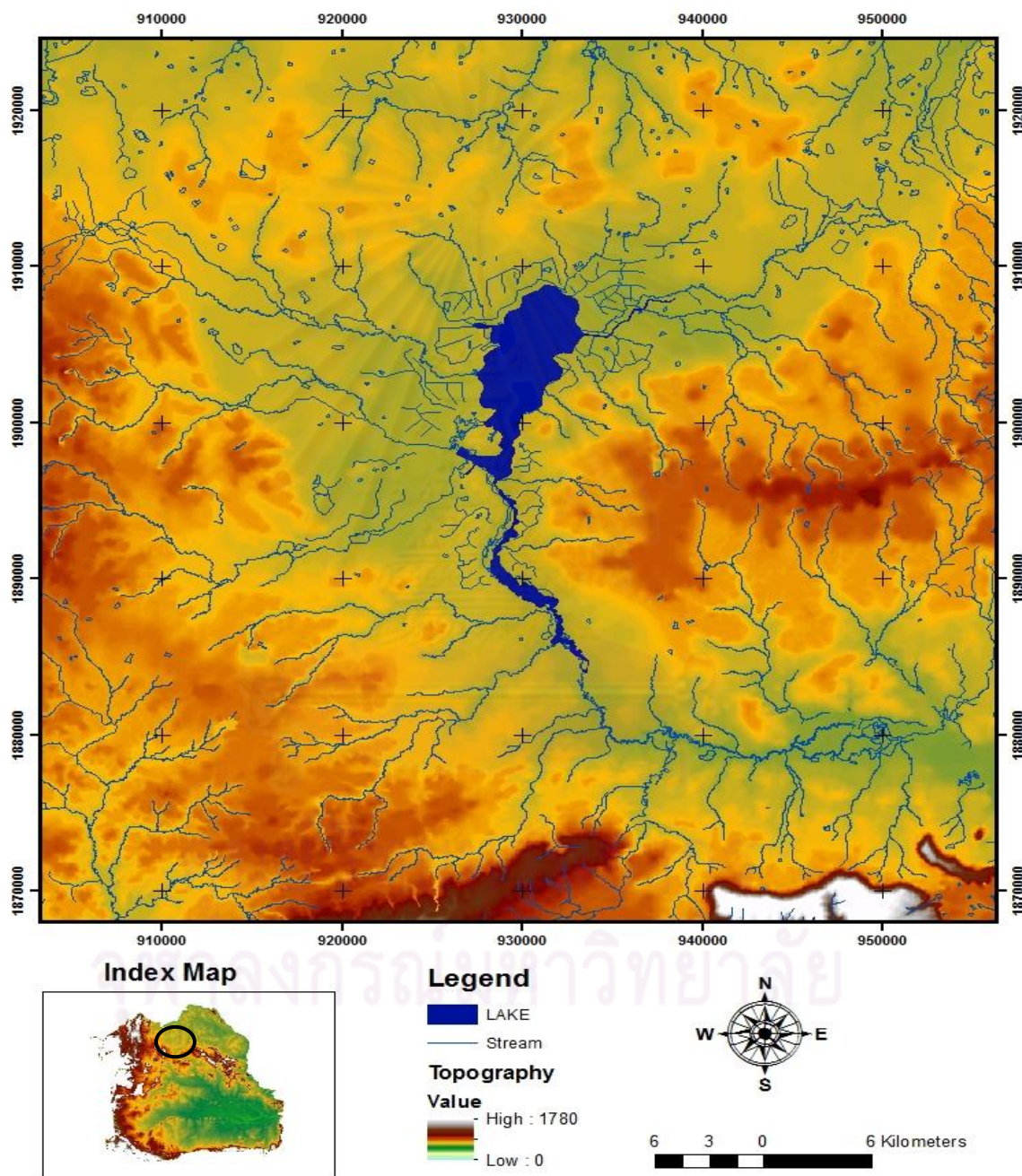


Figure 1-1 The location of Nong Han Kumphawapi (digital data from Thai Royal Survey).

1.5 Expected output

The expected outputs of this thesis consist of:

- Change in lake geography during recent time
- Lake sediment stratigraphy
- Paleoenvironment
- Paleogeography

1.6 Research methodology

To accomplish the aims of this thesis, four sequential steps were designed. Each of which is described as follows:

1.6.1 Preparation

This step includes:

- Literature review of the related research in the study area, in northeast Thailand, and in other countries.
- Acquisition and study of the previous basic data acquisition, i.e. aerial photos, topographic map, and land use map to understand the topography and land use pattern of the study area as general background information.

1.6.2 Map reconstruction

This step includes:

- Aerial photo interpretations (interpreted change in lake boundary).
- Digital Elevation Map (DEM) and topographic, land use, soil and geologic maps were used to reconstruct paleogeography of the area. Software of geographic information system (GIS) and remote sensing (ArcGIS 10 and ERDAS IMAGINE 8.5) are applied in developing, manipulating, and analyzing the digital data.

1.6.3 Field investigation

This step includes:

- Survey the surroundings of Nong Han Kumphawapi based on the L7017 series 1:50000 map.
- Sediment cores were collected with a Russian corer (chamber Ø: 10 cm and 7.5 cm, chamber length: 1 m) and with 0.5 m overlap. Coring was made along several transects to be able to follow the different layers over longer distances. The most complete sequence was selected for high-resolution multi-proxy sub-sampling in the laboratory.

1.6.4 Laboratory analyses

Firstly, the lithostratigraphy was carefully described by its physical properties, by following a Swedish term, introduced by H. von Post (1862).

Prior to sub-sampling we performed non-destructive, high-resolution (<0.5 mm) magnetic susceptibility (MS) and X-ray fluorescence (XRF) analyses on all selected sequences. Magnetic susceptibility is used as a relative proxy indicator for variations in the composition of lake sediments, especially in the content of iron-bearing minerals. Magnetic minerals in lake sediments can be derived from many sources, such as catchment erosion, bedrock, subsoil, and topsoil in the lake drainage basin and the measurements thus provide information on the mineral input from catchment run-off. MS was measured with the MSCL core logger. XRF measurements allow analyzing all major elements between Al and U, and can contribute information on catchment processes, atmospheric deposition of lake status changes. XRF measurements were done using the Itrax core scanner. Both instruments are available at the Department of Geological Sciences at Stockholm University.

Loss-on-ignition (LOI) analysis allows estimating the organic matter and carbonates content of lake sediments, and thus gives information about the nature of the sediment and sediment sources (e.g. in lake organic matter sources, paleo-productivity). LOI is expressed as percentage of the dry weight of each sample. LOI analysis was performed on the most complete sediment sequence. Samples were taken in contiguous 1 cm increments and had a volume of ca. 3 cm³.

The remaining core fragments from CP3A were sub-sampled in contiguous 5 cm intervals for ¹⁴C dating in order to obtain a preliminary chronology. The samples were selected for Accelerator mass spectrometry (AMS) ¹⁴C dating. These samples were measured by AMS at the QUB ¹⁴CHRONO centre. The resulting ¹⁴C dates were then calibrated (Reimer et al., 2004). All radiocarbon determinations are presented at the 2σ calibrated range, or the median of that range.

1.7 Components of the thesis

This thesis is composed of 6 chapters, including this introductory chapter 1. Chapter 2 contains reviews of previous studies of the site and adjacent areas. The application of remote sensing and Geographic Information Systems (GIS) are also briefly reviewed. The site description is given in Chapter 3, which is divided into 5 parts, including location and topography, geology, vegetation, climate and archaeology. Chapter 4 provides all methods which were used in this study. The chapter starts with GIS and map reconstructions and then presents the fieldwork procedures and laboratory analyses. The Previous investigations from the related technical literature are also given. Based on the data preparation and the different analytical steps, the results are presented in chapter 5. Chapter 6 contains discussions of the results and the conclusions.

CHAPTER II

LITURATURE REVIEW

This section will review two main topics: a) Past Asian monsoon variability and b) The previous studies for Paleogeography, Paleoenvironment and Paleoclimatic change of Nong Han Kumphawapi, Udon Thani Province. These studies over Thailand have limited information, however available for Nong Han Kumphawapi in respect to past monsoon intensity and paleoenvironmental reconstruction (Kealhofer, 1996, Kealhofer and Penny, 1998, Penny, 1999; 2001; White et al., 1995; 2004 and Penny & Kealhofer, 2005).

2.1 Past Asian monsoon variability

Over millions of years, changes in monsoon patterns are controlled by the tectonic uplift of the Tibetan Plateau, which changes the thermal contrast between the Indian Ocean and the southern Asian mainland (Kutzbach, 1981). On time scales of thousands to hundreds of thousands of years, monsoon variability is controlled by the 23 ka precession cycle of insolation. Interannual to centennial-scale monsoon variability is caused by physical processes internal to Earth's climate system, such as the El Niño-Southern Oscillation (ENSO) and local atmosphere-ocean-land interactions (Wang et al., 2003). These processes occur on time scales that are most important from a human perspective, but are less well understood.

Decadal to millennial-scale variability in monsoon precipitation and its underlying causes have therefore attracted considerable attention during the past years. Marine sediments, cave speleothems, annually laminated corals and tree rings from Asian monsoon regions have added new knowledge to our current understanding of the factors that controlled inter-annual to millennial monsoon variability in the past and provide

important constraints for climate modeling scenarios (Overpeck and Cole, 2007). In contrast, the spatial and temporal pattern of sub-millennial scale monsoon variability and its impact on land cover in SE Asia are still unresolved. This shortcoming stems from the fact that temporally well-resolved paleoenvironmental studies are missing for large parts of SE Asia. Given that global and regional climate models increasingly use terrestrial paleo data to test their performance, past changes in land cover (e.g., vegetation, dust, lake and wetland extent) are important variables to better understand feedbacks between different Earth systems.

Speleothems from China (Wang et al., 2008), India (Sinha et al., 2005), Yemen (Shakun et al., 2007) and Oman (Fleitmann et al., 2007), and marine records from the Arabian Sea (Sirocko et al., 1996) and the Indian Ocean (Rashid et al., 2007) suggest a strong coupling between Asian monsoon and climate variability in the North Atlantic region on sub-millennial time scales during the past 110 ka: weakened (increased) Asian summer monsoon during cold (warm) Northern Hemisphere intervals. The observed relationship between Asian monsoon variability and cold (stadial) Northern Hemisphere intervals during the Last Glacial (110-11.5 ka) is generally explained by westerly transport of cold air from the Atlantic region and an intensified outflow of cold/dry air from the Siberian High which led to a stronger northeast (winter) monsoon. Lower SST over the western Pacific on the other hand would have caused a reduced sea-land thermal contrast resulting in a weak summer monsoon. This climatic situation was reversed during Northern Hemisphere warm (interstadial) intervals.

The sparse lake sediment and peat studies for the Last Glacial Maximum (LGM) and the end of the Last Glacial period (ca. 20-11.5 ka) (see e.g. summaries by (Wang et al., 2005; Morill et al., 2003)) imply terrestrial and aquatic ecosystem response associated with changes in monsoon strength and intensity, but also dependent on local/regional controlling

factors, such as e.g. sea level changes and ecotone boundaries (Hope et al., 2004). Drier climatic conditions caused by the strong northeast monsoon during the LGM led to a depression of the tree-line, expansion of high-altitude montane forests and grasslands, and increased fire intensity (Hope et al., 2004). The first increase in summer monsoon strength and higher moisture availability around ~15 ka initiated a change in vegetation and also triggered higher lake levels (Herzschuh et al., 2005; Maxwell, 2001). However, the decadal to centennial-scale climate shifts recorded in speleothems are rarely observed in lacustrine archives. Moreover, the lack of good chronological control renders it unclear how the observed shifts in vegetation and lake level correlate to precipitation changes reconstructed in other archives. Vegetation reconstructions in China (Wang et al., 2007) (Hong et al., 2003) and Japan (Nakagawa et al., 2003) suggest for example that changes in monsoon intensity were partly in concert with North Atlantic climate variability and partly off-set. Transitions between different monsoon phases may also have been more gradual (Shakun et al., 2007) and may even have lasted longer (Zhao et al., 2003) than their North Atlantic counterparts.

The distinct increase in summer monsoon intensity ~11.5 ka, resulting from a rapid northward shift of the ITCZ (Fleitmann et al., 2007) is a clear feature in many paleo archives across SE Asia (Morill et al., 2003). However it is unclear whether the response to the strengthened summer monsoon was abrupt or gradual, synchronous or asynchronous over Asia. This issue is difficult to constrain based on ^{14}C -dated archives with a poor temporal resolution, since ^{14}C plateaux during this time interval complicate ^{14}C calibration (Reimer et al., 2004) and as such precise age assignments and correlations between archives. Also the gradual weakening of the summer monsoon during the mid-late Holocene, which was caused by the declining precession cycle of summer insolation, is temporally not well constrained. Whether the monsoon weaken gradually (Fleitmann et al., 2007) or abruptly (Morill et al., 2003; Abram et al., 2007) during the mid-Holocene and whether this decline

was synchronous or asynchronous is therefore still debated. Lake levels and vegetation in Indonesia (Dam et al., 2001), China (Herzschuh et al., 2005; Hong et al., 2003; Wang et al., 2007 and Morill et al., 2006), India (Sinha et al., 2006), Taiwan (Liew et al., 2007) and the Australasian region (Hope et al., 2004) responded to the general trend of a strong early Holocene monsoon and to the gradual weakening during the mid-late Holocene. But these studies rarely exhibit the sub-millennial shifts in monsoon intensity suggested from speleothem and marine records, which imply close links with high-latitude temperature variations, variations in solar activity and/or changes in oceanic and atmospheric circulation (Gupta et al., 2003; Hu et al., 2008; Wang et al., 2005).

Marine paleo-proxies (Stott et al., 2007; Visser et al., 2003) and speleothems from the equatorial western tropical Pacific region (Partin et al., 2007), as well as Himalayan ice core records (Thompson et al., 2000) draw a more complicated picture with links to Southern Hemisphere climate and a possible tropical Pacific influence on the North Atlantic region. Indeed, El-Niño like conditions in the tropical Pacific weakened the Asian monsoon in the 1700s (Buckley et al., 2007). Moreover, ^{14}C measured on tree rings from central Thailand (Hu et al., 2004) follows a Southern Hemisphere trend during parts of the Little Ice Age, when studies further to the northeast evoke a link to Northern Hemisphere climate.

2.2 The previous studies for Paleogeography, Paleoenvironment and Paleoclimatic change of Nong Han Kumphawapi, Udon Thani Province.

Penny (1999) investigated Paleoenvironment of the Sakon Nakhon Basin by using evidence from pollen and charcoal. ^{14}C dating based on pollen concentrates, returned age of 14350 years BP for the lowermost sediments. Pollen did not preserve in these sediments, suggesting oxidation and a dry period. The sediments dating to c. 9,500 – c. 10,200 years BP were dominated by *Pinus*, *Celtis* and *Uncaria/Wedlandia* type (lowland forest). Since, regional vegetation species were poor (17 aboreal pollens), Penny (1999) suggested

flooded or permanently water-logged conditions. Nong Han Kumphawapi was probably an open water lake with high energy sediment transport and sparse and open vegetation around the shore. Higher precipitation due to a relatively stronger southwest monsoon circulation is interpreted from the change to homogenous lacustrine clay and the increase in sedimentation rate. At 9,800 years B.P., arboreal pollen taxa become dominant and the pollen diversity increases markedly. Penny (1999) interprets this as a change in environment conditions, since dry deciduous or semi-deciduous forests expand. The appearance of mixed deciduous and dry evergreen forests between 8,000 and 6,900 years B.P. suggests climate conditions is substantially more humid than present. Between c. 6,400 and c. 6,600 years B.P., pollen analysis shows a dramatic decrease in lowland forest taxa, while *Pinus* and *Cephalanthus* type pollen increase together with charcoal particles. This suggests a decrease of lowland forests and more frequent, widespread, or more intense fires. The increase of secondary forest taxa and the decline in charcoal particles around 2,840 years B.P. are interpreted as a re-establishment of dryland forests and an expansion of secondary forests. In conclusion, this study provided the first picture of environmental change and human/environment interaction from the late Pleistocene to the present in the Sakon Nakhon basin.

According to Kealhofer and Penny (1998), who combined pollen and phytolith data from the same core, the Late Pleistocene (between >14,000-<8,250 year B.C.) environment of Nong Han Kumphawapi was characterized by the development of herbaceous swamp and swamp forest communities. Early Holocene (ca. 8,000-7,000 year B.C.) vegetation changes reflect the rapid expansion and diversification of mixed-deciduous forests, which may however have been disturbed by anthropogenic burning. The shift in the burning regimes during the Middle Holocene (ca. 7,000-3,000 year B.C.) is indirect evidence for agricultural activities. During the Late Holocene (3,000 year B.C.-Present) reduction in dry-

land forest and the subsequent establishment of secondary-growth forests, suggests a further change to burning regimes.

White (2004) reported data from KUM3, which is one of the sediment cores from Nong Han Kumphawapi, and which has been the subject of several publications (Kealhofer, 1996; Penny et al., 1996; Kealhofer and Penny, 1998; Penny, 1999). White (2004) combined the data from pollen analysis (Penny et al., 1996; 1999), charcoal particle concentration (Penny et al., 1996; 1999) and phytolith analysis (Kealhofer, 1996) with archaeological data of the study area and adjacent areas. The bottom sediments of the lake have an age of $12,270 \pm 70$ B.P. uncal. The pollen data suggest dry climate with low abundance of trees and low total species diversity and phytolith data show burning regime of the ground cover (Kealhofer, 1996, 2002). During the Pleistocene/Holocene transition, phytoliths show a shift from savanna adapted grasses to bamboid taxa (ground cover of dry dipterocarp forest). During the early Holocene, a gradual increase in the abundance and diversity of forest pollen suggest an increase in precipitation and climate condition were thus interpreted as having become more humid than at present. The abundance and diversity of forest pollen types increase above 250 cm depth, which has an age of ca. 8610-7100 B.P. uncal. The environment of this period was dominated by mixed deciduous/dry evergreen forests (Penny, 1998). The middle Holocene (170 cm depth) pollen taxon diversity is more than double that recorded during the terminal Pleistocene. The early to middle Holocene settlements in the Kumphawapi catchment have not yet been identified. However, Kealhofer (1996) claims that charcoal concentrations suggest burning and human activities. This event occurred from before ca. 5,500 B.P. uncal. to 3,500 B.P. uncal. , and is seen as a peak in microscopic charcoal concentrations at 90 cm depth. Coincident the diversity of dryland tree pollen taxa decrease dramatically The high charcoal zone ends around 60 cm where the beginning of Late Holocene (ca 1,800 B.C. cal.) is. Here the charcoal

concentrations have fallen relative to the very high values observed between 90 and 60 cm depth. The environment around Nong Han Kumphawapi was dominated by a swamp and forest trees. Around 890 B.C. cal. (2690±70 B.P. uncal.) some pollen taxa reappear and suggest a recovery phase in forest cover. However, the relationship between paleoclimate, paleoenvironment and cultural history of this region still need to be discussed, especially in respect to the archaeological evidence for societies practicing plant cultivation in the Sakon Nakhon basin.

There are two groups of interpretations as follow:

A) According to Higham (1996) and Bellwood (1997) agriculture appeared during the later part of the 3rd millenium B.C. cal., after a long period of forest disturbance and when the amount of charcoal decreases sharply. This suggestion is based primarily on dates in Thailand and elsewhere in Southeast Asia, which are associated with a particular widespread ceramic decoration.

B) White (1986, 1987) suggests that agriculture appeared during the 4th millennium B.C. cal. This suggestion is based primarily on dates from basal deposits in Ban Chiang and Ban Tong, two long-term settlements in the Kumphawapi catchment.

ศูนย์วิทยทรัพยากร
จุฬาลงกรณ์มหาวิทยาลัย

CHAPTER III

SITE DESCRIPTION

3.1 Location and Topography

This chapter will focus on the northeastern region of Thailand where Nong Han Kumphawapi, the study area is located. The Northeastern region (Isan) is one of six physiographic regions of Thailand (Figure 3-1).

The Khorat Plateau is a dominant feature of Northeastern Thailand. The Plateau has an area of approximately 170,000 km² or about 1/3 of the total area of the country (from Department of Geology and Mineral Resources of Thailand). The plateau lies between latitudes 14° and 19° N and between 101° and 106° E. A “saucer shape” is often used to describe the Khorat Plateau (Moore, 1988; Smitinand, 1989; Miura et al., 1992; cited in Penny, 1998) which reaches a maximum elevation of 120-220 m above sea level (a.s.l) in the northern and western part. The altitude gradually decreases in the southwest corner where it is 65 m a.s.l. (Thriramongkol, 1983). The Petchabun and Dong Phrayayen Mountain ranges are north to south trending and separate the west of the plateau from the central basin. The Sunkumphang and Phanomdongrak Mountain ranges extend from east to west and form a boundary between the south and the north. The eastern part of the Khorat Plateau is bounded by the Mekong River. The Phu Phan range divides the Khorat Plateau into two basins: the Sakon Nakhon Basin (approximately 58,000 km²) in the north and the Khorat Basin (approximately 112,000 km²) in the south (Figure 3-2). Two major fluvial systems drain the Khorat Basin: the Mun river originates in the west and southwest highlands of the Khorat Plateau, and the Chi river in western Petchabun and in the northern Phu Phan mountain ranges. Both rivers drain to the southeast and converge west of Ubon Ratchathani before flowing to the Mekong. The Sakon Nakhon Basin is drained by the Songkhram River, which is the largest river. It originates in the northern part of the Phu Phan mountain range and flows north and east-south-east to the Mekong River. Apart from these larger river systems a series of smaller streams flow directly north to the Mekong.

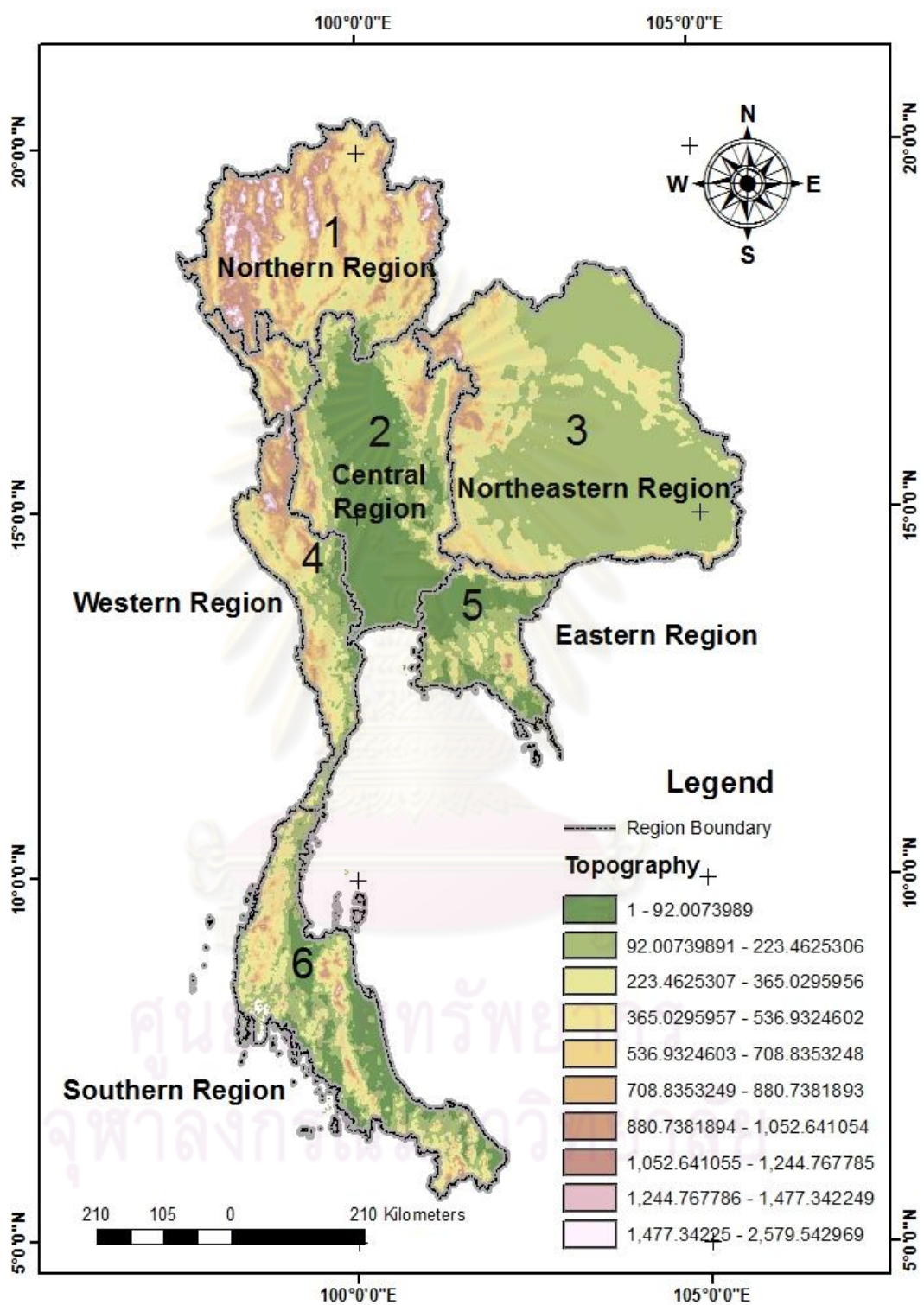


Figure 3-1 Physiographic regions of Thailand (digital data from The Royal Thai survey)

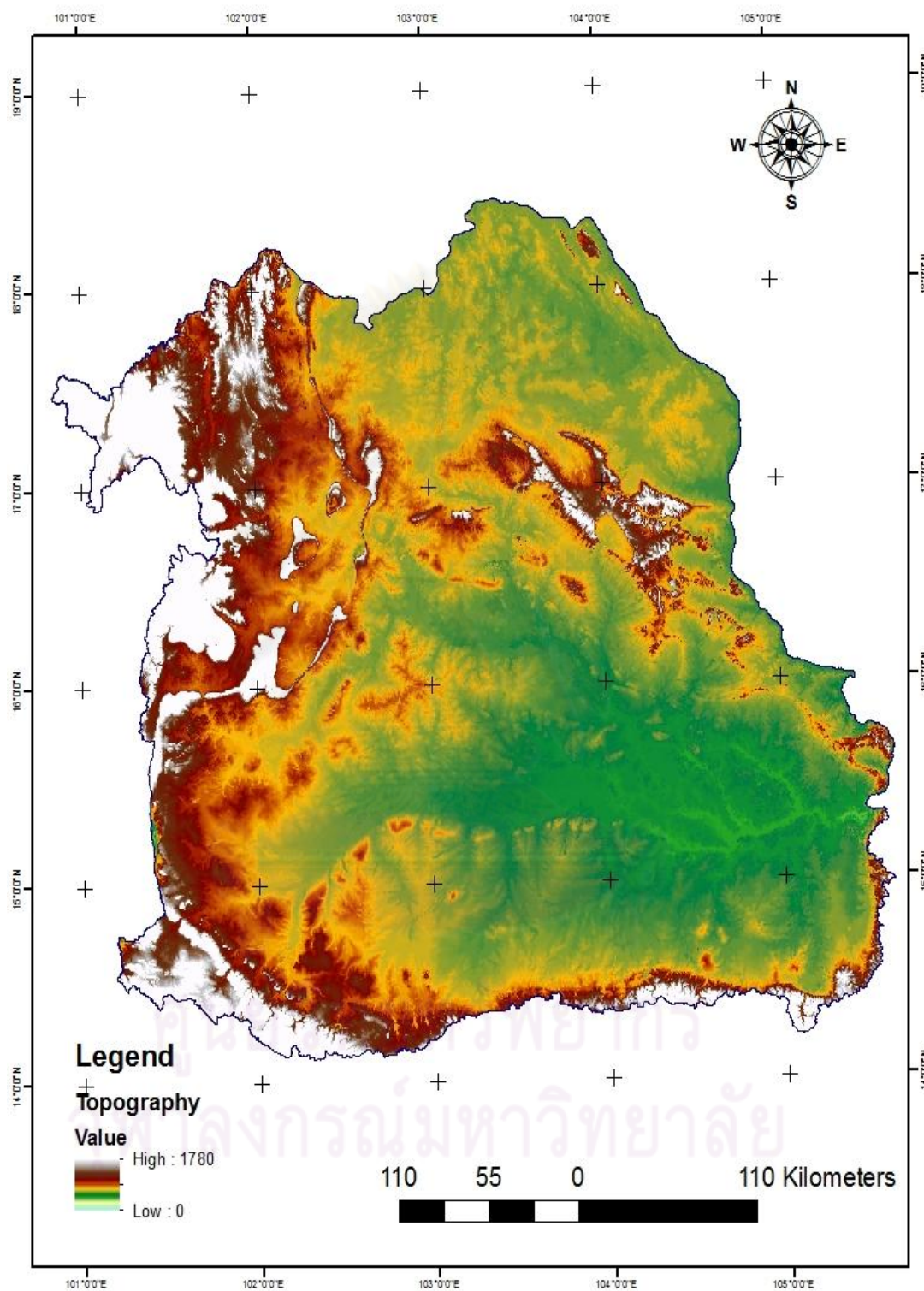


Figure 3-2 Location and major topographic features of the Khorat Basin and the Sakon Nakhon Basin (digital data from The Royal Thai survey)

Nong Han Kumphawapi ($17^{\circ}11'N$ and $103^{\circ}02'E$) is a natural lake located in the Sakon Nakhon basin, approximately 36 km southeast of Udon Thani. The lake occupies an area of approximately 32 km^2 and is situated at approximately 160 – 170 m a.s.l. It occupies a broad alluvial floodplain with a low local relief and is surrounded by hills rising to over 200 m a.s.l. Kumphawapi is a shallow (< 4m water depth) lake. Its length is 13 km from north to south and its widest part is 5 km from east to west. Altogether 11 small streams drain the surrounding low hills, including Huai Phai Chan Yai, a primary inflow which originates in the northwestern part of the Phu Phan mountain range and flows into the northeastern side of the lake. Runoff from Huai Phai Chan Yai and numerous streams drain south into Lam Pao River. Most of the lake area is covered with floating plant communities with an extensive herbaceous swamp. The southern part of the lake is characterized by a salt mound that rises 10-15 m above the surrounding swamp and which is called Ban Don Kaeo.

There are two theories regarding the origin of the lake:

- 1) The depression occupied by the lake was formed by dissolution and collapse of the underlying salt sequences (Maha Sarakham Formation) of the Upper Cretaceous (Rau and Supajanya, 1985);
- 2) Abandonment of a palaeochannel of the Mekong River, whose current channel is some 90 km to the north (Moore, 1998; Parry, 1990).

Since Thailand joined the Mekong Chi Mun Project Plans, a dam was built to block the Lam Pao River in order to expand the storage capacity of the lake for dry season irrigation purposes and to protect from flooding. The dam was finished in 1994 and includes 5 floodgates and 124 km of dyke (8 m wide and 6 m high) around Nong Han Kumphawapi (Table 3-1 and figure 3-3). Above the dam and along the dyke 14 electrically powered pump stations were installed to pump water from the lake into the irrigation canal systems which irrigate 35.9 km^2 of agricultural area. The details of the lake after damming are shown below.

Table 3-1 The properties of Nong Han Kumphawapi after the dam was built.

Nong Han Kumphawapi reservoir	
Catchment area	1,310 km ²
Runoff water	311 million m ³ per year
Water surface area	36 km ²
Trough level	+166.00 m(MSL)
Catchment level	+199.50 m(MSL)
Catchment volume	102 million m ³



ศูนย์วิทยทรัพยากร
จุฬาลงกรณ์มหาวิทยาลัย

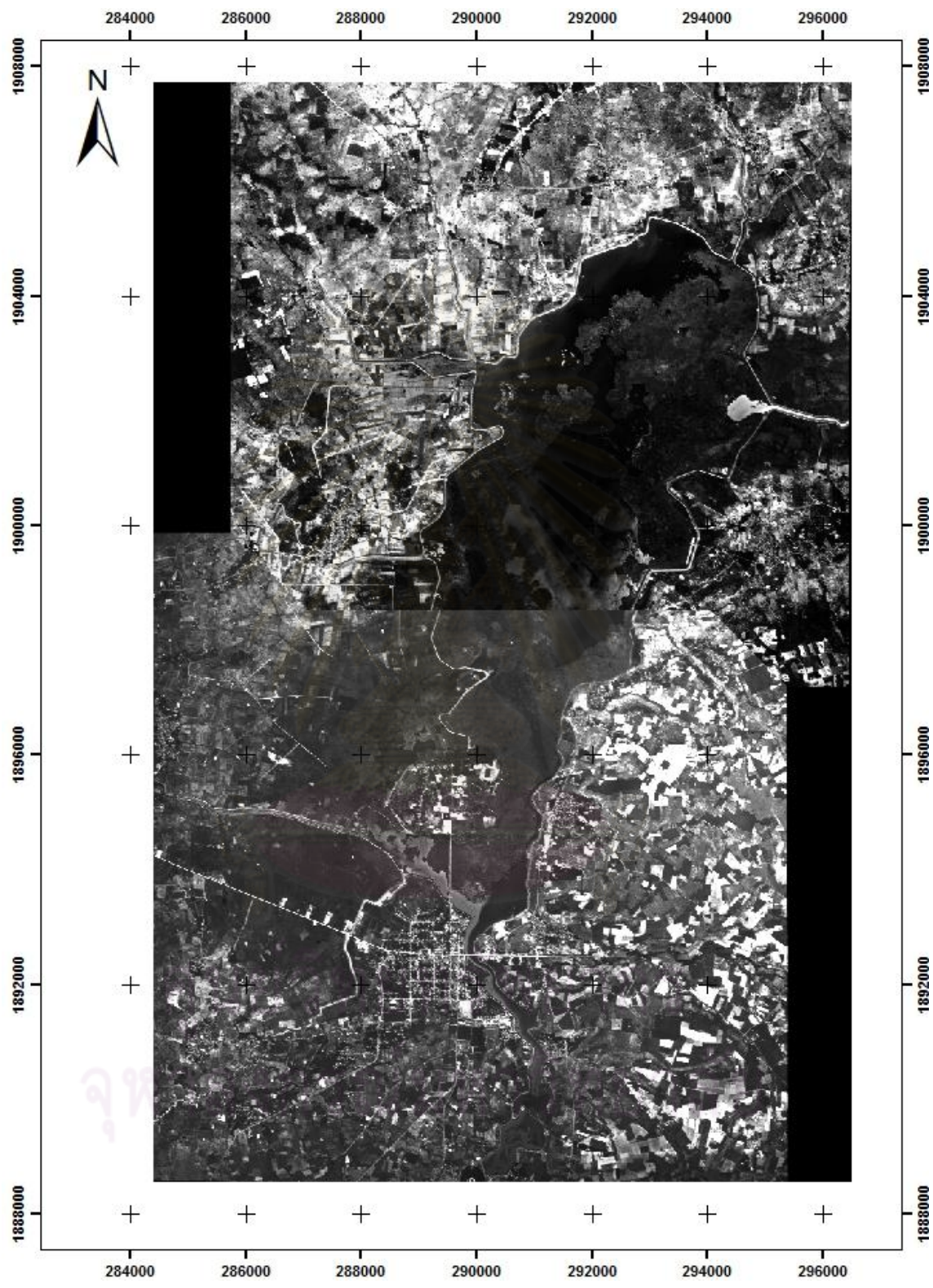


Figure 3-3 Aerial photos from 1996 of Nong Han Kumphawapi after the dam was built (data from The Royal Thai Survey)

3.2 Geology

3.2.1 Khorat Plateau

The Khorat Plateau is located on the Indochina microplate and includes the Sakon Nakhon Basin (approximately 58,000 km²) in the northern part and the Khorat Basin (approximately 112,000 km²) in the southern part. These two basins are divided by the Phu Phan anticline which is northwest-southwest trending. The plateau is a broad syncline bounded to the west by the Shan Thai microplate and to the north by the South China Plate (El Tabakh, 1999) (Figure3-4).

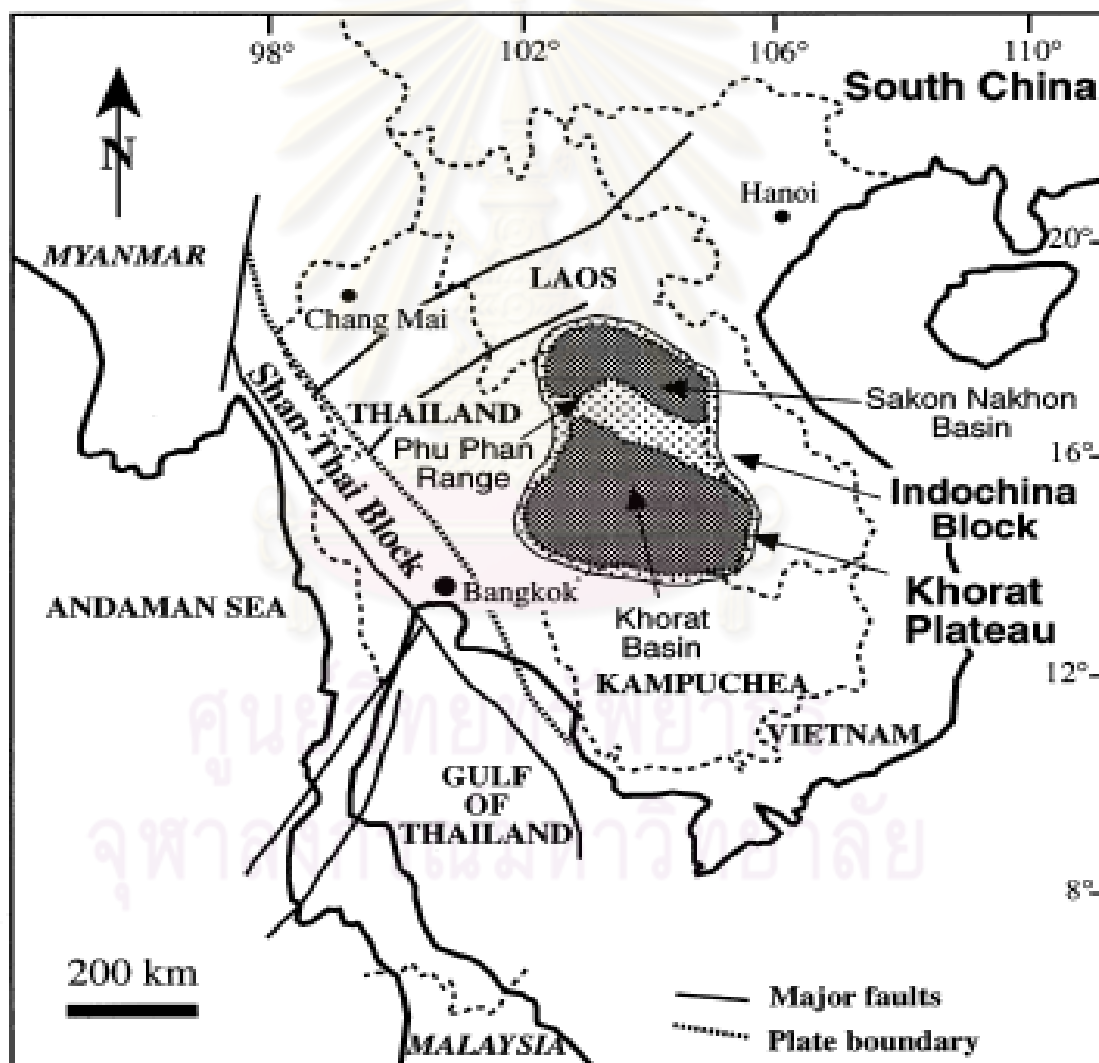


Figure 3-4 The general tectonic elements of the region and the location of the Khorat and the Sakon Nakhon basins (after El Tabakh, 1999).

Much of the sedimentary succession of the Khorat Plateau is a non-marine red bed, called the Khorat Group. It is a terrestrial deposit of Mesozoic age and consists of siltstone, sandstone, mudstone and conglomerate with a thickness of 4,000 m. These Late Triassic to Cretaceous-Tertiary sediments overlie partly eroded upper Paleozoic sediments (Figure 4). An important formation that influences the present day geomorphology is the Maha Sarakham Formation because of the dissolution of the salt sequences. Following the report of the Department of Mineral Resources of Thailand, the Khorat Group can be divided into 9 formations (figure 3-5 and 3-6) which are from bottom to top:

1.) Huai Hin Lat Formation

This formation is of Mesozoic age and contains conglomerates and sandstone and rhyolite. According to Iwai et al. (1996), the Huai Hin Lat formation consists of sandstone, siltstone and grayish mudstone with fossil leaves, bivalves (*Euestheris mansuyi*), pollen and spores (Haile, 1973) and dinosaur remains (Buffetaut and Ingawat, 1982). The Hua Hin Lat formation lies unconformably over Permian limestone, which suggests a Late Triassic age.

2.) Nam Pong Formation

This formation is made up of siltstone, sandstone and conglomerate.

3.) Phu Kradung Formation

This formation consists of siltstone, greenish gray sandstone, mudstone and conglomerate with limestone rock fragments. In the Phu Kradung mountain range, it is 100 m thick.

4.) Phra Wi Han Formation

This formation is composed of sandstone and thin layers of grayish black siltstone. Its thickness ranges from 56 to 136 m.

5.) Sao Khua Formation

This formation contains siltstone, mudstone and conglomerate, mixed with sand.

In the Sao Khua area, its thickness is around 512 m. Gastropods (*Naticoid*), bivalves (*Trigoniodides* sp. and *Plicatounio* sp.) (Meesook et al., 1995) indicate an early Cretaceous age.

6.) Phu Phan Formation

This formation is made up of thick layers of sandstone, alternating with conglomerates and has a thickness of about 114 m.

7.) Khok Kruat Formation

This formation consists of siltstone, sandstone and caliche-siltstone with are 709 m. thick.

8.) Maha Sarakham Formation

This formation consists of siltstone, shale, sandstone and mudstone alternating with evaporates, such as gypsum, anhydrite, and potash salts (sylvinite, carnalite, halite, tachyhydrite) (Moore, 1988). The evaporites attain a thickness of 200 m, while the whole Maha Sarakham Formation is about 600 m thick. The salt units occupy an area of approximately 21,000 km² in the Sakon Nakhon Basin (Rau & Sapajanja, 1985) and of approximately 36,000 km² in the Khorat Basin. The salt facies impact on the surface features due to the dissolution of underlying salt sequences and diapiric salt domes or plugs. Paleomagnetic studies indicate a late Cretaceous age and from isotope analysis suggests an age of 100 million years.

9.) Phu Tok Formation

This formation consists of reddish fine sand stone, about 200 m thick. There is no evidence for Tertiary rocks would belong to the lowest part of the Cenozoic era on the Khorat Plateau.

Quaternary sediments on the Khorat Plateau consist of gravel beds and lateritic soil which crop out along the northern and southern margin of the basin. Petrified wood has also been found in Late Cretaceous to Early Quaternary gravel beds. In addition, tektites were found on top of gravel beds and lateritic soils around the Khorat Plateau and indicate an age of more than 0.7 million years.

ERA	TIME SCALE	SYSTEM PERIOD	SERIES EPOCHS	LITHOLOGY	FORMATION	GROUP	DEPOSITIONAL ENVIRONMENTS	TECTONIC EPISODES
CENOZOIC	2.0	Quaternary		Gravel	Unnamed		Alluvial	
		Tertiary		Siltstone Mudstone	Phu Tok		Fluviatile	India collides with Asia-Folding of Khorat Plateau
MESOZOIC	144	Cretaceous		Rock salt Mudstone	Maha Sarakham		Evaporitic	
				Sandstone Shale	Khok Kruat	KHORAT GROUP	Fluviatile	
				Sandstone	Phu Phan		Fluviatile	
		Jurassic	Upper	Sandstone	Sao Khua		Fluviatile	
			Middle	Sandstone	Phra Wihan		Fluviatile	
			Lower	Sandstone	Phu Khradung		Fluviatile	
		Triassic	190	Upper	Rhaetian		Shale Sandstone	Nam Phong
Norian-Carnian	Shale Sandstone				Lower Nam Phong (Huai Hin Lat)		Fluviatile	
	200	Middle Lower-		L.S Conglomerate	Triassic Fill		Fluvio-Lacustrine	Khorat Unconformity Indosinian Orogeny

Figure 3-5 Mesozoic and Cenozoic stratigraphy of the Khorat Basin in NE Thailand and summary of the geological history of the Indochina microplate during the Mesozoic and the Cenozoic (After El Tabakh et al., 1999).

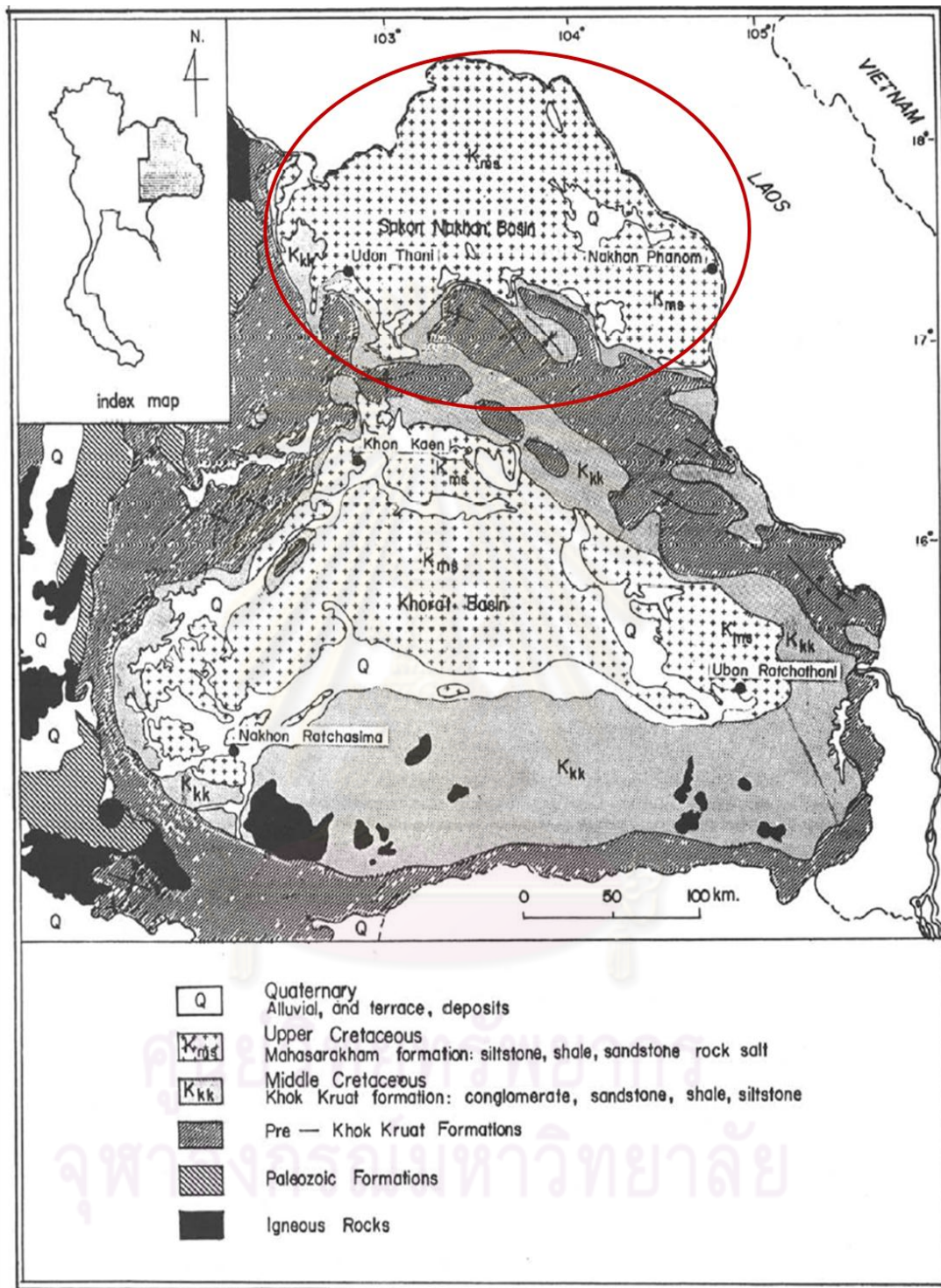


Figure 3-6 Geologic map of Khorat Plateau, including Sakon Nakhon Basin and Khorat Basin

3.2.2 The Sakon Nakhon Basin

Sakon Nakhon Basin occupies an area of approximately 1,000 km² and is drained by the Songkram River and its tributaries originating in the northern part of the Khorat Plateau (Dheeradilok, 1983). The subsurface geophysical survey of Manjai (2004) shows that the Phu Tok Formation makes up a large part of the Sakon Nakhon Basin and those salt domes from the Maha Sarakham Formation reaches to the subsurface.

Quaternary sediments are found in and along the alluvial plains of Sakon Nakhon and Nakhon Phanom provinces. According to the report of DMR (1998) and following Wongsomsak (1992), the Quaternary stratigraphy of the Sakon Nakhon Basin can be divided into 7 units including from oldest to the most recent (Figure 3-7 and 3-8):

Colluvial deposits: the oldest unit occurs near the mountains in the undulating terrain and consists of bedrock fragments mixed with red brown sand and silt.

High Terrace deposits: this flat plain area is situated more than 18 meters above Mekong River level and is composed of well-rounded gravel with sandy clay matrix and tektites.

Middle Terrace deposits: These are situated 13 meters above the Mekong River and include rounded gravel mixed with sand or silt and clay.

Low Terrace deposits: These are at 8 meters above the Mekong River level and are composed of sand or silt with clay.

Valley plain deposits: These occur along tributary rivers and cut across older units. Clay mixed with poorly sorted sand are the dominant sediments.

Flood plain deposits: the youngest unit occurs along the main rivers of this basin and composes of sand or silt mixing with clay layer overlay sandy clay and gravelly sand layers (Sinsakul et. al., 2002).

The Quaternary sediments in the Sakon Nakhon basin are thus mainly of fluvial origin but have experienced uplift throughout the Pleistocene. Dating of tektites found in the High Terrace deposits has been made in comparison to Australian and Southeast Asian tektites, which have an age of 600,000 – 700,000 years B.P. (Bunopas et al., 1976), assuming that deposition occurred more or less of the same time.

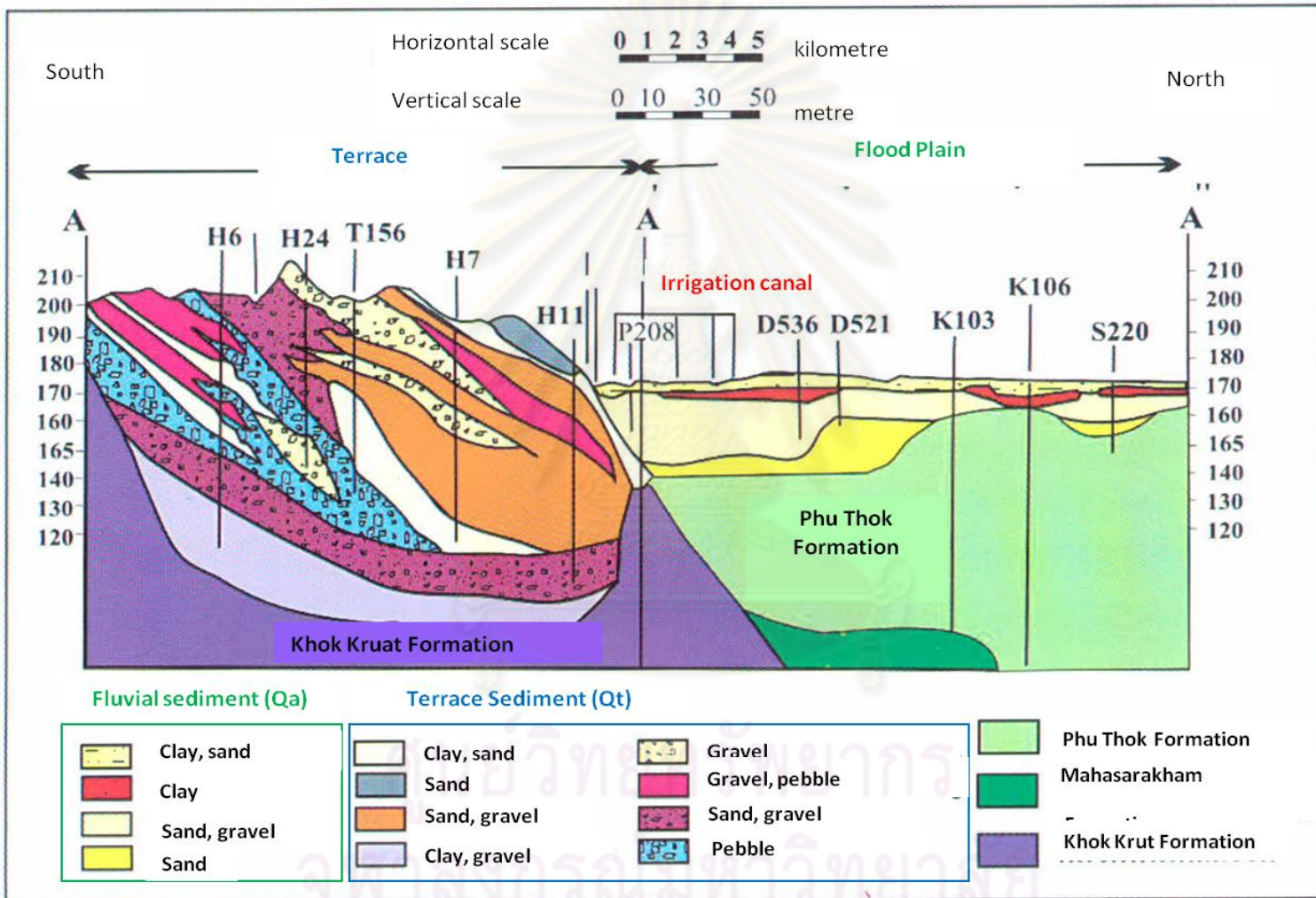


Figure 3-7 Profile of the Quaternary deposit of the Northeastern region of Thailand (after Wongsawat et al., 1992)

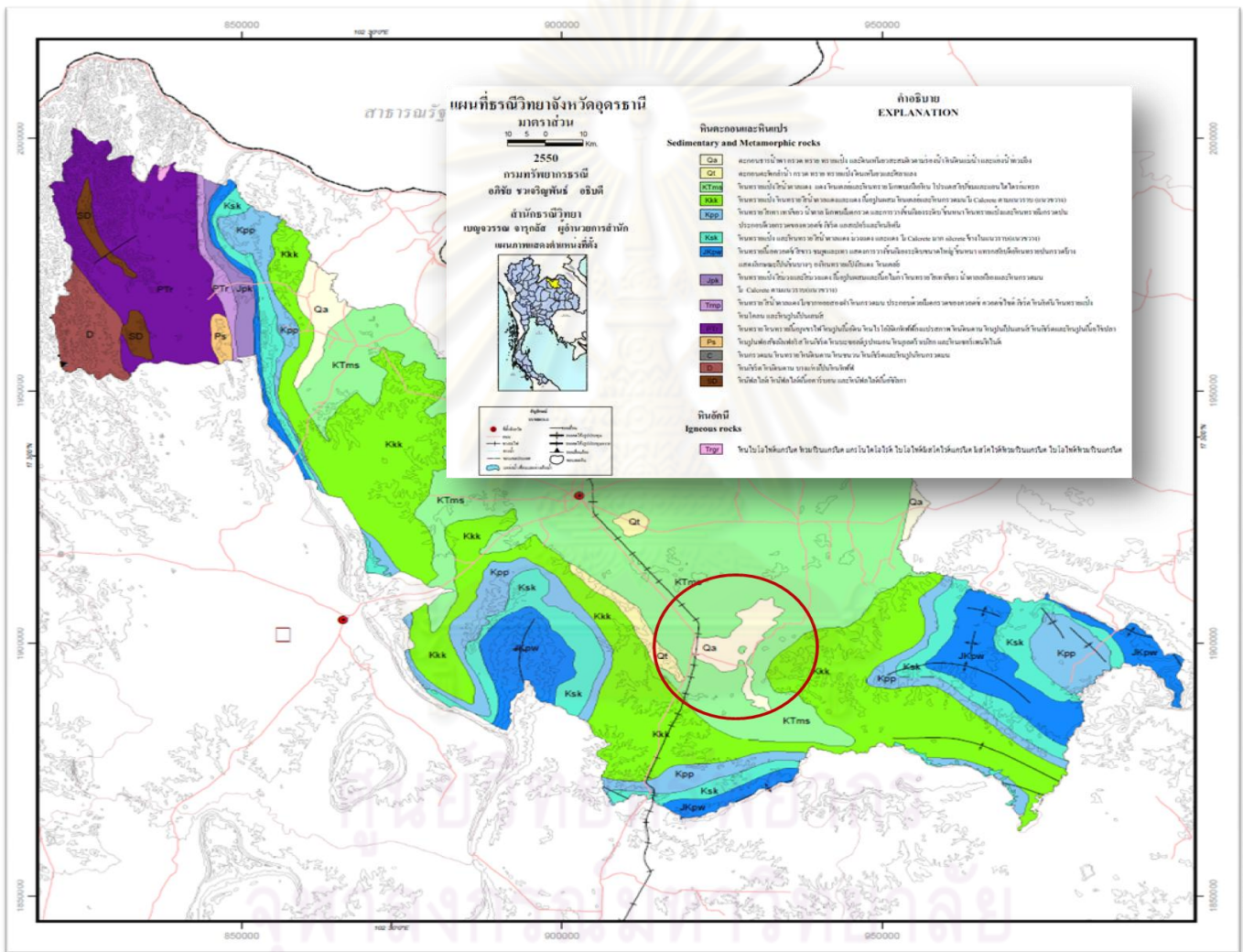


Figure 3-8 Geological map of Udon Thani Province.

3.3 Climate

3.3.1 Monsoon characteristics and seasons

Thailand's climate can be classified into two types, according to the Köppen system (Arbhabhirama et al., 1988; Khedari et al., 2002), a tropical monsoon climate (*Am*) and a tropical savanna climate (*Aw*). The characteristic of the type (*Am*) is a short dry season but a very rainy wet season. The type (*Aw*) has a longer dry season and a prominent but not extraordinary wet season. The Inter Tropical Convergence Zone (ITCZ) moves over Thailand in a northerly direction during May and in a southerly direction during September. This causes the climate of Thailand to be influenced by two major air streams (Figure 3-9), the northeast and the southwest monsoon (Khedari et al., 2002). The southwest monsoon brings high humidity air mass from the Indian Ocean to Thailand during mid May to mid October, while the northeast monsoon brings cool and dry air masses from the Siberian anti-cyclone to the major part of Thailand during November until February.

The climate of Thailand is generally divided into three seasons which are:

The rainy season is influenced by the southwest monsoon from mid-May to mid-October. Rainfall peaks in August to September during the retreat of the southwest monsoon. In addition abundant rainfall comes from tropical cyclones, which reach Thailand from August to October.

The winter season is influenced by the northeast monsoon from mid-November to mid-January. The amount of rainfall is less than during the rainy season, although the eastern part of the Southern peninsular usually receives much more rainfall than the western, leeward side (Khedari et al., 2002). The reason for this is that the northeast monsoon picked up moisture over the Gulf of Thailand.

The summer season is a transition period between the shifts from the northeast to the southwest monsoon and occurs between mid-February and mid-May. The hottest month of the year is usually April.

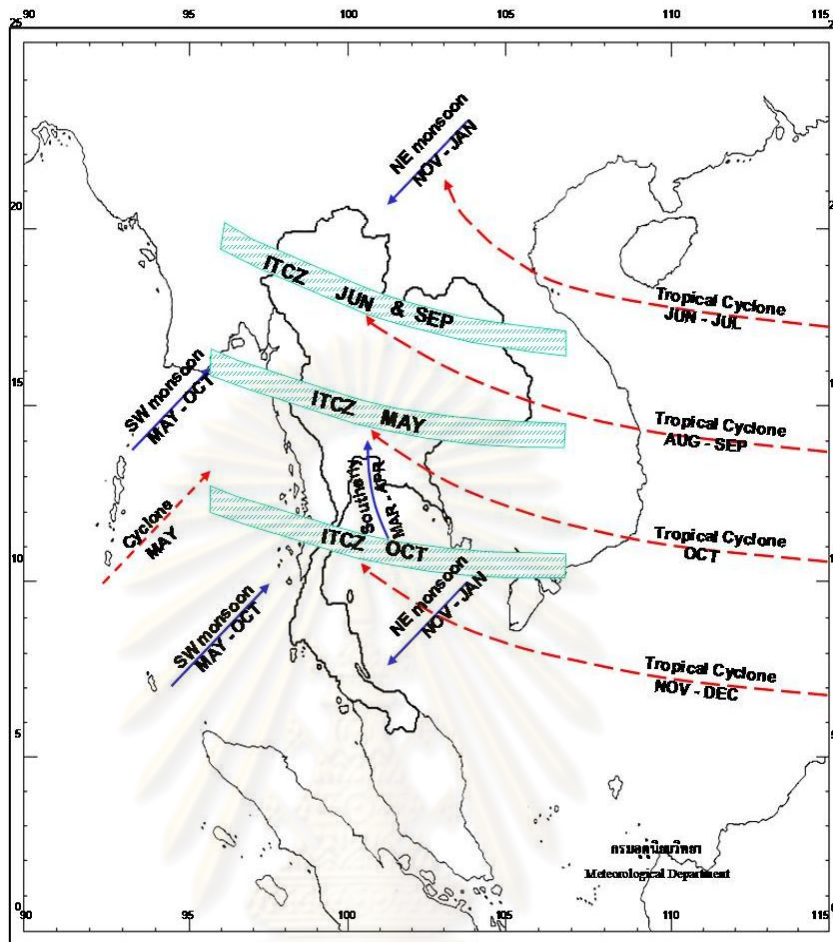


Figure 3-9 The present Monsoon Season and Tropical Storm in Thailand
(Department of Meteorology, Thailand)

3.3.2 Temperature

Thailand is located in the tropical zone and means annual temperatures are therefore $\sim 27^{\circ}\text{C}$. However temperatures vary depending on topography and seasons in the different regions. Highly variable temperatures between day and night, and summer and winter occur in regions that are located inside the continent, such as the upper central region, the upper eastern region, the northern region and northeastern region. The highest temperatures during the summer season are about 40°C in the afternoon and April occur during December to January are the coldest months of the year, with temperatures below 0°C in the high areas of the northern and northeastern regions. Temperatures in nearshore regions vary not much between day and night, or between the summer and winter seasons.

3.3.3 Precipitation

The average annual rainfall over the whole country is 1,572.5 mm. The western and eastern regions are windward areas and experience the highest amount of rainfall. The Khlong Yai district in, Trad province, has for example an average annual rainfall of 4,000 mm. Low precipitation areas are the central part of the northern region and the central region, and the western part of the northeastern region. The western part of northeastern region has lesser rainfall than the eastern part because it is located on the leeward side of the Phu Phan Mountain range and of the west highland margin of the plateau. The southern part has high rainfall almost all year but in summer the western side of peninsular, which is a windward side, has higher rainfall than the eastern side. In winter, the eastern side of the peninsular has higher rainfall than western side because the northeast monsoon that moves across the Gulf of Thailand brings high humidity.

3.3.4 Tropical Cyclones

Thailand occupies an area between two tropical cyclone systems: the Pacific Ocean and the South China Sea to the east and the Gulf of Bengal and the Andaman Sea to the west. Cyclones move over Thailand more frequently from the east than from the west. The average number of cyclones that move over Thailand is 3-4 per year and most often these reach the northern and northeastern regions, especially the upper part of both regions. Tropical cyclones usually move from the west to the northern and northeastern part in May and from the east between June and August. September to October are the months with highest frequency of tropical cyclone. In November and December, tropical cyclones only reach the southern region.

3.3.5 Climate of Northeastern Region and Udon Thani

The tropical savanna climate (Aw) or tropical wet and dry climate is a characteristic for northeastern of Thailand following Köppen's classification. This type of climate is characterized by a long dry season and a prominent but not extraordinary wet season (Khedari et al., 2002). In addition, this region is influenced by the southeast monsoon and

by tropical cyclones from the South China Sea and the Pacific Ocean. Temperatures are generally warm almost all year round.

a) Monsoon characteristics and season

In general, three different seasons can be recognized: The rainy season from May to October with rain spells during June and July. Low pressures and tropical cyclone have high frequencies with late in the rainy season and cause flooding in the region (Figure 9). The winter season in the northeast corresponds to the northeast monsoon which brings cold and dry weather over the region. Temperatures start to drop during late October and remain low until February, with the coldest period in late January (Figure 3-9). The summer season is warm and characterized by tropical cyclone. Temperatures start to rise in March and tropical cyclones occur from late of April to May. Thunderstorms are frequent because of cold air masses from China move southward and converge with local warm air masses.

b) Rainfall and temperature

Instrumental data from the Department of Meteorology of Thailand for 1951-2004 shows that the average annual rainfall in the northeastern region is about 1,410 mm and for Udon Thani Province about 1,455 mm (1951-2008). Figure 3-10 shows that most of the rainfall occurs during August and September (261.9 and 262.5 mm, respectively). The highest rainfall in Udon Thani Province is also during August and September (285.5 and 261.5 mm respectively) (Figure 3-11 and table 3-2) due to the influenced of both the southwest monsoon and tropical cyclones. These cause high relative humidity, relatively low evaporation and moderately high temperatures. In addition, flooding generally occurs in September and October. Parry (1992) shows that the discharge of the Mun River can increase from less than $10 \times 10^7 \text{ m}^3/\text{s}$ during December and April to $280 \times 10^7 \text{ m}^3/\text{s}$ during September and October. December and January are the driest months in the northeast with mean monthly precipitation of about 2.8 and 4.7 mm, respectively (data for 1951-2004). The record for 1951-2008 for Udon Thani shows lowest means monthly minimum rainfall during December and January (2.7 and 6.1 mm respectively).

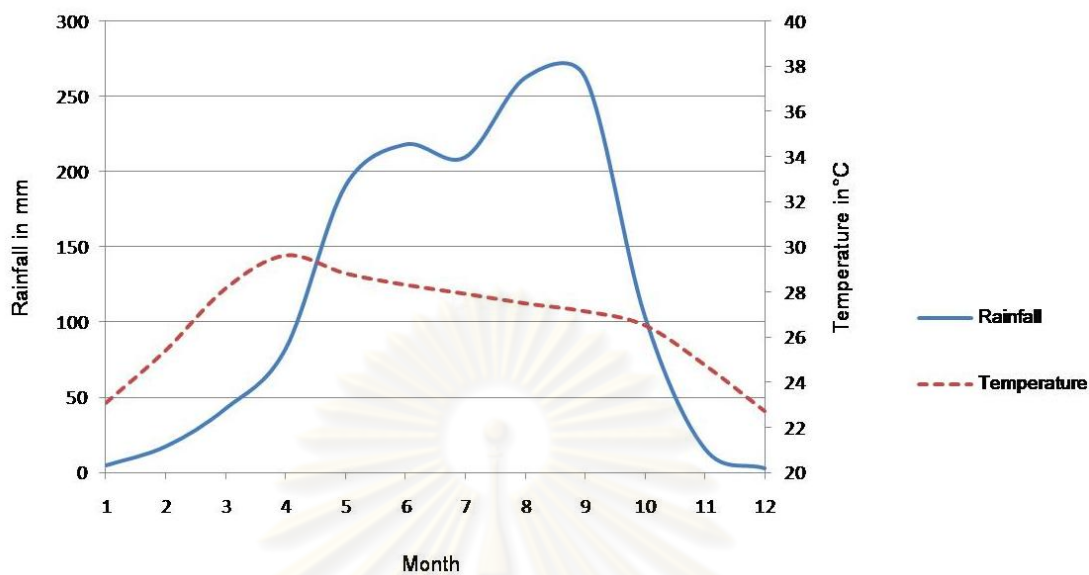


Figure 3-10 Average monthly rainfall and temperature of northeastern Thailand for 1951-2004 (data from Department of Meteorology of Thailand).

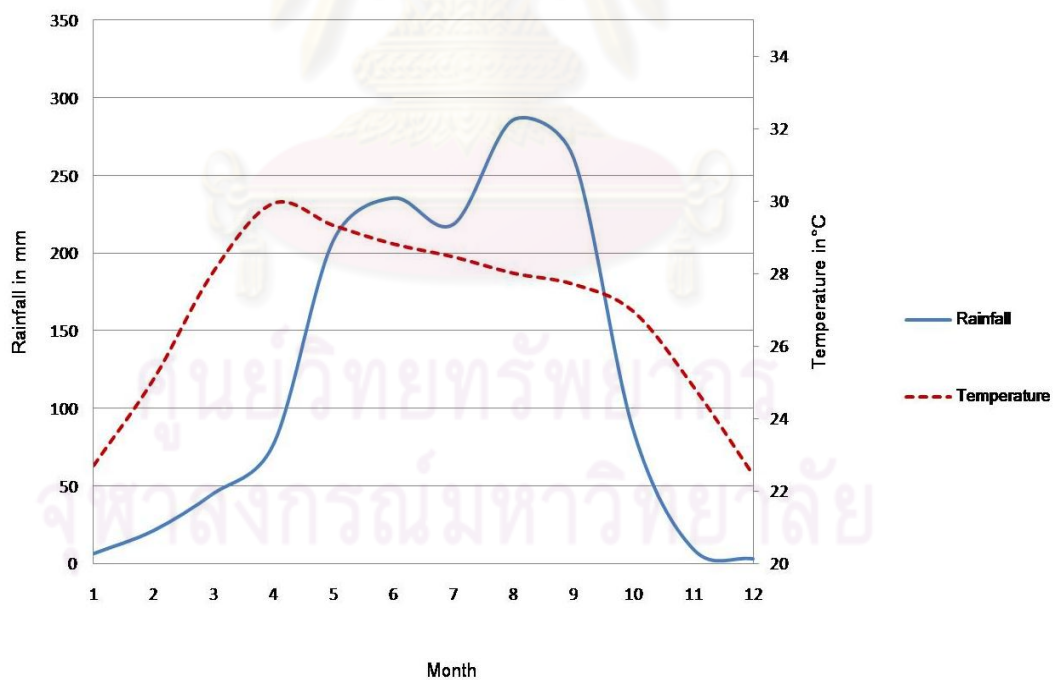


Figure 3-11 Average monthly rainfall and temperature for Udon Thani Province, for 1951-2008 (data from the Department of Meteorology of Thailand).

Table 3-2 Mean monthly temperature and rainfall data for Udon Thani Province, for the years 1951-2008 (Data from Department of Meteorology of Thailand).

<i>Month</i>	<i>Mean Temperature (°C)</i>	<i>Maximum Temperature (°C)</i>	<i>Minimum Temperature (°C)</i>	<i>Mean Precipitation (mm)</i>
January	22.7	29.7	15.7	6.1
February	25.1	32	18.2	21
March	28.1	34.7	21.5	44.9
April	29.9	36	23.9	76.5
May	29.3	34.2	24.5	207.9
June	28.8	32.9	24.8	235.2
July	28.4	32.4	24.6	218.2
August	28	31.7	24.3	285.5
September	27.7	31.5	23.9	261.4
October	26.9	31.3	22.6	85.9
November	24.9	30.4	19.4	9.1
December	22.4	29	15.9	2.7

3.4 Vegetation

Thailand is located between two biogeographical regions, Indochina and Sunda typical (i.e. Malaysia, Sumatra, Borneo and Java). This makes Thailand a center of three important forest elements: Indo-Burmese, Indo-Chinese and Malesian. Plants communications are thus of an Indo-Malayan type and are called Tropical Dry or Deciduous Forest (Udavardy, 1975).

Thailand's floristic regions are divided into seven zones (Smitinand, 1989) according to climate and topography of each region. The biogeographical of Northeastern region occupied the upper Khorat Plateau which is high terrain and low hill with the peaks are about 1,200-1,500 m high i.e. Phu Luang, Phu Kradueng, Phu Ruer and Phu Hin Rong Kla. The plant communities of the Khorat Plateau belong to in the Indo-Chinese zone, which relates to hot and dry climate, a short rainy season and a long dry season. The characteristic of forests in the Northeast region are deciduous dipterocarp forest, coniferous forest, dry evergreen forest and few amounts of hill evergreen forest.

3.4.1 Plant communities of Nong Han Kumphawapi

White (1995) interpreted aerial photographs dating from 1950s (Figure 3-12) and concluded that forests around Nong Han Kumphawapi are mostly deciduous and influenced by soil rather than climate, and that some semi-evergreen and riparian/inundated forests also occur. According to Penny, 1998 the lake is surrounded by an extensive floating herbaceous swamp while a mosaic of floating vegetation mats and sheltered channels cover much of the lake area (Figure 3-13 and 3-14). Penny (1998) cites following species: *Nelumbo nucifera* (Nymphaeaceae), *Ipomoea aquatic* (Onagraceae), *Ludwigia adscendens* (Onagraceae), *Nymphoides indicm* (Menyanthaceae), *Nymphaea lotus* var. *pubescens* and *Salvinia cucullata* (Salviniaceae). In disturbed areas where the lake had been excavated to provide material for the ridge construction, either sedges or *Nelumbo nucifera* tend to occur monospecifically (Penny, 1998). Data from the Office of Natural Resources and Environmental Policy and Planning shows that at least 15 types of hydrophytes were found in Nong Han Kumphawapi. These include submerged plants such as *Hydrilla verticillata*, *Ceratophyllum demersum*; floating plants such as *Eichornia crassipes*, *Ipomoea aquatia*, *Salvinia cucullata*, *Pistia stratiotes*, and *Lemna trisulca*; floating-leaf plants such as *Nelumbo nucifera* Gaertn. (Nymphaceae); emergent plants such as *Scirpus grossus*, *Polygonum chinense*, *Typha angustifolia*, *Eleocharis dulcis*, and *Phragmites-karka*; and herbaceous such as *Schismatoglottis calyptrate*, *Brachiaria mutica*, *Imperata cylindrical*.

The lake is surrounded by paddy fields which used to be flood plains, and other agriculture areas where kenaf (*Abelmoschus manihot* var. *pungens*, Malvaceae), maize (*Zea mays*, Poaceae), cassava (*Manihot esculenta*, Euphorbiaceae), sugar cane (*Saccharum officinarum*, Poaceae), sorghum (*Sorghum vulgare*, Poaceae), castor bean (*Ricinus communis*, Euphorbiaceae), peanut (*Arachis hypogaea*, Papilionaceae), and

sesame (*Sesamum indicum*, Pedaliaceae) are planted (Arbhabhrama et al., 1988; Parnwell, 1988 and Penny, 1998).

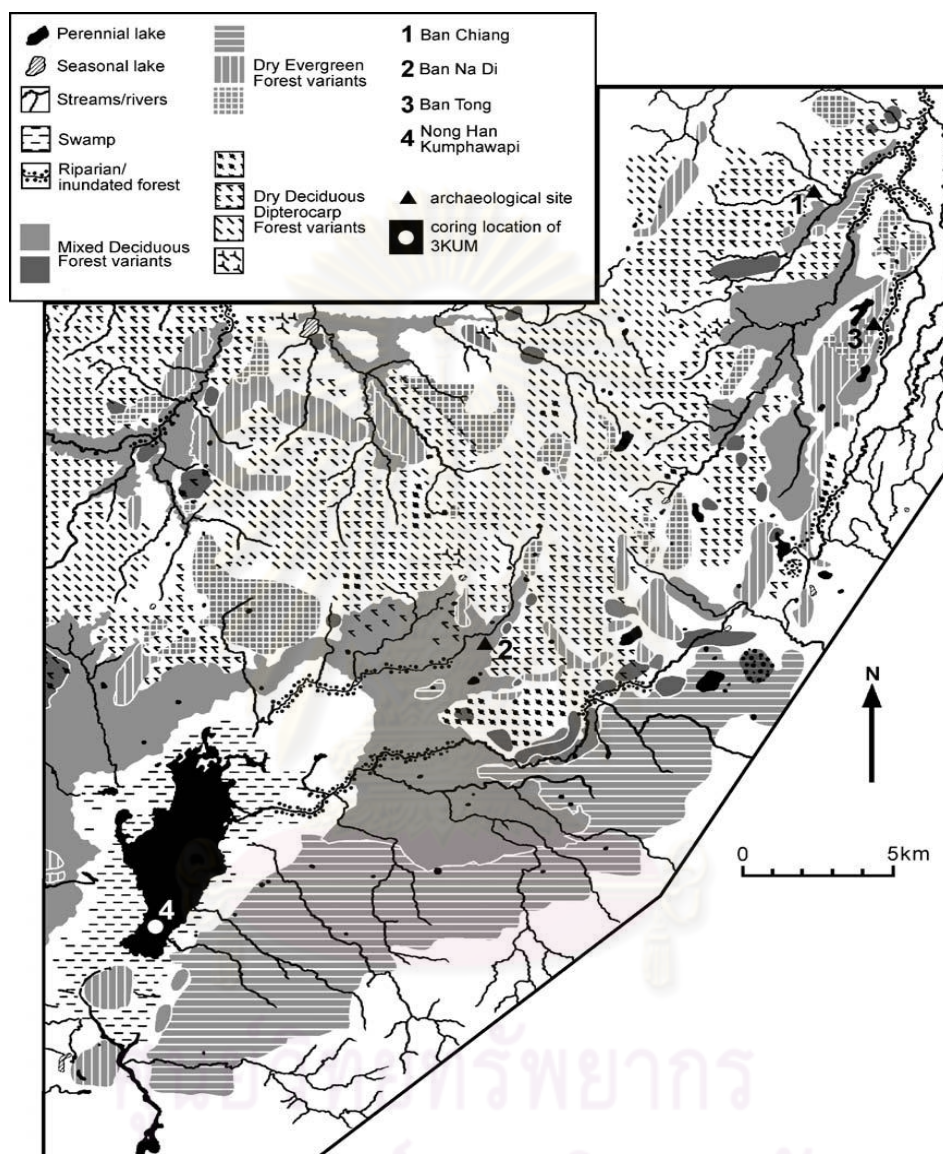


Figure 3-12 Vegetation map of the Ban Chiang/Nong Han Kumphawapi region, prepared by White (2004) based on interpretation of aerial photographs from the 1950s in conjunction with the ethnoecological field research undertaken in 1979–1981 and 1994.



Figure 3-13, 3-14 Photos of Nong Han Kumphawapi and its surrounding.

3.5 Archaeology

The first occupation of the Sakon Nakhon Basin occurred in the 4th millennium B.C. (Higham and Kijngam, 1979). At that time dry deciduous dipterocarp forest covered the area. Both pre-historical and historical sites have been found in the Sakon Nakhon Basin. Ban Chiang is for example one of the important pre-historical sites in Udon Thani Province.

Ban Chiang is located approximately 30 km to the north-east of Kumphawapi in the Upper Song Khram River area, of the Nong Han District. Ban Chiang is famous for its pottery, which has a beige background, and is decorated with dark red spirals. Bronze artefacts are evidence for an early development of metal technology. Ban Chiang seems to have been occupied from ca. 5,600 B.P. to A.D. 200. According to Kijngam and Higham, 1980, Ban Chiang provides a prehistoric sequence, which can be divided into six phases, and dated from 3500 B.C.(5500 B.P.) to 250 A.D., based on changes in pottery style and developments in metal technology. The earliest phases present the use of bronze at the site and iron was present from phase IV (starting c. 1600 B.C or 3600 B.P.) (Table 3-2). Base on the excavation in 1974 and 1975 (conducted by Pisit Charoenwongsa and Chester Goman) the Ban Chiang cultural sequence represents 4,000 years of continuous occupation, from ca. 3,600 B.C. to A.D. 200. and on the basis of ceramic styles, burial rites and soil stratigraphy, the sequence is divided into three periods and dated by thermoluminescence dating: an Early Period from 3,600 to 1,000 B.C. (5,600-3,000 B.P.); a Middle Period from 1,000 to 300 B.C. (3,000-2,300 B.P.); and Late Period from 300 B.C. to A.D. 200 (2,300 B.P. to A.D. 200). White (1986) revised the age of the cultural sequence base on radiocarbon dating and suggested the following division into: An early period, 4,300 to 2,900 B.P.; a Middle Period from 2,900 to 2,300 B.P.; and Late Period from 2,300 B.P. to A.D. 300. However, these dates are still being discussed.

Table 3-3: The Ban Chiang cultural sequences (After Kijngam and Higham, 1980 (Table 1))

Phase	Pottery style	Age yr B.P.	Age ca. B.C.
I and II	Black to grey burnished and incised design	5,600-4,900	c. 3,600-2,900 B.C.
III	Cordmarked vassels with elaborate curvilinear incised design	4,000	c. 2,000 B.C.
IV	Incised and painted pottery	3,600	c.1,600 B.C.
V	Painted pottery	3,000-2,500	c. 1,000-500 B.C.
VI	Red slipped	2,300-1,700	c. 250 B.C.-250 A.D.

Higham and Kijngam (1979) suggested that the Ban Chiang settlement became established near permanent lake and streams and was surrounded by a deciduous dry Dipterocarp forest. During phase I-III, the occupants practiced the slash and burn technique for rice cultivation, hunted and collected and raised domestic pigs, cattle, dog and chickens. Remains of domestic water buffalo and iron which are present in phase IV, seem to indicate wet rice cultivation and ploughing. However, there are still many open questions that need to be answered; 1) Are more site like Ban Chiang present in Northeastern Thailand? 2) What was the nature of the settlement pattern of the Ban Chiang culture? 3) Is there a possibility that the wet rice cultivation developed in the dry Khorat Basin to the south?

In order to answer these questions, Higham and his team (Kijngam and Higham, 1980) undertook intensive site surveys in two areas, of which the first one is at the headwaters of the Lam Pao River in Amphoe Kumphawapi, Udon Thani Province. The other area is located to the south of the confluence of the Lam Pao and Chi rivers in Amphoe Mahasarakham, Mahasarakham Province.

This section will focus on the Kumphawapi study area. The prehistorical sites around Kumphawapi contain inhumation burial, which is related with soil types and rivers.

Prehistoric settlements in the area were usually not on the flood plain but on the so-called Low terrace (Roi Et sandy loam soils). Many small streams drain into the Low Terrace, which has fertilized soil suitable for rice cultivation. No prehistoric settlements have been discovered on the Middle or High terrace (Khorat soils) and in the Lam Pao River valley. The distribution pattern shows a fairly dense network of sites but all these certainly not contemporary. The author (Kijngam and Higham, 1980) suggests that the early prehistoric sites may have occupied the margins of the Kumphawapi flood plain and that later sites occupied the more hazardous terrain nearer to the lake (Figure 3-15). Thus, the movement of the settlements could reflect a developing water control method or pressure by expanding population (Higham and Kijngam, 1980). However, the fieldwork report (Kijngam and Higham, 1980) shows the lack of Ban Chiang painted pottery (phase V, c. 1,000-500 B.C. or 3,000-2500 B.P.) in Kumphawapi flood plain sites. The evidence is based on the excavation of three sites in Amphoe Nong Han and Amphoe Kumphawapi;

- 1) Non Kao Noi, The five inhumation burials and curvilinear incised pottery characteristic of Ban Chiang phase III (c. 2,000 B.C or 4,000 B.P.) were found in this site.
- 2) Ban Na Di yielded 11 inhumation burials, which occupied an area of around 1.5 hectares and which were situated on low terrace rice soils. These soils are dependent on wet season flooding from nearby Lake Kumphawapi. Ban Na Di was first occupied during the equivalent of Ban Chiang phase III. There are in-situ concentrations of charcoal, which can be dated back to around 1,400-1,500 B.C. or 3400-3500 B.P. (Kijngam et al., 1980). In addition, the first remains of iron were found in c. 600 B.C. (2,600 B.P.). Numerous rice grains, aquatic resources, cattle, dog and chickens were always found during the main

mortuary phase, but water buffalos were only present from c. 600 B.C. or 2,600 B.P. onwards.

- 3) Ban Muang Phruk yielded only one burial, but the red slipped pottery that closest parallels with the pottery style of Ban Chiang phase VI (c. 250 B.C.-250 A.D. or 2,200-1,700 B.P.) was found.

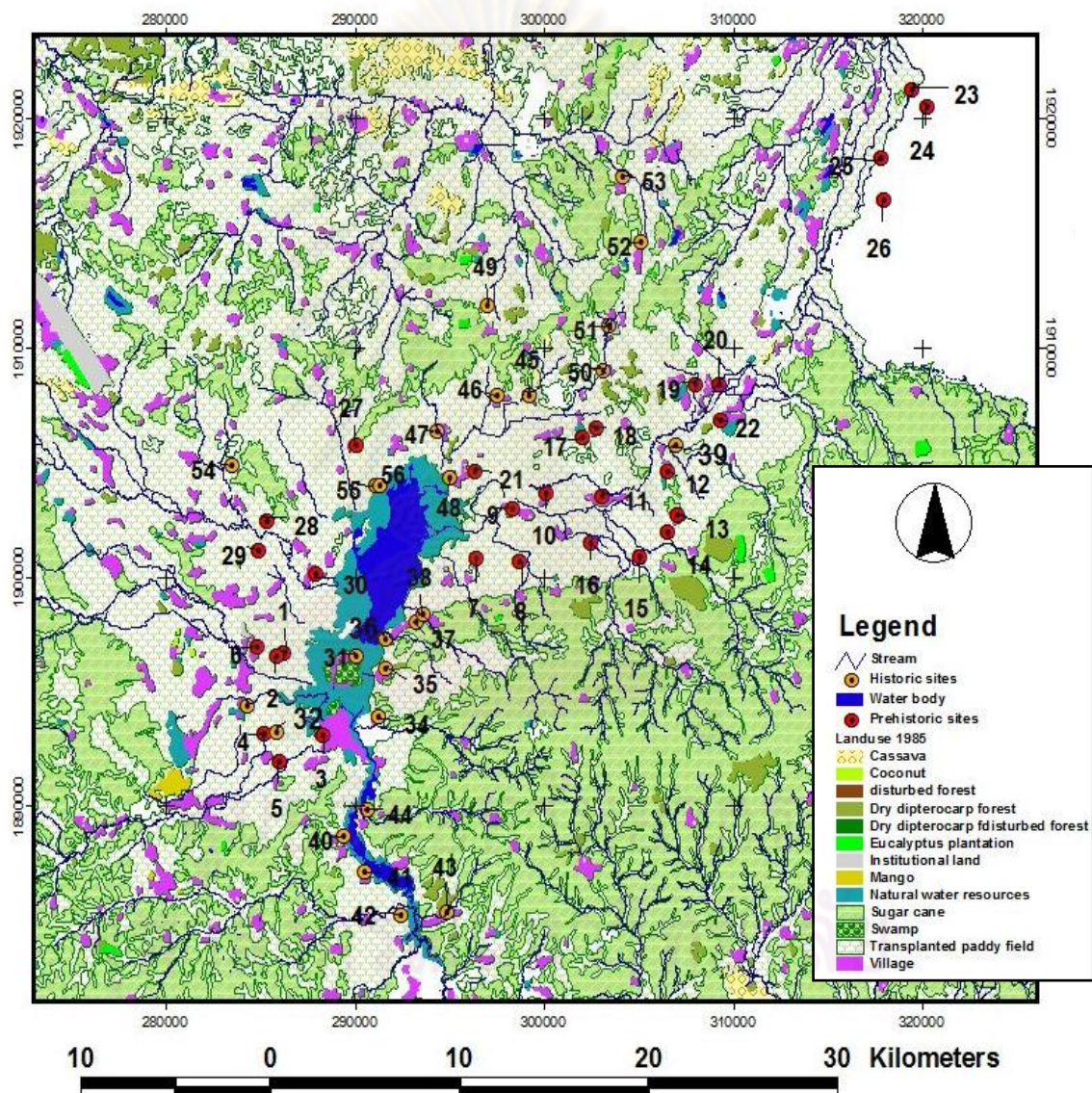


Figure 3-15 Historic and prehistoric sites around Nong Han Kumphawapi.

The data above may lead to these hypotheses: 1) The areas excavated around the Kumphawapi were not occupied during Ban Chiang phases IV and V., or 2) The people living there did not share the Songkhram Valley tradition of richly painted funeral pottery styles. 3) The Songkhram – Lam Pao watershed formed was a cultural division during parts of Ban Chiang sequence.

According to Boonlop and Bubpha, 2009, the report of the Ban Chiang Cultural Tradition Research Project conducted by Bannaurag et al (1992) from the Thai Fine Arts Department (FAD) divided the Ban Chiang Culture into seven clusters:

1. *Nam Suai cluster* is located at the boundary of Pen district, Udon Thani Province and contains three sites, but only Ban Pone has been excavated (Boonlop, 1999).
2. *The Upper Huai Dan cluster* includes 21 sites in Muang and Nong Han Districts of Udon Thani Province. All the excavated sites are located in the Nong Han District and include Ban Pak Top (Schauffler, 1976), Ban Non Na Sang and Ban Sa Beang (Srisuchart and Thosarat, 1976; Bannanurag and Bamrungwong, 1991).
3. *The Upper Song Khram cluster* comprises 15 sites, located between Udon Thani and Sakon Nakhon Provinces. Only five sites have been excavated in Nong Han District; Ban Chiang, Ban Om-Kaew, Ban Thatu, Ban Tong and Non Khi Kling in Ban Nong Sa Pla (FAD, 1988; Bannanurag and Bamrungwong, 1991)
4. *Huai Luang – Mae Nan Song Khram cluster* is located along the Huai Tuan catchments, the tributary of Mae Nam Song Khram. Here 12 sites have been discovered but only one site Ban Dung in Ban Dung District, Udon Thani Province, has been excavated.
5. *Huai Yam – Upper Huai Pla Hang Cluster* is the densest cluster and including

37 sites. Of these only Ban Sang Du in the Waeng Pittayakhom school area has been excavated (Bannanurag and Bamrungwong, 1991).

6. *Huai San Jod cluster* contains six sites were discovered in the Sawang Daen Din Diatrict of Sakon Nakhon Province. Only two of these have been excavated these are Ban Don Thong Chai (FAD, 1994; Kijchotprasert, 1998) and Ban Khok Khon (Boonlop, 1999).
7. *Nong Han Kumphawapi Lake cluster* comprises 29 sites around the lake, located in Kumphawapi and Chaiwan Districts of Udon Thani Province. Ban Muang Pruek and Non Kao Noi, approximately 17 and 2.25 km to the east of the lake, respectively) have been excavated (FAD, 1994; Bannanurag and Bamrungwong, 1991). These two sites have pre-historical inhumation burials. Moreover, there are a number of sites which are coeval with the early Period at Ban Chiang such as: Ban Tong, Non Khi Kling, Ban Pak Top, Ban Don Kaen, Ban Yang, Non Kao Noi (Kijngam et al., 1980; Higham & Kijngam, 1984). Sema stones or Boundary Stones have been found at the Ban Don Kaeo salt dome and can date back to approximately AD 800 based on the presence of Mon inscriptions. Given the proximity of sites such as Ban Na Di, which is one of the most important sites in the Nong Han Kumphawapi Lake cluster and which is located only 8 km to the northeast of the lake was an important resource for Early Period populations in the region, particularly during the winter monsoon when other water resources may not have been available. Rice was however probably not cultivated close to the lakeshore, and prehistoric populations may have only made use of wild rice. It is however obvious that 30 km from Nong Han Kumphawapi, human populations have been present from at least the third millennium BC, and possibly earlier (White, 1995; cited in Penny, 1998).

CHAPTER IV

METHODOLOGY

4.1 Map reconstruction

Satellite image data and aerial photo interpretations were done by using software of geographic information system (GIS) and remote sensing (ArcGIS 9.2 and ERDAS IMAGINE 8.5). The topographic, land use, soil and geology maps were used to reconstruct paleogeography of the area. GIS technique was used to reconstruct geomorphic map of the study area and are applied in developing, manipulating, and analyzing the digital data .

The map reconstruction procedure was done as outlined below:

1) Data collection step:

Collection of existing data (collection of existing maps and reports with relevant data) (Table 4-1)

Table 4-1 Data collection

Data type (Source)	Acquisition year	Remark
Aerial photo (Royal Thai survey)	1951	before the dam was built
	1996	after the dam was built
Vegetation map (White, 2004)	1954	Interpreted from aerial photo
Soil and soil utilization (Land and land development Department)		scale 1:25000 in shape file
Landuse (Land and land development Department)	1985, 2001 and 2009	scale 1:25000 in shape file
Geomorphic map (Kijngam and Higham, 1982)		reported after 1980-1981 archaeology site survey
GIS base map of Udon Thani (Land and land development Department)	1985	

- 2) Aerial photo interpretation (Interpreted lake boundary) based on aerial photos from the 1954 and 1996.
- 3) Create Landuse/ land cover map with the data from Land and land development Department. Compare the results with Vegetation map which is reported by White, 2004.
- 4) Create thematic map (soil map, land form map) and Digital Elevation Model (DEM) from the GIS base map of Udon Thani.
- 5) Combining all data (lake boundary, landuse map, soil and soil utilized map ,DEM and old geomorphic map) to generate paleogeographic map.
- 6) Add the data from archaeology site survey to generate a historical settlement in the paleogeographic map.
- 8) Present output maps.

4.2 Field investigation

We first surveyed the surroundings of Nong Han Kumphawapi based on the L7017 series 1:50000 map to find a good place from where to access the lake. Prior to coring we measured the water depth and tested the sediment depth. The coordinates of the best spots were stored in a GPS. For coring we used a zodiac (Figure 4-1) with a specially constructed platform with space for 3-4 persons and the equipment. In addition, for stabilizing and anchoring the zodiac during the coring operation we used 3-4 bamboo poles. Sediment cores were collected with a Russian corer (Figure 4-2) (chamber Ø: 10 cm and 7.5 cm, chamber length: 1 m) with 0.5 m overlap. Coring was made along several transects to be able to follow the different layers over longer distances. The most complete sequence was selected for high-resolution multi-proxy sub-sampling in the laboratory. The fieldwork and laboratory analyses procedure diagram are shown as follow (Figure 4-3)



Figure 4-1 The Zodiac boat with special platform.



Figure 4-2 Russian corer with lake sediment

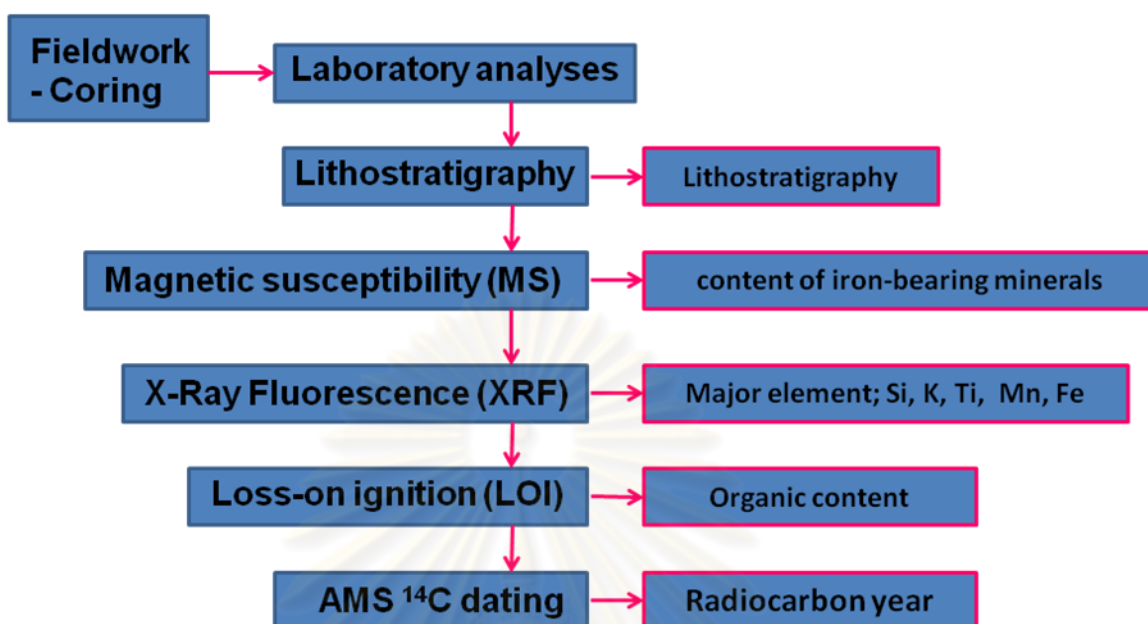


Figure 4-3 Fieldwork and laboratory analyses diagram

4.3 Laboratory analyses

4.3.1 Lithostratigraphy

The lithostratigraphy was carefully described (Figure 4-4) by its physical properties, by following a Swedish classification system, introduced by Hampus von Post (1862). Sediments with an organic content of >30% are defined as gyttja, clay gyttja has an organic content of 6-30% and gyttja clay an organic content of 3-6%. Gyttja is a freshwater deposit (mud) consisting of organic and mineral matter found at the bottom or near the shores of lakes. Hampus von Post (1862) defines a term of gyttja as a light-colored coprogenic deposit consisting of a mixture of plankton particles, mollusk shells, chitin remains from the exoskeletons of insects, pollen and spores of higher plants, and mineral particles, formed in eutrophic water bodies.



Figure 4-4 Process of describing stratigraphies in the laboratory.

4.3.2 Magnetic Susceptibility

Magnetic Susceptibility is the magnetization of a material per unit applied field and describes the magnetic response of a substance to an applied magnetic field (Britannica Encyclopedia). If the ratio of magnetization is expressed per unit volume, volume susceptibility is defined as:

$$K = M / H$$

Magnetic volume susceptibility, commonly symbolized by **K**, is equal to the ratio of the volume magnetization of the material **M** and **H** is the applied external magnetic field strength (Blum, 1997).

Material can be classified into five categories of magnetic behavior according to their magnetic properties; ferromagnetism, ferrimagnetism, canted-antiferromagnetism,

paramagnetic and diamagnetic (Dearing, 1994). Each of these 5 groups shows different reactions when attracted by an external applied magnetic field. Ferromagnetic material is almost pure iron. The magnetic moments are highly ordered and aligned in the same direction and magnetic susceptibility is very high but these will not normally be found in the natural environment. Ferrimagnetism forms the most important kind of magnetic behavior in natural material. The magnetic moments of this group are strongly aligned, but exist as two opposing sets with unequal forces controlled by the crystal lattice structure of certain minerals. Magnetite and a few other Fe-bearing minerals are included in this group. These can be found in igneous and sedimentary rocks and also in nearly all soils. They have high magnetic susceptibility values. Canted-antiferromagnetic material has lower magnetic susceptibility values. Its structure gives rise to well-aligned but opposing magnetic moments, but forces virtually cancel each other out. Haematite is the most common and one of a few iron minerals in this category. All metals and minerals in these three magnetic groups can retain a permanent magnetic field and remain aligned even after the absence of the external magnetic field (Figure 4-5).

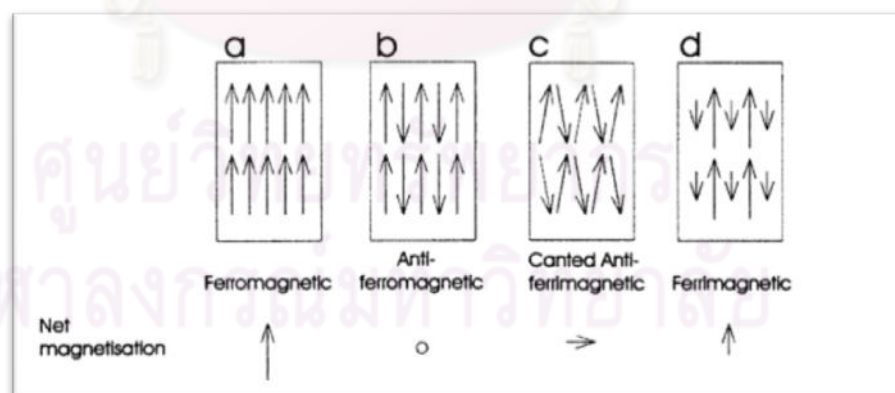


Figure 4-5 Schematic representation of the distribution of magnetization vectors in ferromagnetic materials, (a) ferromagnetic, (b) antiferromagnetic, (c) canted-antiferromagnetic (d) ferromagnetic (Sandgren and Snowball, 2002; McElhinny, 1973)

Paramagnetic matter includes Mn and Fe ions. A large number of minerals normally contain Mn and Fe, and are very common in rocks and soils (e.g. biotite, pyrite, olivine, pyroxene, garnet and carbonates containing iron and manganese) (Sandgren and Snowball, 2002). Their magnetic susceptibility values are weaker and magnetic moments are only aligned in the presence of a magnetic field. Diamagnetism has weak and negative values of magnetic susceptibility and includes non-iron minerals (e.g. quartz, calcium carbonate, feldspar and calcite) and non-mineral diamagnetic substances (e.g. organic matter and water). Consequently, the sum of all the magnetic susceptibility of the ferromagnetic, canted antiferromagnetic, paramagnetic materials and diamagnetic components represents the magnetic susceptibility of sediment material (Dearing, 1994). The susceptibility values of some common minerals and rocks are shown in the Table 4-2:

Table 4-2 Susceptibility values of common minerals and rocks

	κ (10^{-6} SI)	χ (10^{-8} m ³ /kg)
Non-iron-bearing		
Plastic (e.g., perspex, PVC)	~-5	~-0.5
Ice or water	-9	-1/-0.9
Calcite	-7.5 to -39	-0.3 to -1.4
Quartz, feldspar, magnesite	-13 to -17	-0.5 to -0.6
Kaolinite	-50	-2
Halite, gypsum, anhydrite	-10 to -60	-0.5 to -2.0
Serpentinite	3,100 to 75,000	120 to 2,900
Iron-bearing minerals		
Illite, montmorillonite	330 to 410	<u>5</u> to 13 to <u>15</u>
Biotite	1,500 to 2,900	<u>5</u> to 52 to <u>95</u> to 98
Orthopyroxene, olivines, amphiboles	1,500 to 1,800	<u>1</u> to 43 to 50 to <u>130</u>
Goethite ^a	1,100 to 12,000	26 to <u>70</u> to 280
Franklinites	450,000	8,700
Iron ^a	3,900,000	50,000 to <u>2,000,000</u>
Iron sulfides		
Chalcopyrite	23 to 400	0.6 to <u>3</u> to 10
Pyrite	35-5,000	1 to <u>30</u> to 100
Pyrrhotites ^a	460 to 1,400,000	10 to <u>5,000</u> to 30,000

Iron-titanium oxides		
Hematite ^a	500 to 40,000	10 to <u>60</u> to 760
Maghemite ^a	2,000,000 to 2,500,000	<u>40,000</u> to 50,000
Ilmenite ^a	2,200 to 3,800,000	46 to <u>200</u> to 80,000
Magnetite ^a	1,000,000 to 5,700,000	20,000 to <u>50,000</u> to 110,000
Titanomagnetite	130,000 to 620,000	2,500 to 12,000
Titanomaghemite	2,200,000	57,000
Ulvospinel	4,800	100
Average rock values		
Sandstones, shales, limestones	0 to 25,000	0 to 1,200
Dolomite	-10 to -940	-1 to -41
Clay	170 to 250	10 to 15
Coal	25	1.9
Basalt, diabase	250 to 180,000	8.4 - 6,100
Gabbro	1,000 to 90,000	26 to 3,000
Peridotite	96,000 to 200,000	3,000 to 6,200
Granite	0 to 50,000	0 to 1,900
Rhyolite	250 to 38,000	10 to 1,500
Amphibolite	750	25
Gneiss	0 to 25,000	0 to 900
Slate	0 to 38,000	0 to 1,400
Schist, phyllite	26 to 3,000	1 to 110
Serpentine	3,100 to 18,000	110 to 630
^a Remanence-carrying minerals		

Magnetic susceptibility is commonly used as an indicator for variations in lake sediment composition, especially regarding the content of iron-bearing minerals. Most fresh water lake derives their magnetic minerals from many catchment erosion (bedrock, subsoil, and topsoil) and in lake processes. The magnetic susceptibility records can indirectly be linked to paleoclimatic and paleoenvironmental change, and/or human activity in the catchment, because erosion and weathering processes as well as transport and deposition of lake sediments is strongly related to these factors. The type, concentration

and grain size of magnetic minerals found in lake sediments vary according to processes operating in response to changes in climate, human activity and lake status changes (Sandgren and Snowball, 2002).

All materials can be classified according to their magnetic properties during and after they have been attracted by an external magnetic field. If magnetic susceptibility values are positive the material magnetic material can be paramagnetic, ferromagnetic, ferrimagnetic, or antiferromagnetic. Alternatively, if magnetic susceptibility values are negative the material is diamagnetic because the material has a weak magnetic field.

Logging of magnetic susceptibility is one of the standard non-destructive methods to determine changes in the magnetic record of sediment over depth and is expressed in S.I. units. These measurements are extremely useful to correlate stratigraphies derived from different parallel cores and overlapping cores. The advantages of this method can be summarized as follows:

- Measurement can be made on all materials
- Measurements are safe, fast and non-destructive
- Measurements can be made in the laboratory or field with minimal training
- Measurements complement many other types of environmental analyses

4.3.2.1 The multi sensor core logger device

Core loggers are usually controlled by a computer and include a conveyor system with a track motor that moves the sediment core along different stationary sensors in equal steps (Figure 4-6). In this study, a magnetic susceptibility point sensor was used for logging of split cores. The point sensor moves up and down to the sediment surface with spatial resolutions of better than 5 mm. While the point sensor moves down to the sediment surface, an oscillator circuit in the sensor

produces a low intensity (approx. 80 A/m RMS) non-saturating, alternating magnetic field (0.565 kHz for the MS2C sensor and 2 kHz for the MS2E sensor). Any material in the near vicinity of the sensor, that has a magnetic susceptibility, will cause a change in the oscillator frequency. The electronics convert this pulsed frequency information into magnetic susceptibility values (Geotek).

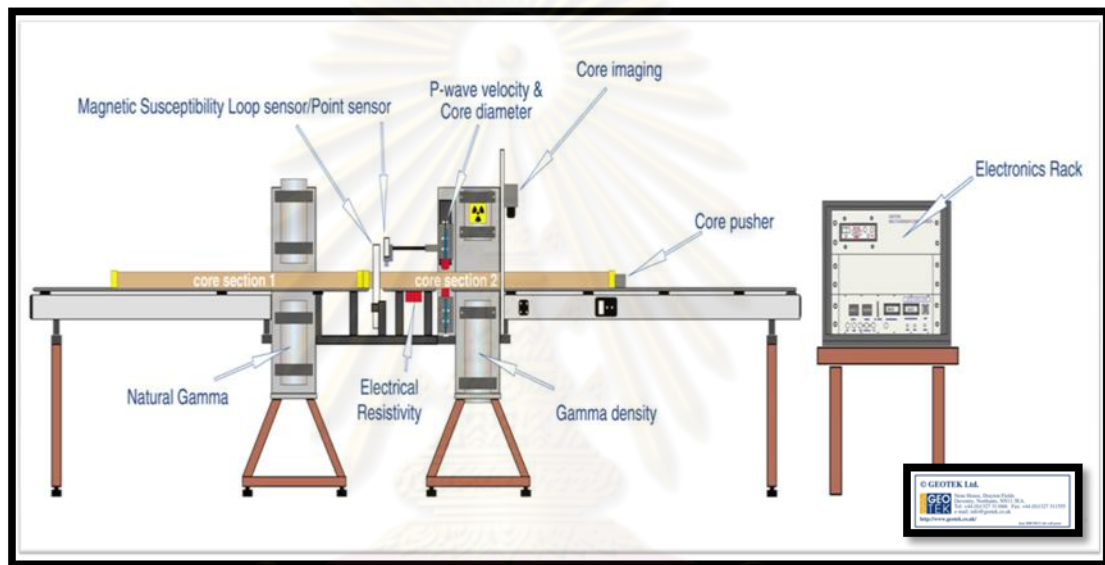


Figure 4-6 The multi-sensor core logger device used in this study. Only the magnetic susceptibility point sensor (after Zolitschka et al., 2001) for logging of split cores was used.

The magnetic susceptibility sensor is electronically set to measure a single standard sample of a stable iron oxide which has been tested and analysed by the manufacturer (Bartington Instruments Ltd.). Therefore, all magnetic susceptibility sensors supplied should record exactly the same value for any given sample, and that value should be the same as a measurement made on a different measuring system. In that sense the magnetic susceptibility system is calibrated absolutely. Since the calibration has been set electronically it should not alter. A calibration sample is provided which can be used to check the long term consistency of the

calibration. The data obtained from the magnetic susceptibility system provides uncorrected, volume specific magnetic susceptibility, which can be converted to either corrected volume specific magnetic susceptibility or mass specific magnetic susceptibility automatically in the Geotek MSCL software.

Split-core logging means a half-cylinder shape sediment core is logged. The Split-core logging steps are shown below.

1. Carefully clean the core surface.
2. Wrap sediment surface with transparent thin plastic film to avoid contamination from the sensor.
3. Adjust the distance between sensor and sediment to the appropriate position which should not be too far or too close. This will reduce the error of the results.
4. Set the frequency of the sensor to measure every 2 cm along the entire core.



ศูนย์วิทยทรัพยากร
จุฬาลงกรณ์มหาวิทยาลัย

4.3.3 X-ray fluorescence (XRF) analysis

X-ray fluorescence analysis (XRF) is a method to determine the composition of an unknown material. By using an x-ray tube or a radioactive source x-rays are produced to incident on the atom and can either be scattered or absorbed through the material. The scattering of the electron can be described by a Compton Scattering process (Figure 4-7). During the absorption process, the x-ray will transfer all of its energy to the atom. When there is enough energy in the incident photon to overcome the atom's work function, the innermost electron is emitted. The result of the absorption is emission of an electron from an innermost shell in the atom which is called the photoelectric effect and the emitted electron is called a photo electron.

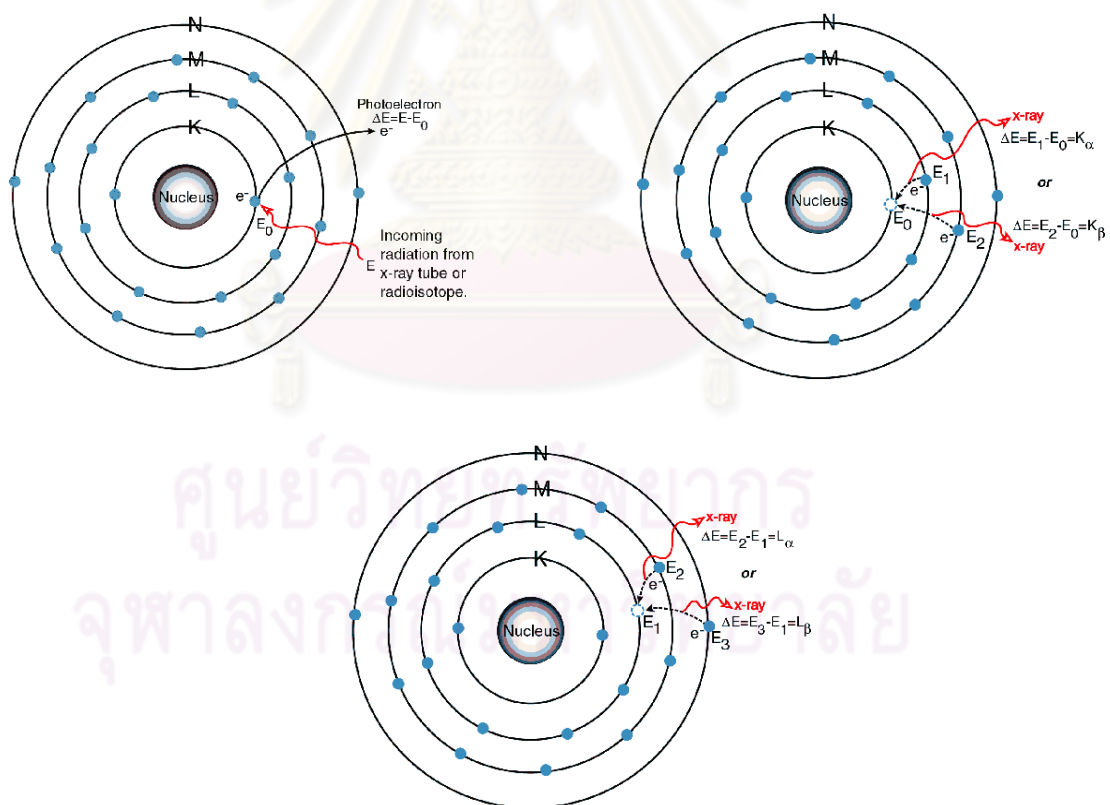


Figure 4-7 The Compton scattering process

After the emission, the atom becomes unstable and an electron in the outer shell moves to the inner vacancy to re-stabilize the atom. This process will emit a secondary x-ray which is from an energy difference between the binding energy of the shells. Since energy level of the secondary x-ray is unique for each atom, the study of these secondary x-rays is a non destructive way to determine the type of atom.

4.3.4.1 The ITRAX core scanner

X-ray Fluorescence Analysis was performed with the ITRAX core scanner (Figure 4-8), at the Department of Geological Sciences at Stockholm University. XRF Core scanning is non-destructive provides, high resolution geochemical records for terrestrial and marine sediments and drilled rock cores (Croudace et. al, 2006). The ITRAX can measure split sediment cores of up to 1.8 meters length and at a resolution as fine as 200 μm . It also can produces optical and X-radiographic images which are useful for guiding sample selection for further detailed sampling.

a) Scanning procedure and control software

The standard ITRAX procedure runs the following steps shown below (Table 4-3 (Croudace et. al, 2006)):

1. Loading a split sediment core onto a horizontal cradle with core top position to the right.
2. Scanning is initiated from the software and follows a logical and guided sequence involving inputs:
 - (i) To define the core length to be scanned
 - (ii) Setting the excitation voltage and current to the X-ray tube
 - (iii) Initiating a surface topographic scan of the core. This topographic scan is made in relation to a horizontal reference plane and is used to ensure

that any subsequent positioning of the XRF detector does not lead to a collision of the detector with the sediment surface and, importantly, that the detector-sample distance is monitored and remains constant. The scanning occurs by a regular left to right incremental movement of the core perpendicular to the long axis of the rectangular beam. This initial scan takes approximately 5 min after which the core is automatically returned to its start position.

- (iv) Involves defining the likely elements in the sample from a periodic table as well as adjusting and refining the peak-fitting parameters using one or more representative parts of the core sample. This optimization takes place with the operator ensuring that the best peak-fitting functions are chosen.
- (v) To record a reference response for the X-radiographic detector by automatically driving the core out of the path of the X-ray beam. This step calibrates and normalizes the response of the X-ray line camera diode array and takes approximately 1 min after which the core is returned to its start position.
- (vi) The final step in the Navigator panel is to enter the Batch Analysis Mode where the user defines the core name, reviews instrument count times, dwell times and scan
- (vii) Limits before starting the scan process.

Table 4-3 The standard ITRAX procedure.

Operator task or input	Result
Load split sediment core on to horizontal sample cradle	Sample ready for scanning
Define kV and mA setting for 3 kW Mo X-ray tube	Excitation condition set
Define core dimension to be scanned	Dimensional limits set for scanning
Initiate surface scanning/photographic procedure (approximately 5 min)	Surface topography profile determined and digital photographic image of core captured
Enter the scan increment size and the dwell time for the radiographic scan	Radiographic parameters set ready for the radiographic scan
Establish XRF parameters and select the elements likely to be present	Elements selected and spectral-fitting parameters refined
Set reference response for the radiographic camera by automatically removing the core from the X-ray beam	Calibration of the X-ray line camera diode array
Enter dialogue menu where data file storage locations are named and the XRF count time defined	Automated process commences with the acquisition of an incremental (digital) radiographic scan. The core is then returned to zero ready for next stage
Instrument commences XRF analysis	Incremental XRF scans acquired and stored

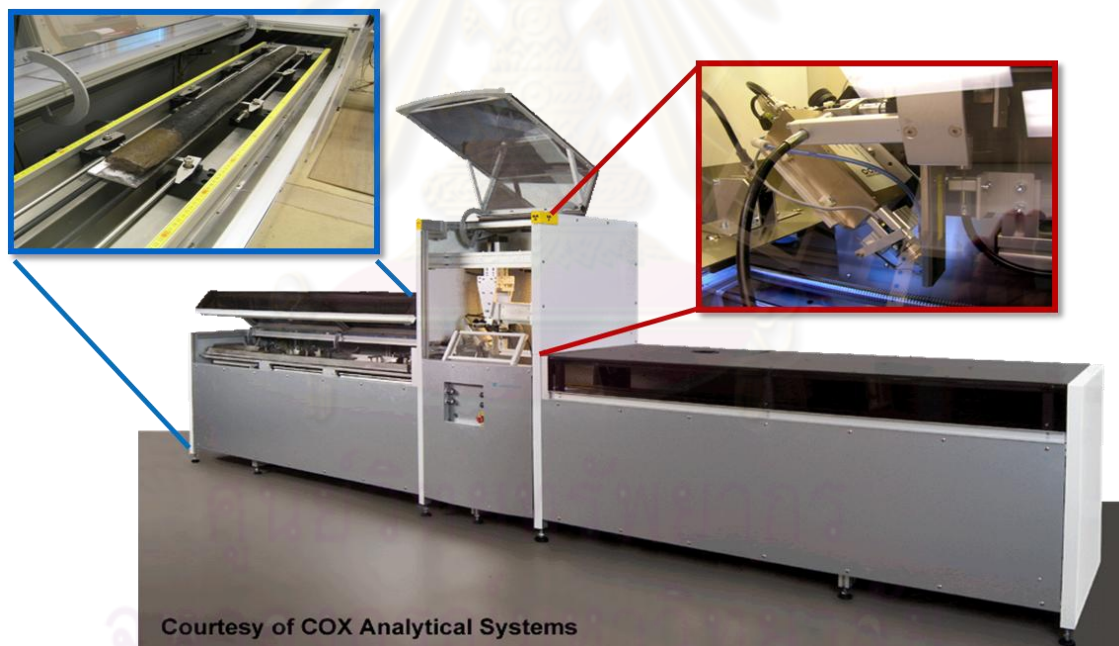


Figure 4-8 The Itrax core scanner

4.3.4 Loss on ignition (LOI)

Loss on ignition analysis is an inexpensive and simple method to investigate past environmental changes in lake sediments. Climatic changes can influence sediment composition, which is controlled by factors such as productivity, inorganic inputs, and decomposition and also influence the patterns of sediment accumulation which is controlled by factors such as basin morphology and water level. The LOI method allows estimating the organic matter and carbonates contents of lake sediments, and thus gives information about the nature of the sediment and sediment sources. It is expressed as percentage of the dry weight of each sample.

LOI is based on differential thermal analysis. Organic matter begins to ignite at about 200°C and is completely depleted at about 500°C. Carbonate minerals are destroyed between 700-950°C. The conditions of using the LOI method depend on the ignition temperature and on the length of time of ignition which may influence the results (Heiri et al., 2001). In this study, the organic content is estimated from weight loss-on-ignition at 550°C, following Dean (1974). Carbonate (CO₂ evolved from carbonate minerals) content is estimated from weight loss-on-ignition at 950°C (Dean, 1974; Bengtsson and Enell, 1986; Heiri, 2001).

4.3.4.1 Loss on ignition analysis step

LOI analysis was performed on 379 samples from coring point KMP-CP3A. These were sampled in contiguous 1 cm increments and had a volume of ca. 3 cm³. The analysis in this study was done as outlined below (Figure 4-9 a-d).

In the preparation step, crucibles were cleaned and dried by heating them overnight in an oven at 105°C.

- a) The crucibles were then placed in a desiccator for 2 hours and weighed. The sediment samples were subsequently placed in the crucibles, which were weighed again. Crucibles and sediment samples were then dried in an oven at 105°C overnight, placed in the desiccator for 4 hours, and re-weighed.

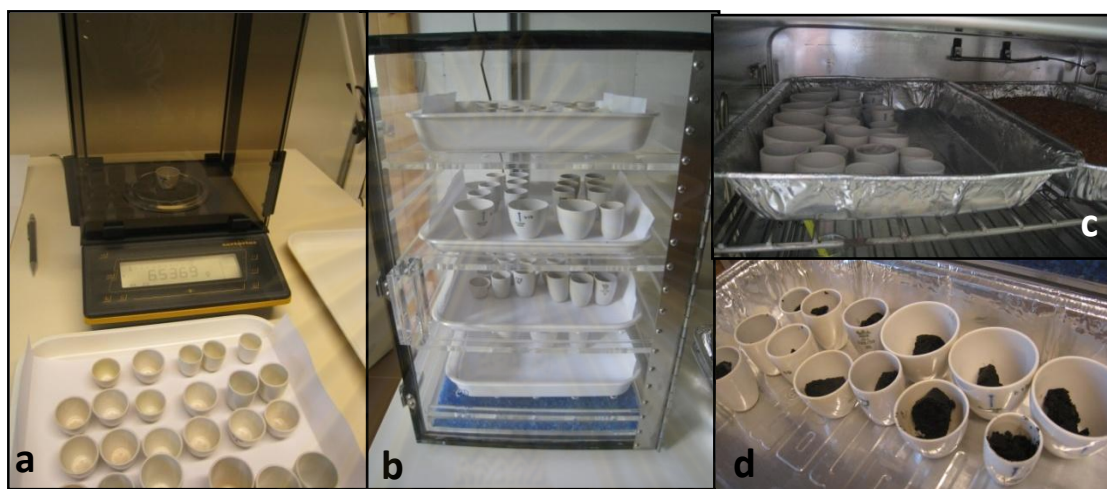


Figure 4-9 a-d: The different preparation steps.

- b) In a first step of the LOI reaction, organic matter was combusted to ash and carbon dioxide at temperatures of between 500 – 550°C. In this study, crucibles (with samples) were dried in a muffle furnace at 550°C (Dean, 1974; Bengtsson and Enell, 1986) for 4 hours. After burning they were placed in a desiccator for 2 hours and re-weighed.

LOI % was calculated by using the equation below:

$$LOI_{550} = \frac{(DW_{105} - DW_{550})}{DW_{105}} \times 100$$

LOI_{550} = LOI at 550°C as percentage

DW_{105} = Dry weight before the first combustion (The sediment's constant weight)

DW_{550} = Dry weight after heating to 550°C

[g]



Figure 4-10 A muffle furnace

- c) In a second step, carbonate was combusted at a temperature of 950°C. For this the crucibles (with samples) were dried in a muffle furnace (Figure 4-10) at 950°C for 4 hours, placed in a desiccator for 2 hours and re-weighed. LOI % was calculated by using the equation below:

$$LOI_{950} = \frac{(DW_{550} - DW_{950})}{DW_{105}} \times 100$$

LOI_{950} = LOI at 950°C as percentage

DW_{105} = Dry weight before the first combustion (The sediment's constant weight)

DW_{550} = Dry weight after heating to 550°C

DW_{950} = Dry weight after heating to 950°C

[g]

4.3.5 Radiocarbon Dating

4.3.5.1 Introduction

Radiocarbon dating is one of the most widely used of all radiometric techniques which are usually employed as a chronostratigraphic technique in paleolimnology. It allows precise age control of lake-sediment sequences and thus enables comparisons and correlations on local, regional and global scales. Lake sediments usually contain certain amounts of organic carbon in form of terrestrial, telmatic and limnic plant and animal debris which are suitable for radiocarbon dating (Björck and Wohlfarth, 2001). Radiocarbon dating reveals an estimated age of formerly living organisms by measuring the proportion of the carbon-14 isotope ^{14}C ($T_{1/2}=5730$ yr) in their carbon content. The maximum measurable age of organic materials is up to about 50,000 years.

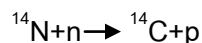
This method was invented in 1951 by W. F. Libby, an American chemistry professor. There are many textbooks, journals and articles which discuss the background and principles of radiocarbon dating (see e.g., Walker, 2005; Björck and Wohlfarth, 2001). The principles and limitations of the radiocarbon method will be briefly reviewed below.

Carbon has three principle isotopes which occur naturally: ^{12}C , ^{13}C and ^{14}C . ^{12}C and ^{13}C are both stable but ^{14}C is unstable or radioactive. The most abundant of these is ^{12}C (98.89%), followed by ^{13}C (1.11%), while ^{14}C ($1.0 \times 10^{-10}\%$) is only present in small quantities (Walker, 2005). The equilibrium concentration of ^{14}C and ^{12}C is:

$$\frac{^{14}\text{C}}{^{12}\text{C}} = 10^{-12}$$

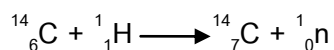
In other words, one ^{14}C atom exists in nature for every 1,000,000,000,000 ^{12}C atoms.

^{14}C is formed in the upper atmosphere by the effect of cosmic ray neutrons upon nitrogen 14 (Higham, 1994). The reaction is:



n = a neutron, p = a proton

Libby described the reaction by the following formula.



Cosmic ray flux leads to the collision of free neutrons with other atoms and molecules. One of the effects of these nuclear reactions is the displacement of protons from nitrogen atoms (^{14}N) to produce carbon atoms (^{14}C). The ^{14}C formed is rapidly oxidized to $^{14}\text{CO}_2$ and enters the atmosphere. It is then absorbed by the oceans and by living organisms during tissue building. Plants and animals which utilize carbon in biological food chains take up $^{14}\text{CO}_2$ during their lifetimes and are in equilibrium with their contemporaneous life-medium (atmosphere, ocean or fresh-water). When a plant or animal dies, the uptake of $^{14}\text{CO}_2$ stops. So, there is no replenishment of ^{14}C , only decay. The ^{14}C atom decays back to ^{14}N by emitting a weak beta particle (β), or electron (e^-), which possesses an average energy of 160 keV. The decay can be shown as below and production of ^{14}C and its cycle are shown in Figure 4-11.

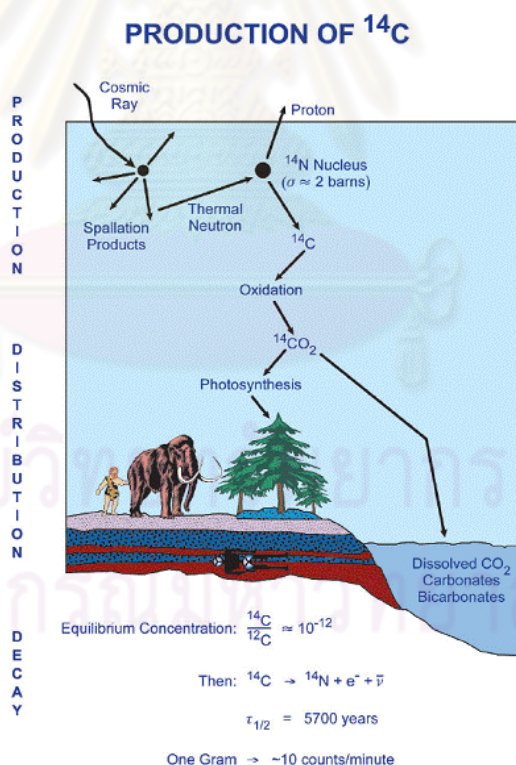
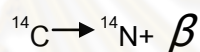


Figure 4-11 Production of ^{14}C and its cycle (LA Currie, 2004 after D. J. Donahue)

(Parameter values are approximate.).

Libby's early work indicated that after $5,568 \pm 30$ years (Walker, 2005), half of the ^{14}C in the original sample will have decayed and after another 5,568 years, half of that remaining material will have decayed, and so on (see Figure 4-12). However, the half-life of ^{14}C has been recalculated at 5730 ± 40 years (Walker, 2005; Godwin, 1962). The old half-life is still used in many published papers, which means that, all dates should be multiplied by 1.03 in order to obtain an accurate radiocarbon date (Walker, 2005).

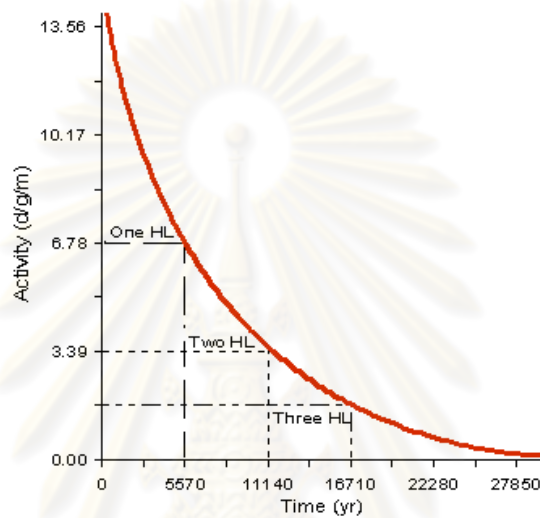


Figure 4-12 The decay curve of radiocarbon

(<http://www.geo.arizona.edu/palynology/geos462/10radiometric.html>)

Uncalibrated radiocarbon ages are usually reported in radiocarbon years "Before Present" (BP). "Present" being defined as AD 1950. A raw BP date cannot be used directly as a calendar date, because the level of atmospheric ^{14}C has not been strictly constant. The level of ^{14}C is affected by both natural processes and human activities. Natural processes are variations in cosmic ray intensity which are in turn affected by variations in the Earth's magnetosphere. In addition, there are substantial reservoirs of carbon in organic matter, the ocean, ocean sediments (methane hydrate), and sedimentary rocks. Changes in the Earth's climate can affect the carbon flows between these reservoirs and the atmosphere, leading to changes in the atmosphere's ^{14}C fraction.

However, the level has also been affected by human activities. From the beginning of the Industrial Revolution in the 18th century to the 1950s, ^{14}C in the atmosphere and

hydrosphere was diluted because ^{12}C was increased by the use of fossil fuel in industry, the so-called "Industrial Effect". This decline is also known as the Suess effect, and also affects the ^{13}C isotope. In 1952 A.D., the beginning of nuclear weapon tests caused an increase in ^{14}C so-called "Atomic Bomb Effect". Thus, the intensity of ^{14}C today cannot be used as a primary intensity for dating. In addition, the U.S. National Bureau of Standard has made Oxalic acid as an International Primary Standard for dating by changing it from 19th century trees.

As a consequence, the radiocarbon method shows limitations on dating of materials that are younger than the industrial era. Due to these fluctuations, greater carbon-14 content cannot be taken to mean a lesser age. The upper limit of reliable radiocarbon dating can be placed around 40,000-50,000 years BP, although it has been claimed that this limit may reach as much as 60,000-70,000 years BP (Penny, 1998; Geyh and Schleicher, 1990; Stuiver et al., 1979; Pilcher, 1991). Since the content of radiocarbon has varied through time, radiocarbon measurements need to be calibrated to be comparable to real ages.

4.3.5.2 Dating of macrofossils by AMS ^{14}C

After sub-sampling for geochemical and biological proxies, the remaining core fragments from KMP-CP3A were sub-sampled in contiguous 5 cm intervals for ^{14}C dating. A total of 50 samples were sieved (mesh size 0.5 cm) under running water. Sieve remains were identified under the microscope. Only few samples contained however enough organic material for dating. The samples selected for AMS ^{14}C dating were composed of charcoal, seeds and wood fragments (see Table 4-4 and Figure 4-13 a-c). These four samples were dried overnight at 105°C (Figure 4-13 a-c) in pre-cleaned glass vials and were then submitted to the Belfast Radiocarbon Laboratory for analysis.

The reason for selecting, plant macrofossils and charcoals for this study is because this type of material has long been used in radiocarbon dating and is well preserved in a range of depositional contexts, including lake sediment, peats, palaeosols, cave sediment, buries soils, etc (Walker, 2005). In lake sediments, plant macrofossils have different

sources. They may be derived from aquatic plants and may originate from the point of sampling. However, macrofossils found in lake mud have often been transported short distances from the nearby aquatic and lake-margin vegetation; or were washed in from the surrounding terrestrial vegetation, for example by small streams, alternatively transported to the lake by wind (Birks and Birks, 1980). Charcoal is often found in archaeological contexts. Thus, it can provide useful ecological and cultural information (Walker, 2005). In lake sediments, it has proven to be especially valuable as an indicator of past fire regimes, reflecting the influence of both climate (increased incidence of fire under drought conditions: Brunelle and Anderson, 2003) and/or human impact.

Table 4-4 Selected sample for ^{14}C dating

Units	Sample depth (m)	Lab ID	Material
7	4.80-4.85	UBA-12660	Charcoal
4	3.75-3.70	UBA-12661	wood
4	3.70-3.65	UBA-14166	Chara, seeds, charcoal
4	3.60-3.55	UBA-14168	wood
4	3.45-3.41	UBA-12662	wood
3	3.39-3.36	UBA-14169	charcoal
4	3.36-3.33	UBA-14170	wood
3	3,10-3,05	UBA-12663	Charcoal



Figure 4-13 a-c: Plant macrofossils for AMS ^{14}C dating.

4.3.5.3 Laboratory preparation of AMS ^{14}C samples

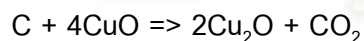
a) Pretreatment

Pretreatment is required in order to get pure carbon from the samples and to get rid of contaminations with old or modern carbon. The main goal of the treatment is to remove carbonates and humic acids that is not a primary material of the sample. The choice of the proper procedure depends on the type of the material subjected to radiocarbon dating. Following the selected samples, wood, charcoal, and seed, the standard procedure acid-alkali-acid (AAA) pretreatment was used. The first acid step is used to remove carbonates and the second alkali step is used to remove humic acids. The additional acid step is being applied to remove contamination with modern atmospheric CO_2 , which occurs during the alkali step (Hajdas, 2006).

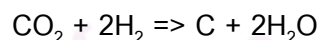
b) Combustion and Graphitization

^{14}C measurements by AMS require that the sample is transformed to elemental carbon in order to produce a stable ion beam with negligible memory effect in the ion source. The purified carbon dioxide acquired from the combustion of organic matter or acidification of carbonates is reduced in a reaction with hydrogen over catalyst (iron or cobalt powder).

The reaction of combustion is



The reaction of graphitization is



The filamentous graphite is pressed into the cathodes (targets). A set of unknown targets together with standard samples (known $^{14}\text{C}/^{12}\text{C}$ ratio) and blank samples (prepared of ^{14}C free materials) for measurements of chemical and machine background is then placed in the ion source of the accelerator.

c) Accelerator Mass Spectrometry (AMS) Method

Two approaches were used to measure the remaining ^{14}C activity in samples relative to the modern standard. The first one is the original method which is also

called **conventional radiocarbon dating technique or beta counting**. This technique detects and counts β emissions, the decay products from ^{14}C atoms over period of time. **Accelerator Mass Spectrometry** is the second method. It uses particle accelerators as mass spectrometers to count the relative number of ^{14}C atoms in a sample and is determined by comparing this ratio with that of a standard of known ^{14}C content (Walker, 2005). The AMS technique has a wide range of dating and tracking applications in the geological and planetary science, and in archaeology and biomedicine. This technique required only 1 mg of pure carbon and the measurement process can be completed in a few hours or days. By contrast, the conventional method requires 1-2 g of pure carbon and it can take a number of days or even weeks to measure a sample (Björck and Wohlfarth, 2001; Walker, 2005; Hellborg and Skog, 2007).

Samples are converted to graphite (or CO_2 source) and mounted on a metal disc and inserted into the ion source through a vacuum lock. Cesium ions (Cs^+) are fired from the ion source by focusing to a small spot on the sample. The negatively ionized carbon atoms (C^-) are produced on the surface of the sample and sent down the beam line towards the first magnet under the vacuum condition. At this point the beam is about 10 microamps which corresponds to 10^{13} ions per second (mostly the stable isotopes). At the first magnet, also called the injector magnet, the mass of interest is selected and the intense neighboring stable isotopes are rejected by bending the negative ion beam by 90° . Then the evacuated beam line is sent down to the tandem accelerator (see figure 4-14 and 4-15) which consist of two accelerating gaps with a large positive voltage in the middle which is called the terminal. It is charged to a voltage of up to 10 million volts by two rotating chains. At the terminal, there is an electron stripper, a gas or very thin carbon foil, the negatively ionized carbon atoms are accelerated towards the positive terminal.

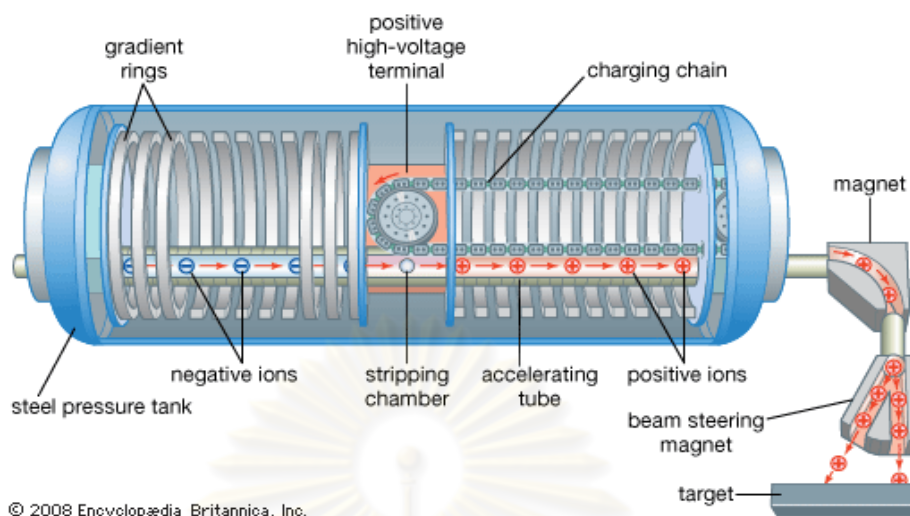


Figure 4-14 Example of a tandem accelerator (Encyclopedia Britannica, 2008)

During the passage through the stripper, four electrons are lost from the C^- ions (five in some AMS systems), and they emerge with a triple positive charge (C^{3+} , or C^{4+} if five electrons are stripped). Repulsion from the positive terminal leads to a second acceleration of the carbon ions through focusing magnets or the analyzing and switching magnets, where deflection occurs according to mass by selecting only the highly charged ions that are produced in the terminal stripper (Highly charged molecules are unstable since they lack the electrons that bind the atoms together). The signal of the stable isotope ^{13}C (and sometimes ^{12}C) is measured by using Faraday cups, and the ^{14}C signal is collected by a gas ionization detector where the ions are slowed down and come to rest in propane gas. These electrons are collected on metal plates, amplified, and read into the computer. For each atom, the computer determines the rate of energy loss and from that deduces the nuclear charge (element atomic number) to distinguish interfering isobars.

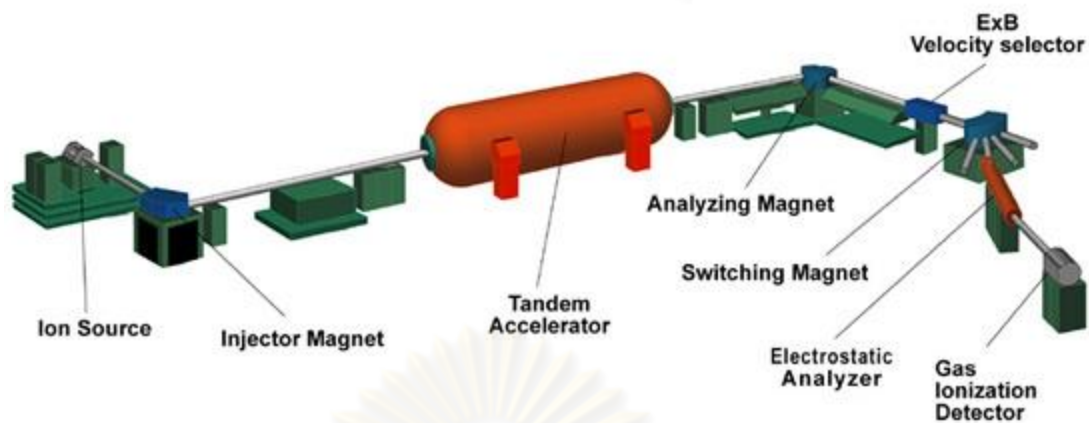


Figure 4-15 The AMS systems

(<http://www.physics.purdue.edu/primelab/introduction/ams.html>)

ศูนย์วิจัยทรัพยากร
จุฬาลงกรณ์มหาวิทยาลัย

CHAPTER V

RESULTS AND ANALYSIS

5.1 Map reconstruction

5.1.1 Aerial photos interpretation

The results of the aerial photo interpretation show the difference in lake surface area before and after the construction of the dam. The lake boundary was reduced after the lake surface area changed from 36 km³ to 44 km³ by making a 124 km long dyke (8 m wide and 6 m high) around the lake.

The dam was finished in 1994 and includes 5 floodgates and 14 electrically powered pump stations. The canal systems were also installed. Figures 5-1 a-b and 5-2 show the lake boundary during the years 1951 and 1996 from aerial photo interpretation.

5.1.2 Correlation of Land-use / Land cover

Land-use maps (from 1985, 2001 and 2009) (Fig 5-4, 5-5 and 5-6) were generated based on the data from the Land use and Land development Department. In addition, these maps were compared with the vegetation map of White (2004) in Figure 5-3. This section reports the change in land-use and land cover of Nong Han Kumphawapi area from the past to present.

ศูนย์วิจัยทรัพยากร
จุฬาลงกรณ์มหาวิทยาลัย

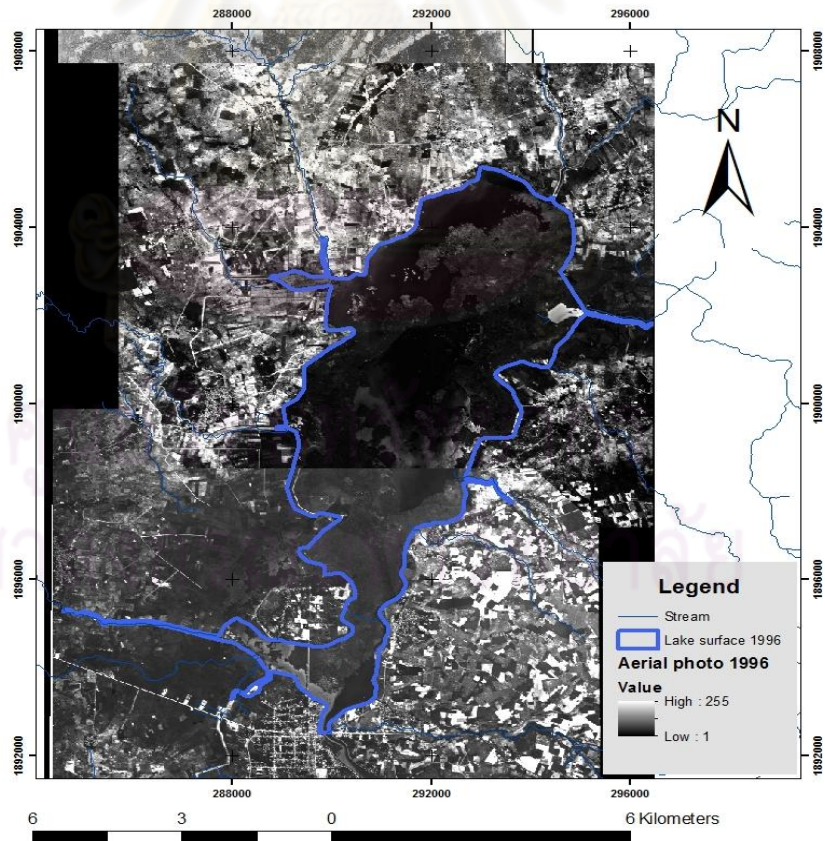
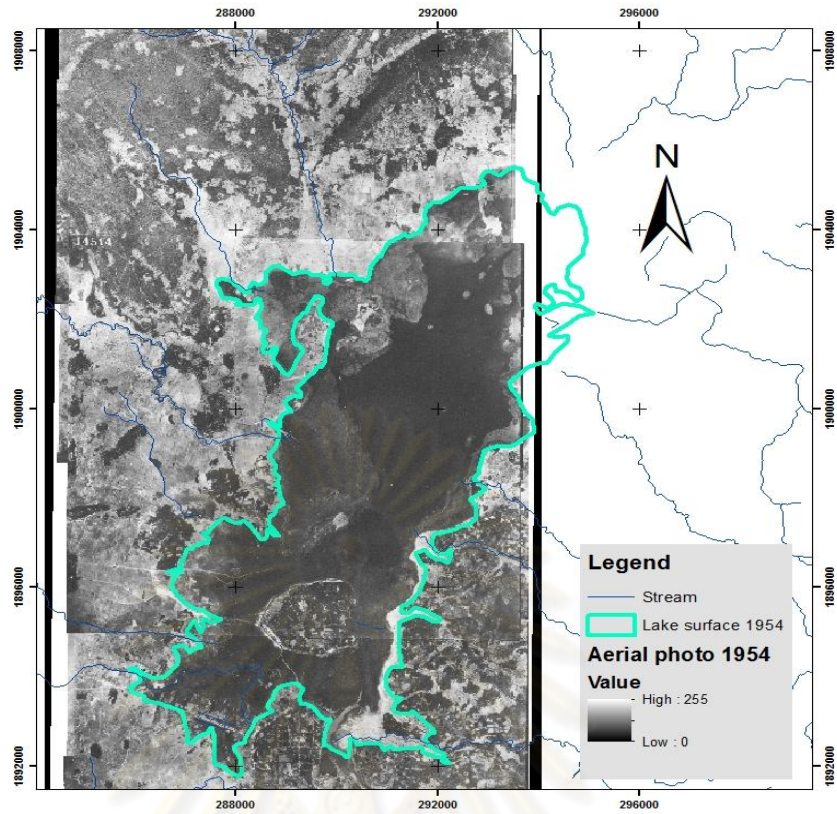


Figure 5-1 a-b Lake surface area based on interpretation of aerial photos from the 1954 and 1996.

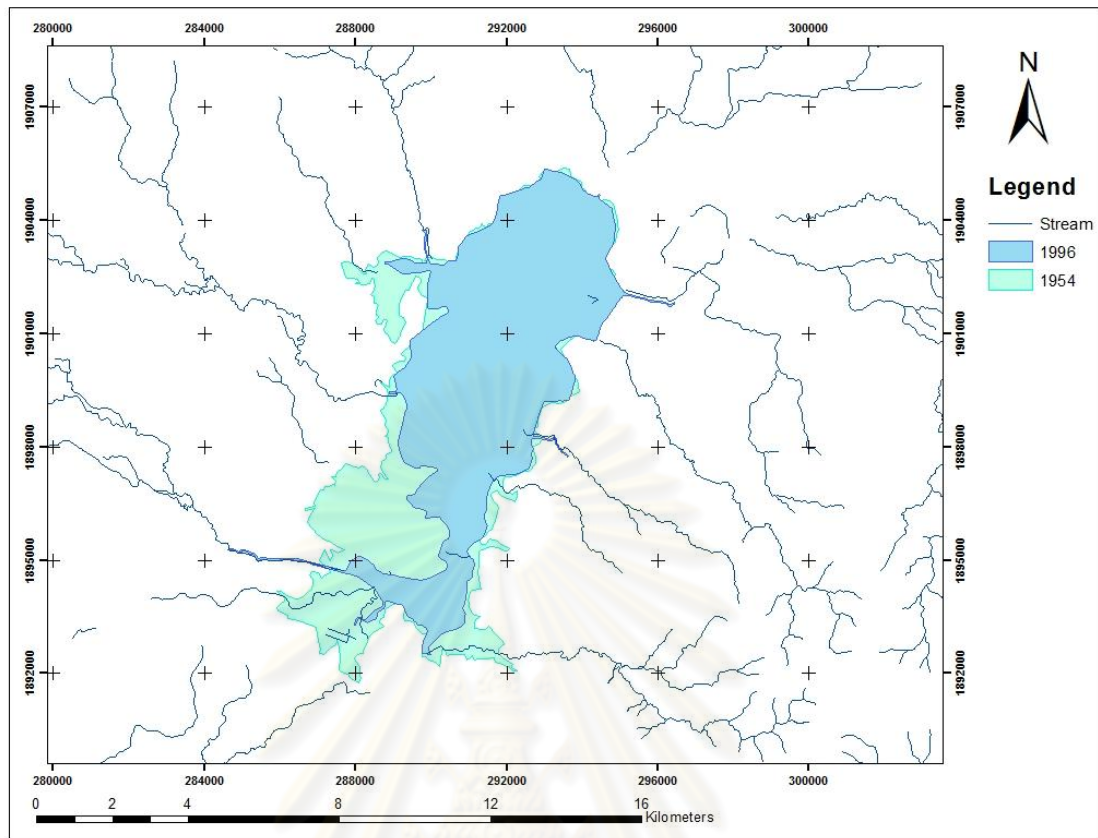


Figure 5-2 Lake surface and lake boundary based on interpretation of aerial photos from the 1954 and 1996.

ศูนย์วิทยทรัพยากร
จุฬาลงกรณ์มหาวิทยาลัย

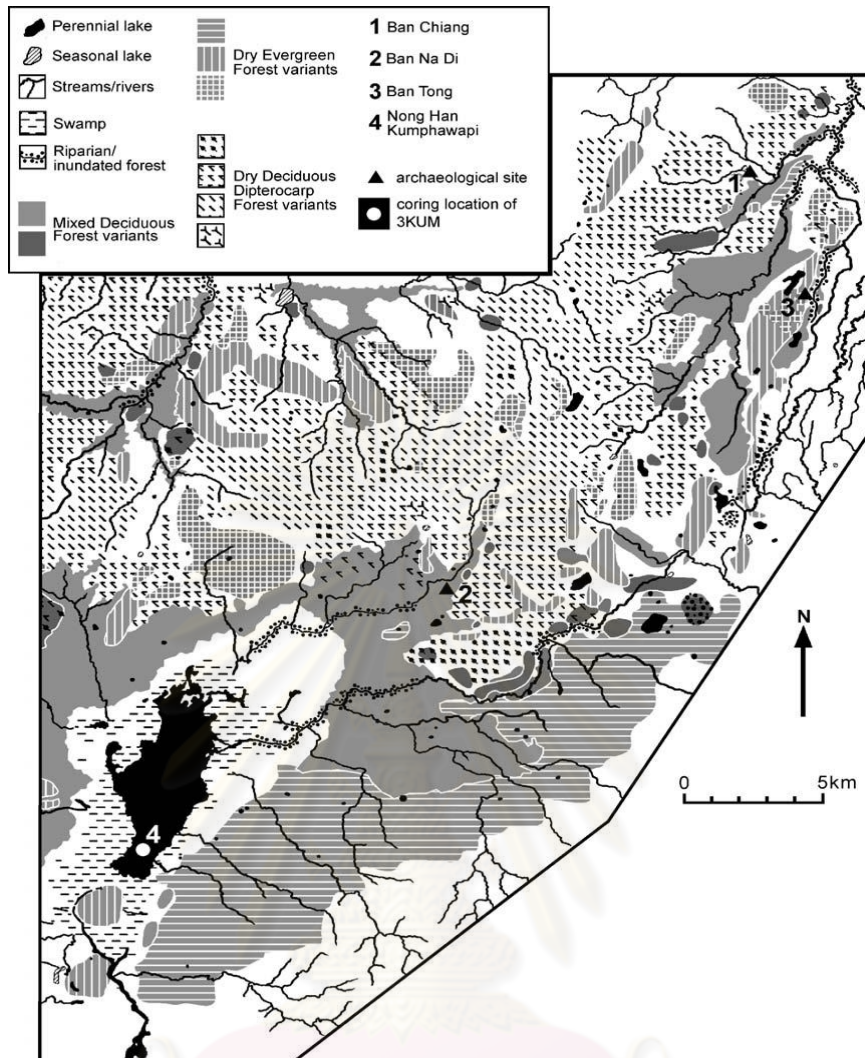


Figure 5-3 Vegetation map of the Nong Han Kumphawapi region, prepared by White (2004).

The map by White (2004) was based on an interpretation of aerial photos from the 1950s and was made in conjunction with ethno-ecological field research undertaken in 1979–1981 and 1994. Nong Han Kumphawapi was classified into perennial lake and swamp areas and the important archaeological sites in this region were included; Ban Chiang, Ban Na Di and Ban thong. The data from the map indicates that a mosaic of natural vegetation types existed recently in this region. Dry deciduous/dipterocarp forests were most common, but with edaphically (plant communities that are found only in specific conditions) influenced zones and pockets of semi-evergreen and

riparian/inundated forest. The vegetation mosaic is reflected in a patchy distribution of a wide range of subtropical natural resources including wild rice, yams, and other useful and edible plants, as well as wild animals.

According to Figure 5-4, land cover changed from natural forests to agricultural areas. Rice paddies and sugarcane plantations dominate in this region. Dry dipterocarp/deciduous forests are mostly disturbed. This map combines the coring point data and heritage sites around Nong Han Kumphawapi. The land-use map from the year 2001 (Figure 5-5) shows the change in plantation; rice paddies and sugarcane still dominate. Eucalyptus and Para rubber plantation are starting to exist in the region. The lake feature had changed after the dam was built in 1994.

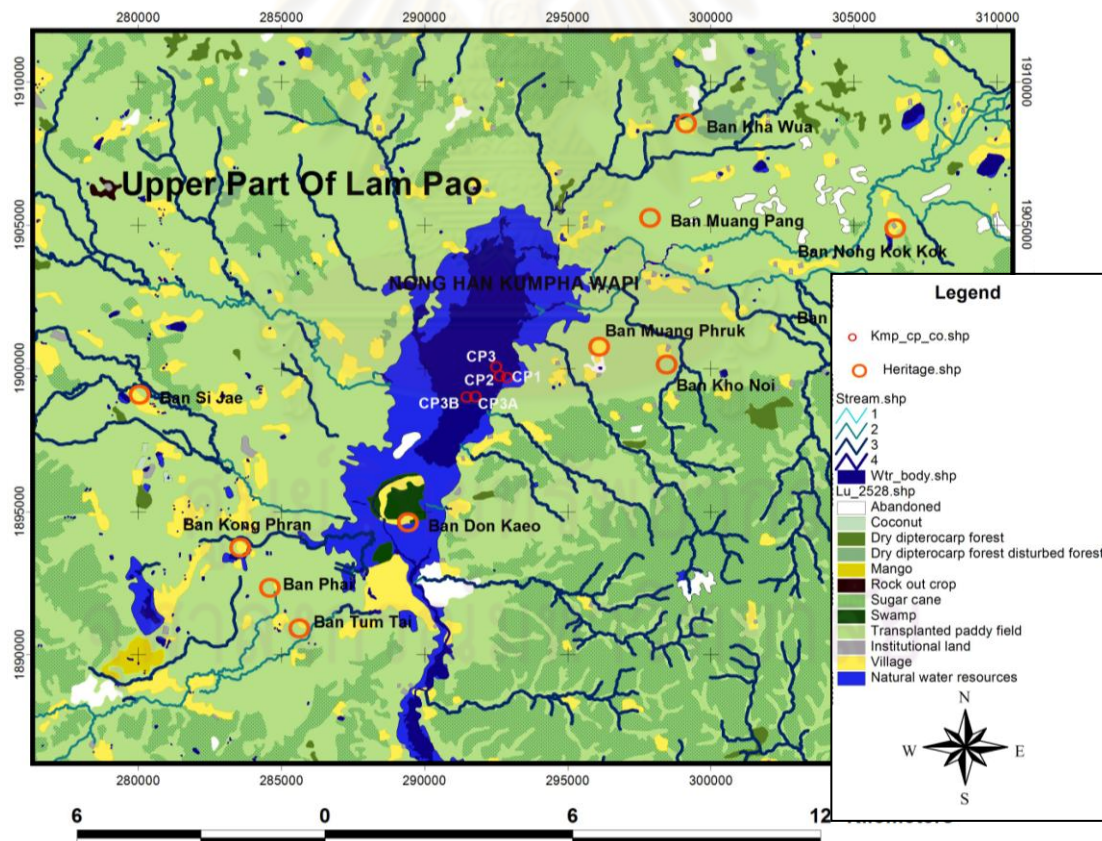


Figure 5-4 Landuse map based on data of Land and Land development Department from the year 1985.

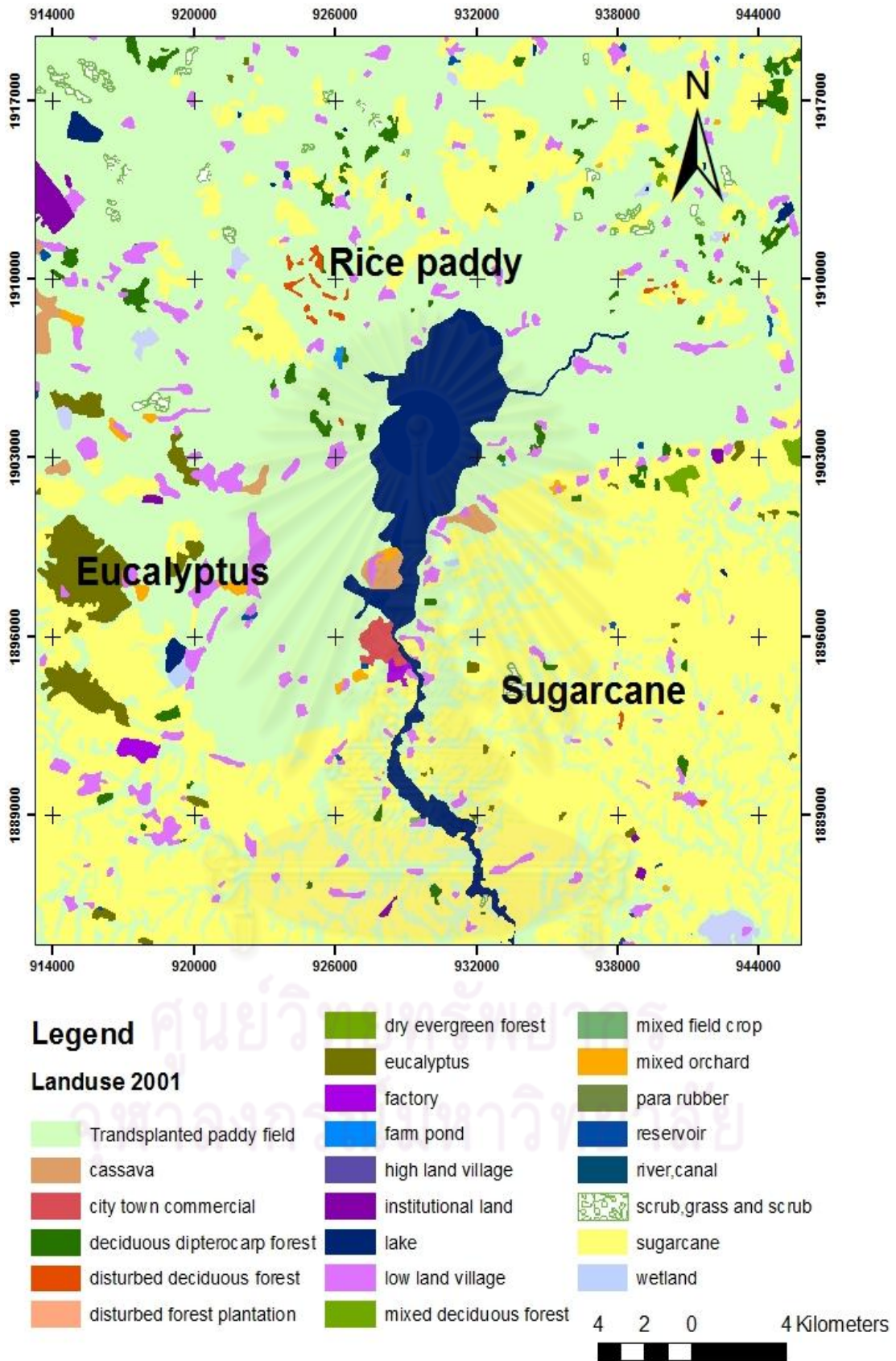


Figure 5-5 Land-use map based on data of Land and land development Department from the year 2001 .

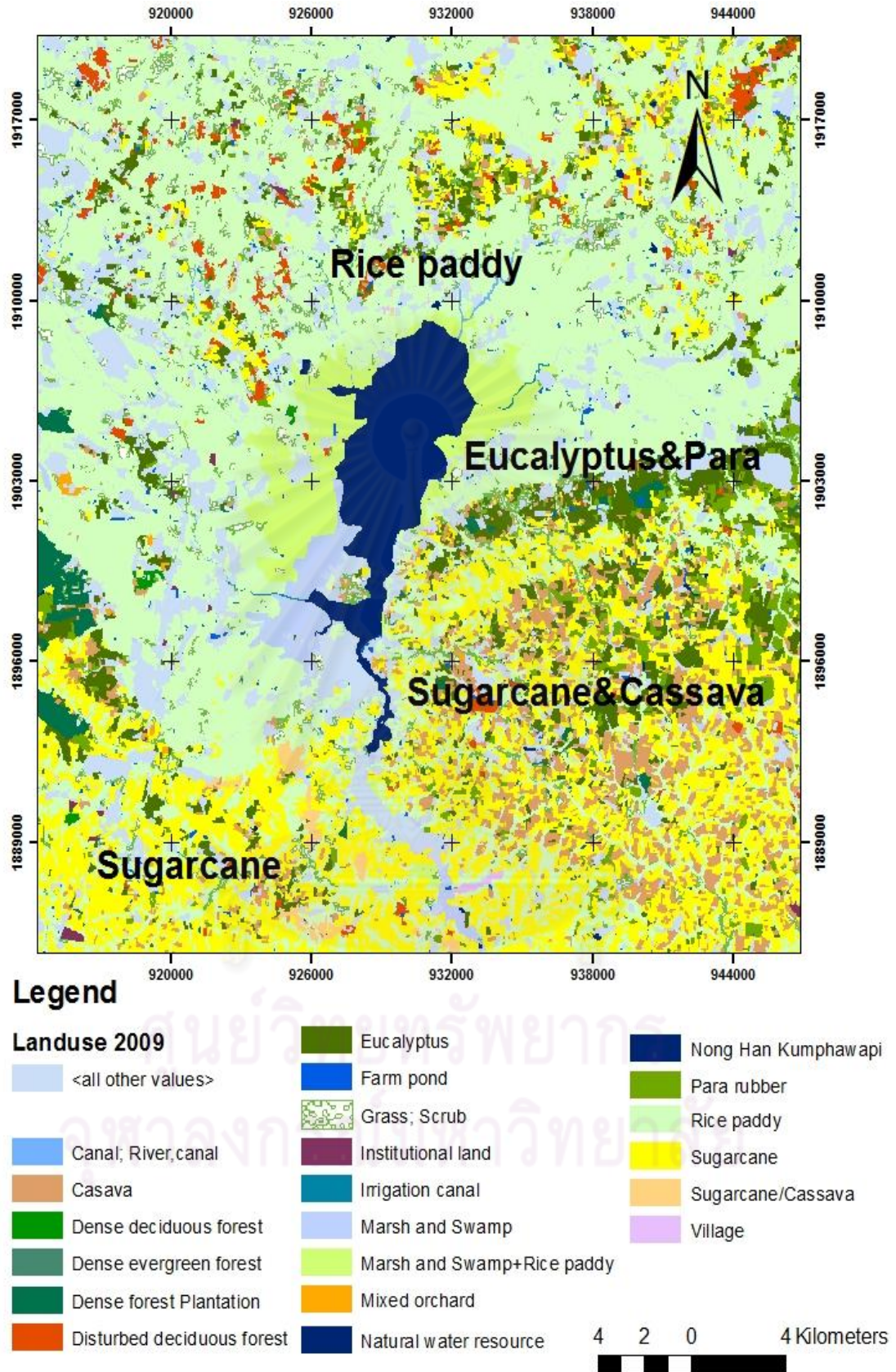


Figure 5-6 Landuse map based on data of Land and land development Department from the year 2009.

Landuse in the map 2009 (Figure 5-6) shows variety of plantations, mosaic of cassava with sugarcane and eucalyptus with para rubber are increasing. The map was classified in more details than the past, recognized from the lake surrounded which were classified into; a) marsh and swamp, b) Marsh and swamp + rice paddy.

In conclusion, the results of this section show the change in lake feature and agricultural pattern in Nong Han Kumphawapi area. The lake was dam due to the irrigation project which supports the expansion of agriculture. Moreover, modern day agricultural take advantage of the landscape mosaic to maintain a broadly based cropping system, although dependent on inundated rice, including both swidden and horticultural techniques. Overall, these results show the impact of human activities in the lake catchment area due to increasing of population and their demand for consumer.

5.1.3 Combined thematic map with old geomorphic map (Kijngam and Higham,1983)

Soil, landform map and Digital Elevation Model (DEM) were generated by the GIS base map of Udon Thani (using ArcGIS10) (Figure 5-7, 5-8 and 5-9). Then group the same unit of soil the same elevation and landform together by using an idea from old geomorphic map of Kijngam and Higham (1983) which is reported after the aecheaology sites survey in 1980-1981 (Figure 5-10). They used suitability of rice cultivation to classified soil type.

Unit 3 in soil map was defined as floodplain clay. This soil type is well suited to rice cultivation. Unit 0 is classified as low terrace which is a moderately suited to rice cultivation. Units 7-8, 13-15, 17, 19, 24, 26, 32 are moderately suited to rice cultivation. These units deposit in low terrace. Units 20-23 are poorly to unsuited to rice cultivation. These units deposit in middle terrace. Units 33-43 are unsuited to rice cultivation. These units deposit in high terrace. In addition, The results of Landform map and DEM correspond with soil map.

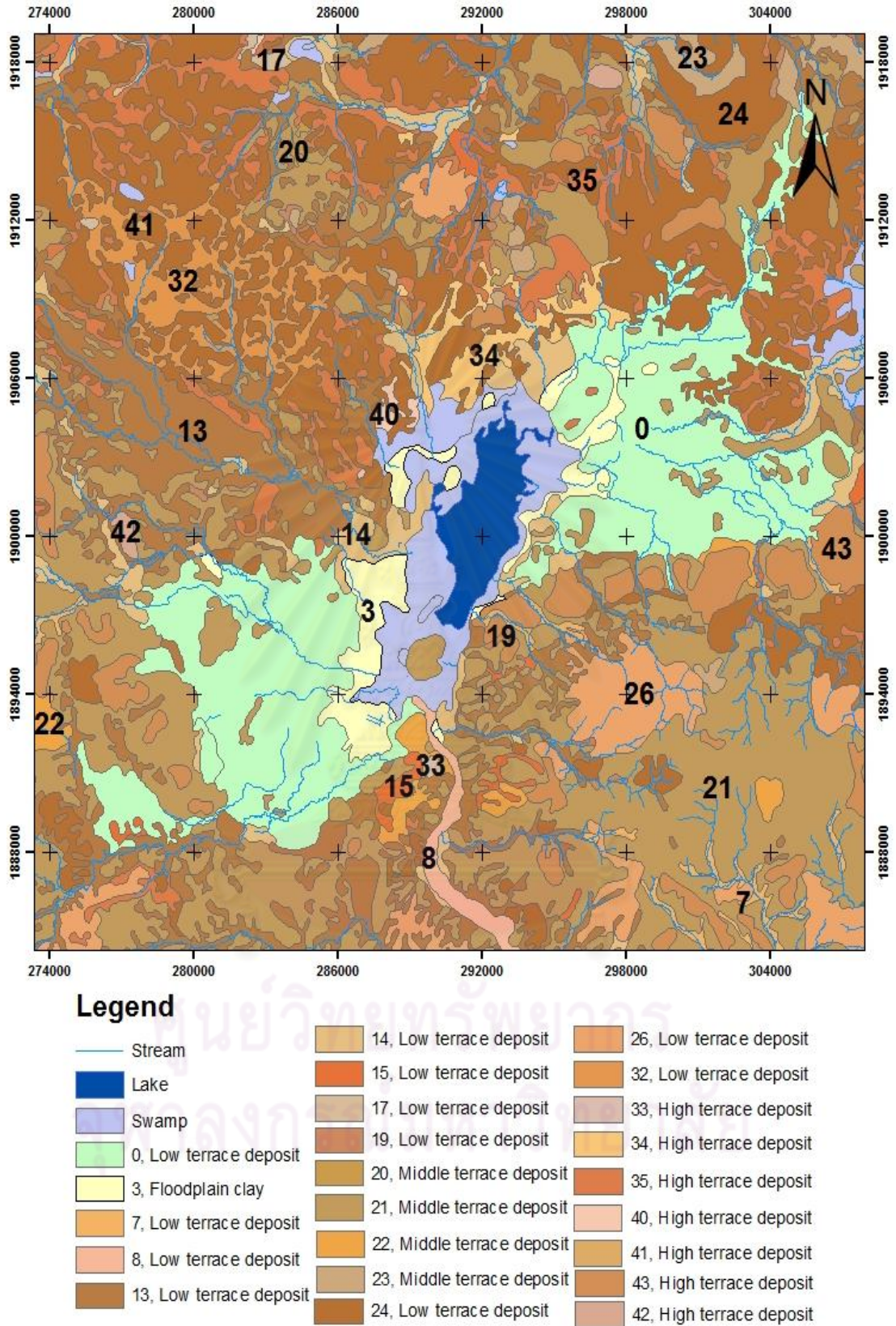


Figure 5-7 Soil map based on the classification of Land and Land development Department (1985).

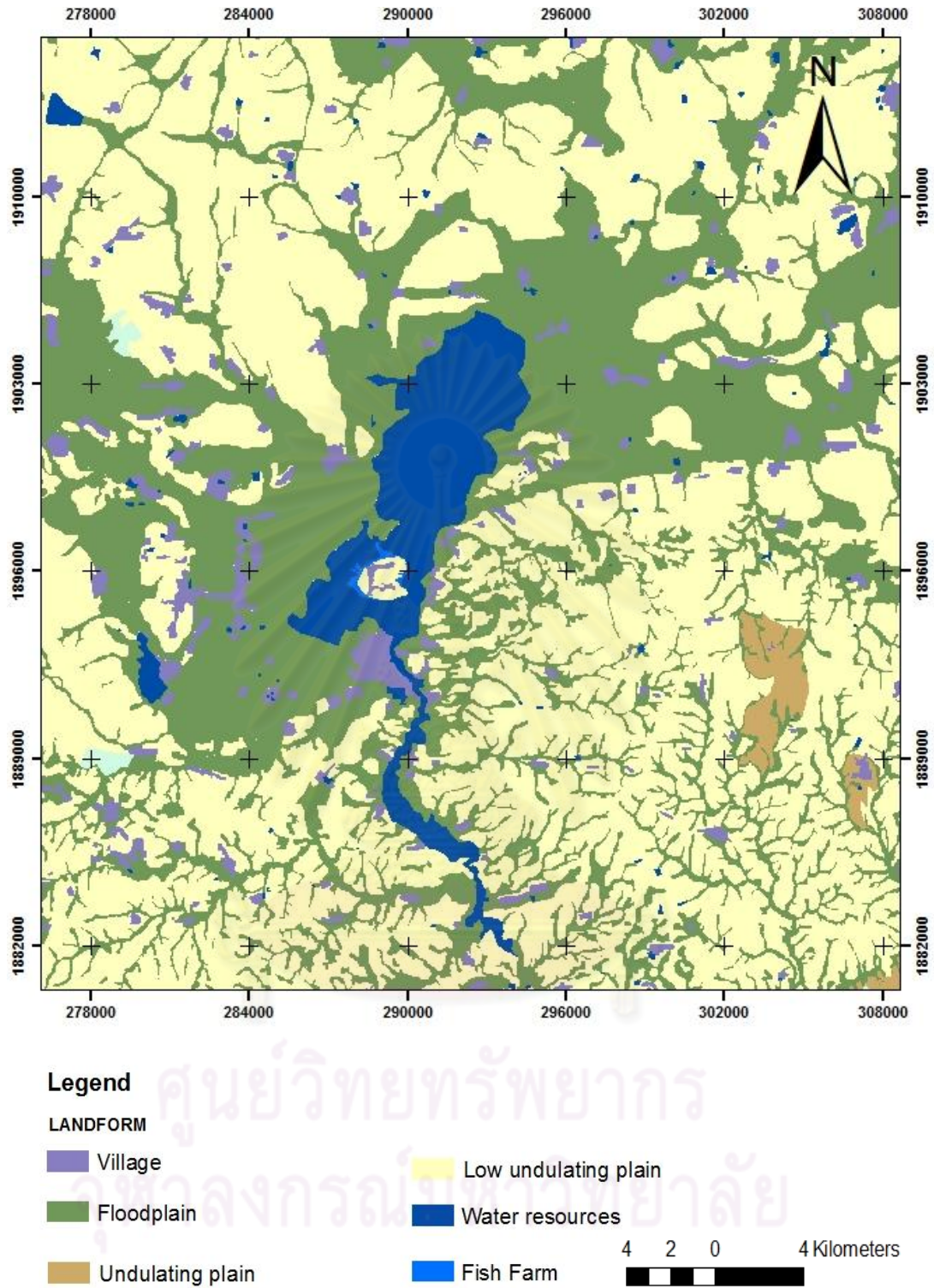


Figure 5-8 Landform map based on classification of land and Land development Department(1985).

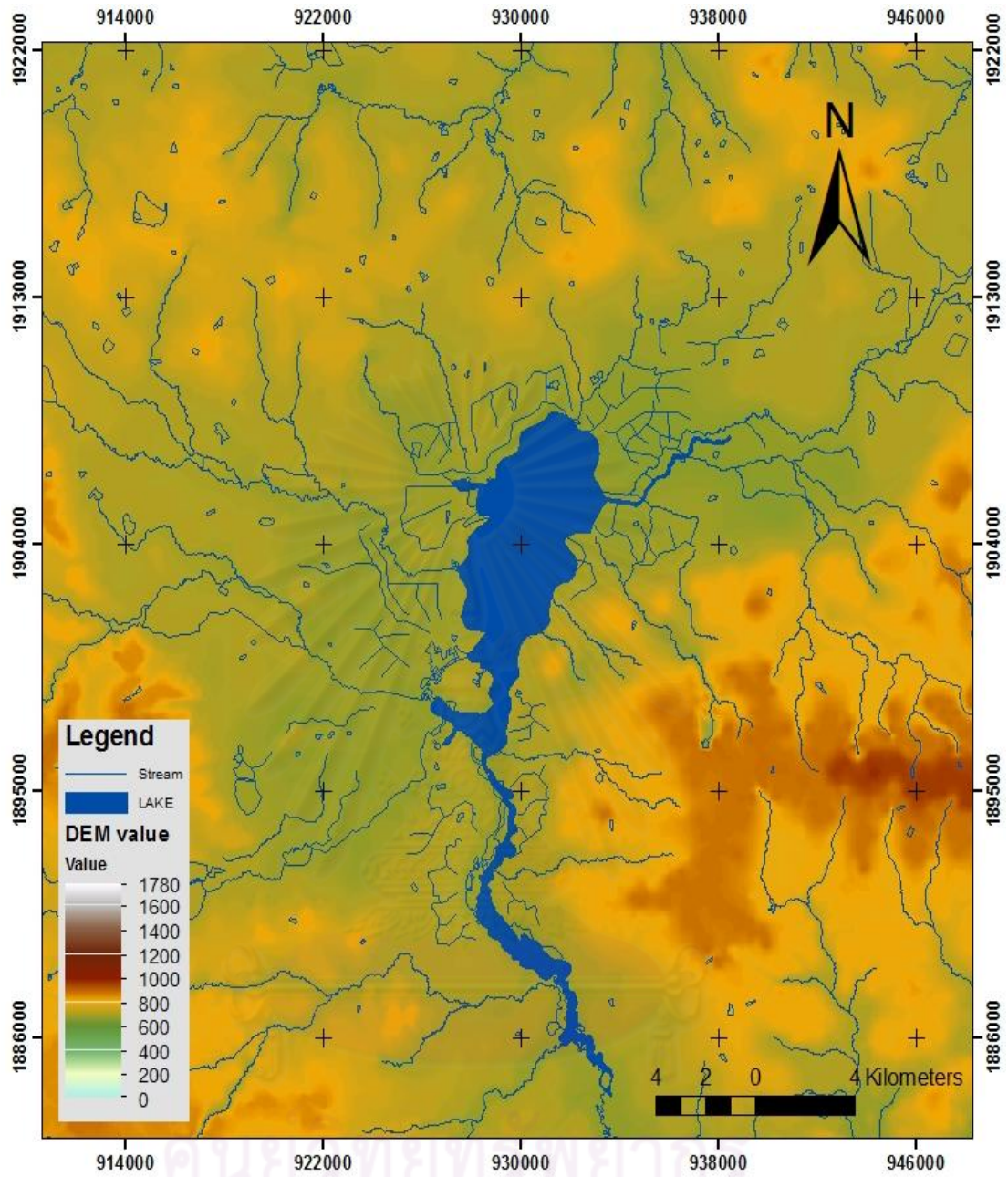


Figure 5-9 Digital Elevation Model (DEM) generated from the database of Land and land development department (1985).

5.1.4 Paleogeographic map

Paleogeographic map with lake flooded conceptual model (Figure 5-11) was generated by combining all results from thematic map and old geomorphic map of Kijngam and Higham 1983 (Figure 5-10). Unit 3 of soil type was interpreted as a lake level during > 6000 yr B.P. because its properties which different from surrounded low terrace soil type. The light blue area with yellow dot outline shows a lake level during 6000-5000 yr B.P. The perennial lake was assumed to be a lake level during 5000-2000 yr B.P. The swamp or floodplain area around the perennial lake was classified to be a lake level during 2000 yr B.P. to present.



Figure 5-10 The old geomorphic map (Kijngam and Higham 1983).

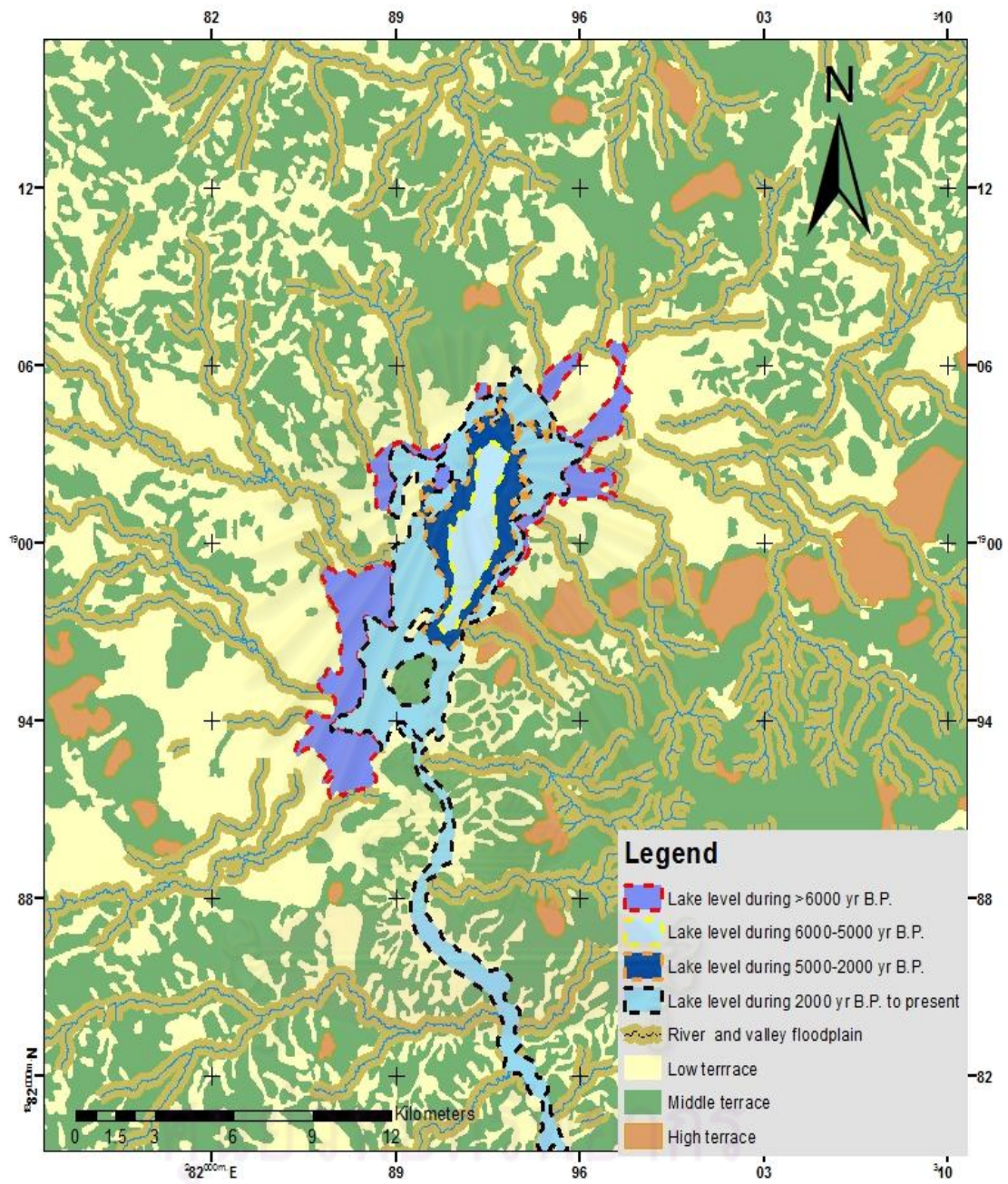


Figure 5-11 Paleogeographic map with the model of lake level.

5.2 Lithostratigraphy of the sediment sequences

Five sediment sequences were obtained from Nong Han Kumphawapi and included CP1, CP2, CP3, CP3A and CP3B. The five coring points are shown on the map below (Figure 5-12). All analyses were done on CP3A, which is presented in more detail below.

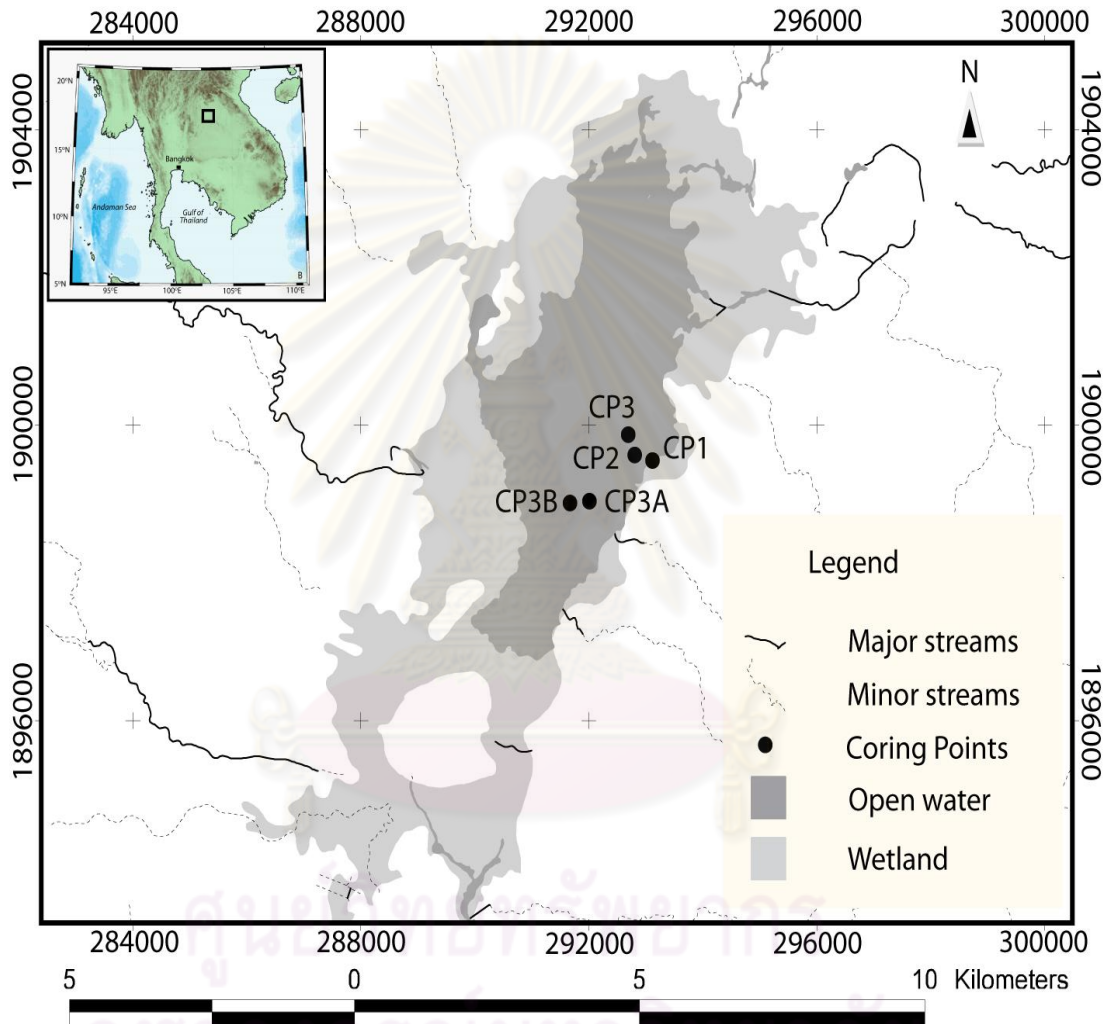


Figure 5-12 Location of Nong Han Kumphawapi and of coring points CP1, CP2, CP3, CP3A and CP3B.

5.2.1 Kumphawapi CP3A

CP3A Core was divided into 20 layers which were grouped into 7 sediment units (Figure 5.13a). The lowermost sediments between 6.00-4.31 m (Unit 7, layer 20) consist of grey gyttja clay. Unit 6 between 4.31 and 4.00 m is composed of olive-brown to greenish- brown gyttja with gradual low boundaries (layers 19 - 18). Unit 5 includes layers 17-15 and is a greenish brown and black to dark brown gyttja with gradual lower boundaries. The sediments in layers 14-11 (3.82-3.33 m depth) are grouped as Unit 4 and consist of blackish-brown peaty gyttja and thick layers of blackish-brown peat; these are overlain by a dark brown- black peaty gyttja with a gradual lower boundary. Unit 3 with layers 10-8 (2.92-3.33 m depth) is composed of a dark brown to black clay gyttja with coarse organic material and a gradual lower boundary. The sediments between 2.92-2.73 m depth were grouped into Unit 2 and consist of dark brown and olive green gyttja (layers 6-7). The uppermost Unit 1 includes layers 5-1 and consists of greenish brown to dark brown clay gyttja with a gradual lower boundary (layers 5-4) and of greenish brown slightly oxidized clay gyttja with a gradual lower boundary (layer 3). These sediments are overlain by oxidized clay gyttja with reddish spots and light laminae (layer 2) and oxidized reddish black clay gyttja at the top (layer 1).

Table 5-1: Lithostratigraphy of Core CP3A, 2.15-6.00 m

Depth below water surface (m)	Description	Layer	Unit
2.15-2.26	Grey in field, now oxidized reddish-black clay gyttja, gLB	1	1
2.26-2.40	Grey in field, now oxidized clay gyttja with reddish spots, light laminations, gLB	2	1
2.40-2.57	grey brown in field, now greenish brown, slightly oxidized clay gyttja	3	1
2.57-2.66	Dark brown clay gyttja	4	1
2.66-2.73	Oxidized greenish brown clay gyttja with reddish-black/brown spots	5	1
2.73-2.80	Olive green gyttja	6	2
2.80-2.92	Dark brown gyttja	7	2
2.92-3.06	Dark brown clay gyttja, oxidized spots	8	3
3.06-3.20	Dark brown clay gyttja with dark spots, Fe stains more distinct	9	3
3.20-3.33	Dark brown/blackish brown clay/coarse organic gyttja,	10	3

sLB*			
3.33-3.50	Dark brown-black peaty gyttja, possibly some clay, gLB**	11+12	4
3.50-3.75	Blackish brown peat, gLB**	13	4
3.75-3.82	Blackish brown peaty gyttja, gLB**	14	4
3.82-3.87	Dark brown gyttja, gLB**	15	5
3.87-3.90	Transition zone: greenish brown and black clay gyttja, gLB**	16	5
3.90-4.00	Greenish brown clay gyttja	17	6
4.00-4.31	Olive brown clay gyttja, gLB**	18	6
	Olive brown claygyttja, gLB**	19	6
4.31-6.00	Grey gyttja clay	20	7
*sLB = sharp lower boundary **gLB = gradual lower boundary			

5.2.2 Kumhawapi CP3B

Sediment core CP3B was divided into 21 layers which were grouped into 7 units (see Figure 5-13b). The lower Unit 7 (6.00-4.395 m depth) is grey gyttja clay. Unit 6 (4.395 - 3.985 m depth) includes layer 20 which is a dark grey brown clay gyttja, layer 19 which consists of olive brown clay gyttja with a very gradual low boundary, and layer 18 which is a brown to grey clay gyttja with a very gradual lower boundary. Unit 5 is composed of layers 17-16 (3.985-3.905 m depth). Layer 17 is a transition zone and layer 16 is a dark brown gyttja, both layers have gradual lower boundaries. These sediments are overlain by Unit 4 (3.905-2.83 m depth) which consists of thick layers of dark brown to black peat (layers 14-15) which is finer and more compact in the lower part. In addition, at the upper part of Unit 4 (layers 11-13) is made up of dark brown to black peaty gyttja and dark brown peaty gyttja with clayey gyttja layers. Unit 3 (2.830-2.745 m depth) includes layers 9 and 10. Layer 10 consists of a dark brown clayey gyttja with gradual lower boundary and layer 9 is a transition zone between the upper gyttja and the lower clayey gyttja. Unit 2 (2.745-2.580 m depth) includes layer 8 which is a dark brown gyttja with a gradual lower boundary. The upper most Unit 1 (2.580-2.00 m depth) includes layers 1-7 and consists of a olive-brown to brown gyttja in the lower part (layer 4-7). These sediments are overlain by a layer of dark grey silty sandy gyttja with stones and (layer 3). The upper most part of this Unit includes layers 1-2. Layer 2 consists of a dark grey clay gyttja with a gradual lower boundary. This layer has a rusty color and is

more compact. Layer 1 consists of black loose clay gyttja with a rusty oxidized surface and a gradual lower boundary.

Table 5-2 Lithostratigraphy of Core CP3B, 2.00-6.00 m

Depth (m) below water surface	Description	Layer	Units
2.00-2.09	Black, fairly loose clay gyttja, oxidized reddish brown surface, gLB**	1	1
2.09-2.30	Dark grey clay gyttja, more compact, rusty color, plant remains, gLB**	2	1
2.30-2.33	Dark grey ?silty sandy gyttja with stones, gLB**	3	1
2.33-2.425	Olive brown clay gyttja, gLB**	4	1
2.425-2.52	Brown clay gyttja, gLB**	5	1
2.52-2.555	Olive brown clay gyttja, gLB**	6	1
2.555-2.58	Brown clayey gyttja, gLB**	7	1
2.58-2.745	Dark brown gyttja, gLB**	8	2
2.745-2.775	Transition zone between upper gyttja and lower (clayey) gyttja, gLB**	9	3
2.775-2.83	Dark brown, clayey gyttja, gLB**	10	3
2.83-2.87	Transition zone: clay gyttja mixed with peaty gyttja	11	4
2.87-2.995	Dark brown peaty gyttja with clay gyttja layers, gLB**	12	4
	Dark brown peaty gyttja with clay gyttja layers, sLB*	12	4
2.995-3.185	Dark brown-black peaty gyttja, gLB**	13	
3.185-3.545	Dark brown-black coarse peat	14	4
3.545-3.905	Dark brown finer, partly more compact peat, gLB**	15	4
3.905-3.94	Dark brown gyttja, gLB**	16	5
3.940-3.985	Transition zone: layers of dark brown gyttja and olive brown clay gyttja, vgLB***	17	5
3.985-4.075	Brown grey clay gyttja, vgLB***	18	6
4.075-4,195	Olive brown clay gyttja, vgLB***	19	6
4,195-4,395	Dark grey-brown clay gyttja	20	6
4,395-6.00	Grey gyttja clay, disturbed in upper part	21	7

*sLB = sharp lower boundary **gLB = gradual lower boundary ***vgLB = very gradual lower boundary

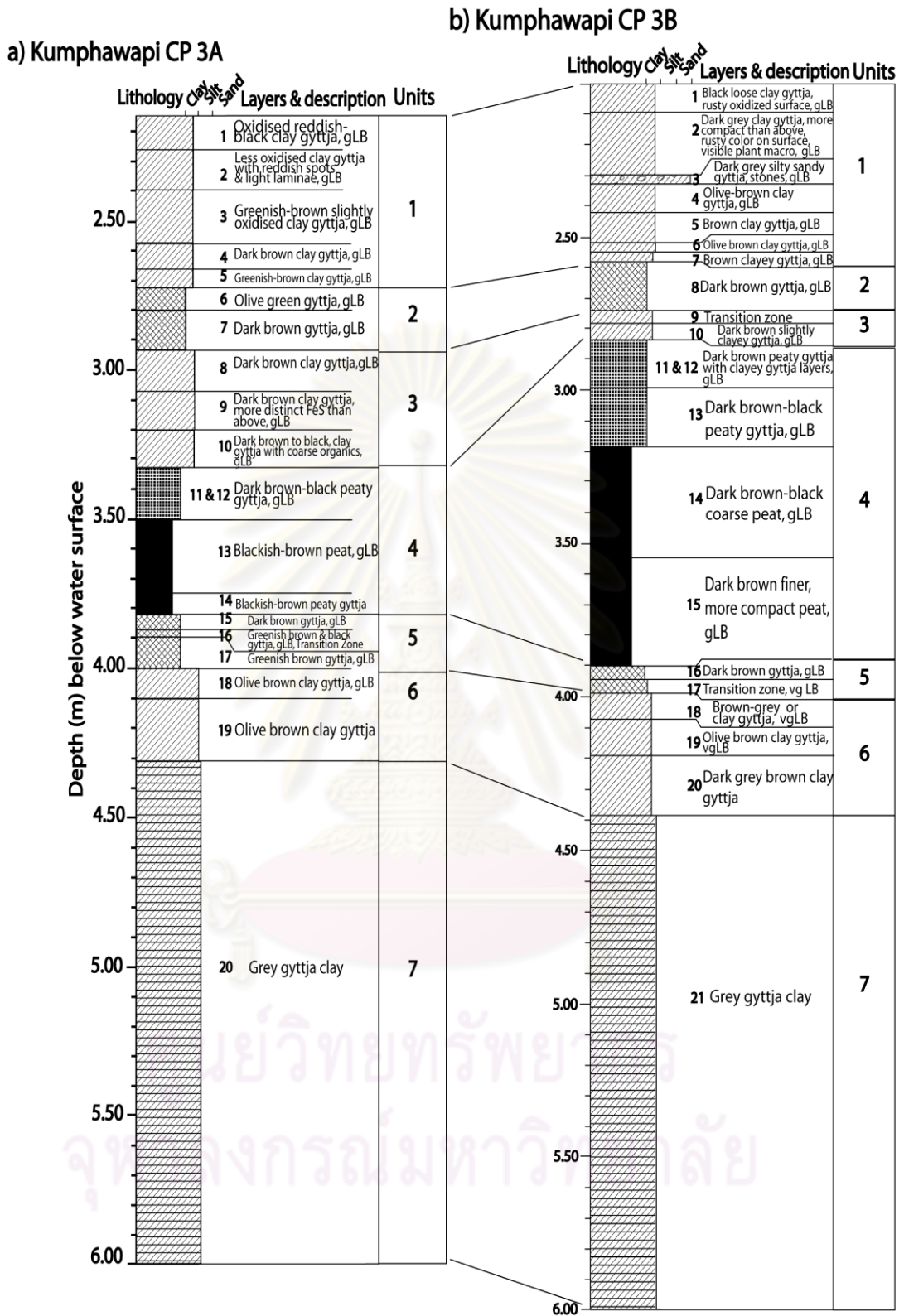


Figure 5-13 Lithostratigraphy of sediment sequences, Kumphawapi

(a) CP3A and (b) CP3B

5.2.3 Correlation between CP3A and CP3B

Although individual layers in the two sequences CP3A and CP3B are somewhat difficult to correlate with each other, sediment units 1-7 have a very good correspondence (Figure 5-13 a, b). CP3A and CP3B both show a change from low organic sediments at the bottom of the sequences to peat and peaty gyttja in the middle part. The upper part (unit 3-1) is characterized by gyttja and clay gyttja.

5.3 Loss-on ignition (LOI), mineral magnetic- susceptibility (MS) and X-ray fluorescence (XRF) of Kumphawapi CP3A

This section will present the results of the chemical analysis of the sediments according to their lithostratigraphy units (see Figure 5-14).

CP3A was divided into 20 layers which were grouped into 7 sediment units. The lowermost sediments (unit 7) between 6.00-4.31 m consist of grey gyttja clay. Magnetic susceptibility is around -2 to 6.5 S.I. units. LOI has values of 3 - 6% and the XRF data shows high values of Si (200-700 counts/s), high values of K (600-1000 counts/s), high values of Ti (2500-5000 counts), very low values of Mn, and high Fe values of 3000-6000 counts/s.

Unit 6 is between 4.31 and 4.00 m. The sediments consist of olive brown gyttja (layers 19-18). Magnetic susceptibility is around-2 to 5 S.I. units and loss-on ignition values are around 6 - 11%. The XRF data show a sharp decrease of Si (< 150 counts/s) and a shift in K values between 10–600 counts/s. In addition Ti values gradually decrease (< 3500 counts/s), while Mn shows very low values and Fe has values of <6500 counts/s.

Unit 5 includes layer 17-15 and is a greenish brown and black to dark brown gyttja. Magnetic susceptibility is around-2 to 3.2 S.I. units, LOI has values of 50-55% and major element counts are low.

The sediments in Unit 4 (3.82-3.33 m depth) consist of blackish-brown peaty gyttja and thick layers of blackish-brown peat; these are overlain by a dark brown- black peaty gyttja. Magnetic susceptibility values are around-2 to 3 S.I. units, LOI values are

around 30-60%, Si has very low values, K, Ti, Mn and Fe counts are low, but show higher values after a depth of 3.5 m.

Unit 3 (2.92-3.33 m depth) consists of a dark brown to black clay gyttja with coarse organics. Magnetic susceptibility is around 0 to 3.5 S.I. units, and LOI values are around 10-50%. Si and Fe counts are low in the lower part of the unit until about 3.20 m depth, where they start to increase and then gradually decrease towards the upper part of the unit. K and Ti counts show a similar pattern.

The sediments of Unit 2 (2.92-2.73 m depth) consist of dark brown and olive green gyttja (layers 6-7). Magnetic susceptibility is around 0 to 5.8 S.I. units, and LOI values are around >30-48%. Si, K and Ti counts are low, while Mn and Fe counts start to increase.

The uppermost unit 1 (layers 5-1) consists of greenish brown to dark brown clay gyttja, greenish brown slightly oxidized clay gyttja, oxidized clay gyttja with reddish spots and light laminae and oxidized reddish black clay gyttja at the top. Magnetic susceptibility is around 1 to 15 S.I. units and LOI values are around 18- 28%. The XRF data show an increase in all major elements counts.

Kumphawapi CP 3A

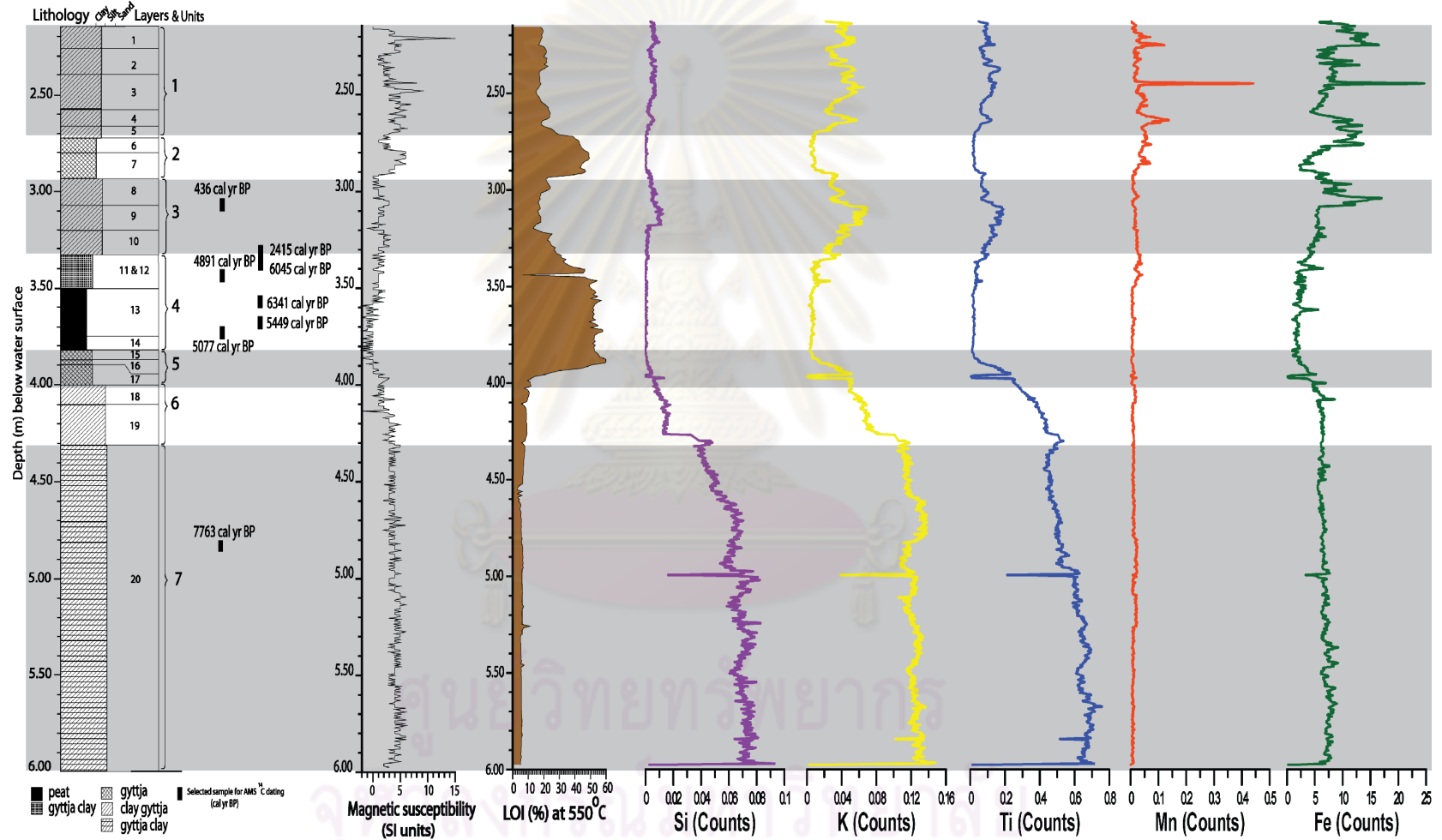


Figure 5-14 Lithostratigraphy , MS, LOI , XRF results and selected sample for ¹⁴C AMS dating

5.4 Chronology

The eight samples selected for AMS ^{14}C dating are shown in Figures 5-15 and 5-16 and in Table 5-3. The oldest sample is around 7,842-7,684 cal years B.P. and the youngest sample dates to around 436 cal years B.P. Samples UBA-14168 and UBA-14170 seem to be outliers, because they gave older ages than samples UBA-12662, UBA-12661 and UBA-14166. More samples are needed to constrain the chronology, and to evaluate whether UBA-14170 and UBA-14168 are really outliers, or whether samples UBA-12662, UBA-12661 and UBA-14166 instead gave too young ages. For the time being and for this work, the chronology will be based on all samples except for UBA-14170 and UBA-14168.

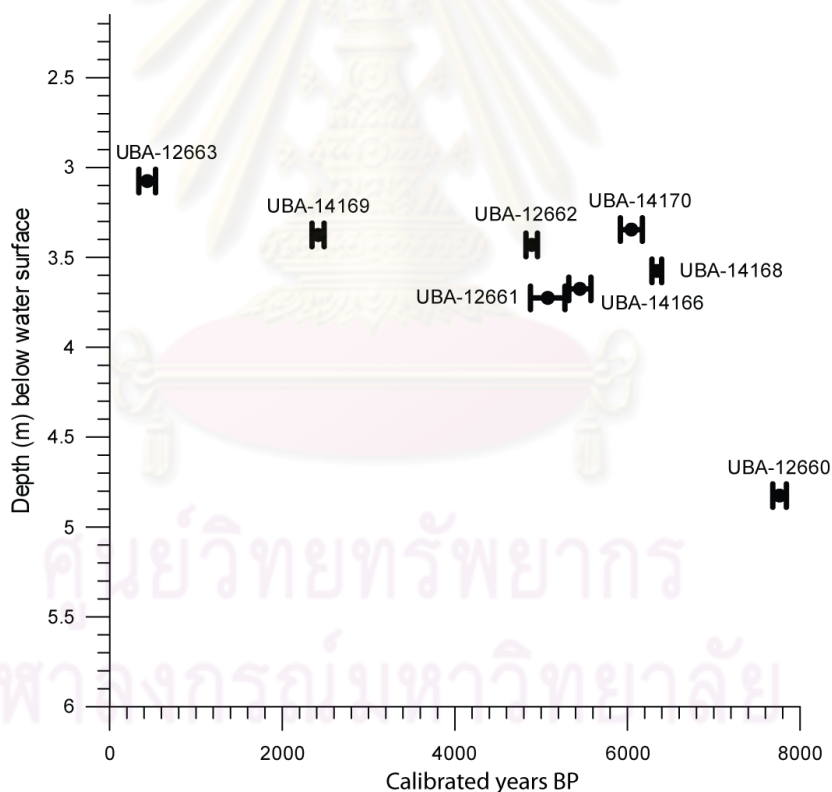


Figure 5-15 Results of ^{14}C AMS dating from Nong Han Kumphawapi are presented at the 2σ calibrated range (see also Table 5-3.).

According to the dating results, a depth of 3.075 m (Unit 3) would correspond to a mean age of 436 cal year BP and 3.375 m depth (Unit 3) to a mean age of 2415 cal

year BP. The top of unit 4 at 3.430 m depth has a mean age of 4891 cal year BP, unit 4 at 3.675 m depth a mean age of 5449 cal yr B.P., while the assumed age for 3.725 m depth is 5077 cal year B.P. The oldest (7763 cal yr B.P.) sample is in unit 7 at 4.825 m depth (Figure 5-15). The age of each sediment unit can be estimate based on an age-depth curve (Figure 5-16) as follows:

The top of Unit 7 (4.31-6.00 m depth), has an age of ca 6,500 cal years B.P. Unit 6 (3.90-4.31 m depth) has an age of between ca 6,500-6,000 cal years B.P., and Unit 5 (3.82-3.90 m depth) an age of between ca 6,000-5,600 cal years B.P. Unit 4 (3.33 - 3.82 m depth) has an age of around 5,600-1,500 cal years B.P. The age-depth curve indicates however a hiatus in the upper part of unit 4 or at the transition between units 4 and 3. This hiatus may have lasted between ~5,000 and 2,000/1,500 cal years B.P. Unit 3 (2.92 m - 3.33 m depth) has an age of around 2,000/1,500 – 200 cal years B.P. The upper part of the sediment core, units 1-2, (2.15-2.92 m depth) dates to between 200 cal years B.P. to present.

Table 5-3 Results of ^{14}C AMS dating of core CP3A

Units	Sample depth (m)	Mean sample depth (m)	Lab No.	^{14}C Age \pm error	Calibrated age yr BP 2σ	Calibrated age yr BP 2σ mean	Material
7	4.80-4.85	4.825	UBA-12660	6936 \pm 34	7842-7684	7763	Charcoal
4	3.75-3.70	3.725	UBA-12661	4432 \pm 30	5277-4877	5077	wood
4	3.70-3.65	3.675	UBA-14166	4689 \pm 30	5577-5321	5449	Chara, seeds, charcoal
4	3.60-3.55	3.575	UBA-14168	5526 \pm 28	6398-6285	6341.5	wood
4	3.45-3.41	3.43	UBA-12662	4282 \pm 30	4958-4824	4891	wood
3	3.39-3.36	3.375	UBA-14169	2385 \pm 24	2345-2486	2415.5	charcoal
4	3.36-3.33	3.345	UBA-14170	5228 \pm 28	6173-5918	6045.5	wood
3	3.10-3.05	3.075	UBA-12663	1639 \pm 29	339-533	436	Charcoal

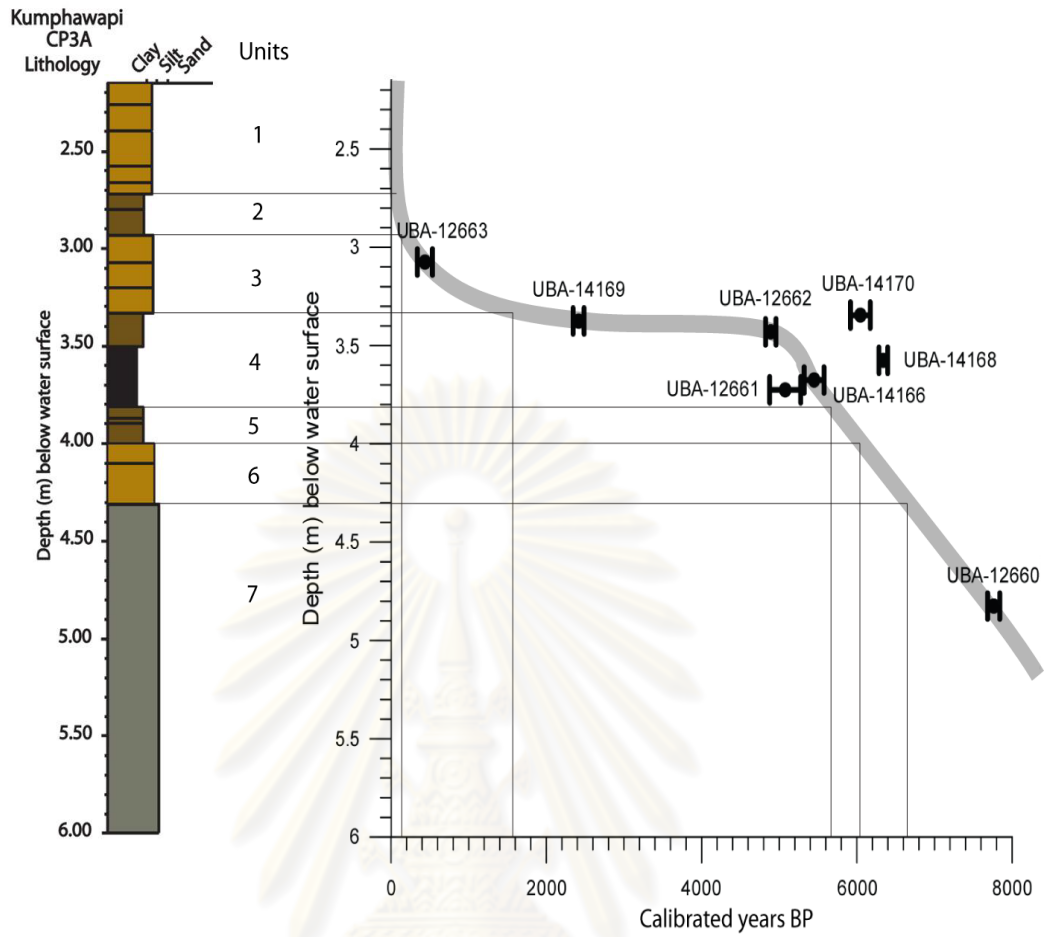


Figure 5-16 Age depth curve for CP3A.

ศูนย์วิทยทรัพยากร
จุฬาลงกรณ์มหาวิทยาลัย

CHAPTER VI

DISCUSSION AND CONCLUSIONS

6.1 Geographical feature, Land-use and land cover change, and Paleogeography of Nong Han Kumphawapi

Changing of the lake surface area in the year 1954 compared with the year 1996 represents reduced in the size from 44 km³ to 36 km³. The correlations of Land-use map from different time provide the change in land-use and land cover of Nong Han Kumphawapi area from the past to present. The oldest land cover map of this area was generated based on interpretation of aerial photos from the 1950s in conjunction with the ethnoecological field research undertake in 1979-1981 and 1994 by White (2004). Dry deciduous/dipterocarp forests were most common in this area, but with edaphically (plant communities that are found only in specific conditions) influenced zones and pockets of semi-evergreen and riparian/inundated forest. The vegetation mosaic is reflected in a patchy distribution of a wide range of subtropical natural resources including wild rice, yams, and other useful and edible plants, as well as wild animals.

Landuse map based on data of Land and Land development Department from the year 1985 shows the changed from natural forest to agricultural areas. The disturbance of dry dipterocarp/deciduous forests had occurred due to the expansion of agricultural area. The land-use map from the year 2001 shows the change in plantation; rice paddies and sugarcane still dominate. Eucalyptus and Para rubber plantation are starting to exist in the region. The lake feature had changed after the dam was built in 1994.

In conclusion, the results of this section show the change in lake feature and agricultural pattern in Nong Han Kumphawapi area. The lake was dam due to the irrigation project which supports the expansion of agriculture. Moreover, modern day agricultural take

advantage of the landscape mosaic to maintain a broadly based cropping system, although dependent on inundated rice, including both swidden and horticultural techniques. Overall, these results show the impact of human activities in the lake catchment area due to increasing of population and their demand for consumer.

6.2 Lithostratigraphic correlation

This section provides a correlation between the lithostratigraphies of this study (CP1, CP2, CP3, CP3A and CP3B) and KUM.3 (Penny, 1998) (Figure 6-1 and 6-2). CP1 consist of clay gyttja for the whole sequence. CP2 and CP3 consist of gyttja clay at the lowermost and overlain by, peat, gyttja and clay gyttja. These three sequences (CP1-CP3) show an incomplete data because they were taken near the lake margin. The sediment data of KUM.3 reveals a fine sand layer at the bottom, which suggests the periodic absence of water. This sequence does not appearing in the CP3A core. The change from sand to clay loam (KUM.3) in the overlying layer can be interpreted as the establishment of more permanent lake conditions. The clay loam sequence in KUM.3 can be well correlated with the gyttja clay in the bottom sequence of CP3A. In the KUM.3 core, the lacustrine clay loam changes to peat, which is interpreted as reflecting the widespread development of fringing swamp or flood plain vegetation due to a lowering of the lake water level, probably as a direct result of more arid condition? This section can be correlated to the changes from gyttja clay to higher organic sediments, such as gyttja and peat, respectively in CP3A. The peat sequence in the middle part of CP3A provides a clear correlation with the peat sequence of Penny's core. The upper part of CP3A consists of clay gyttja and gyttja. These sequences can be correlated with the organic clay in the upper part of Penny's core.

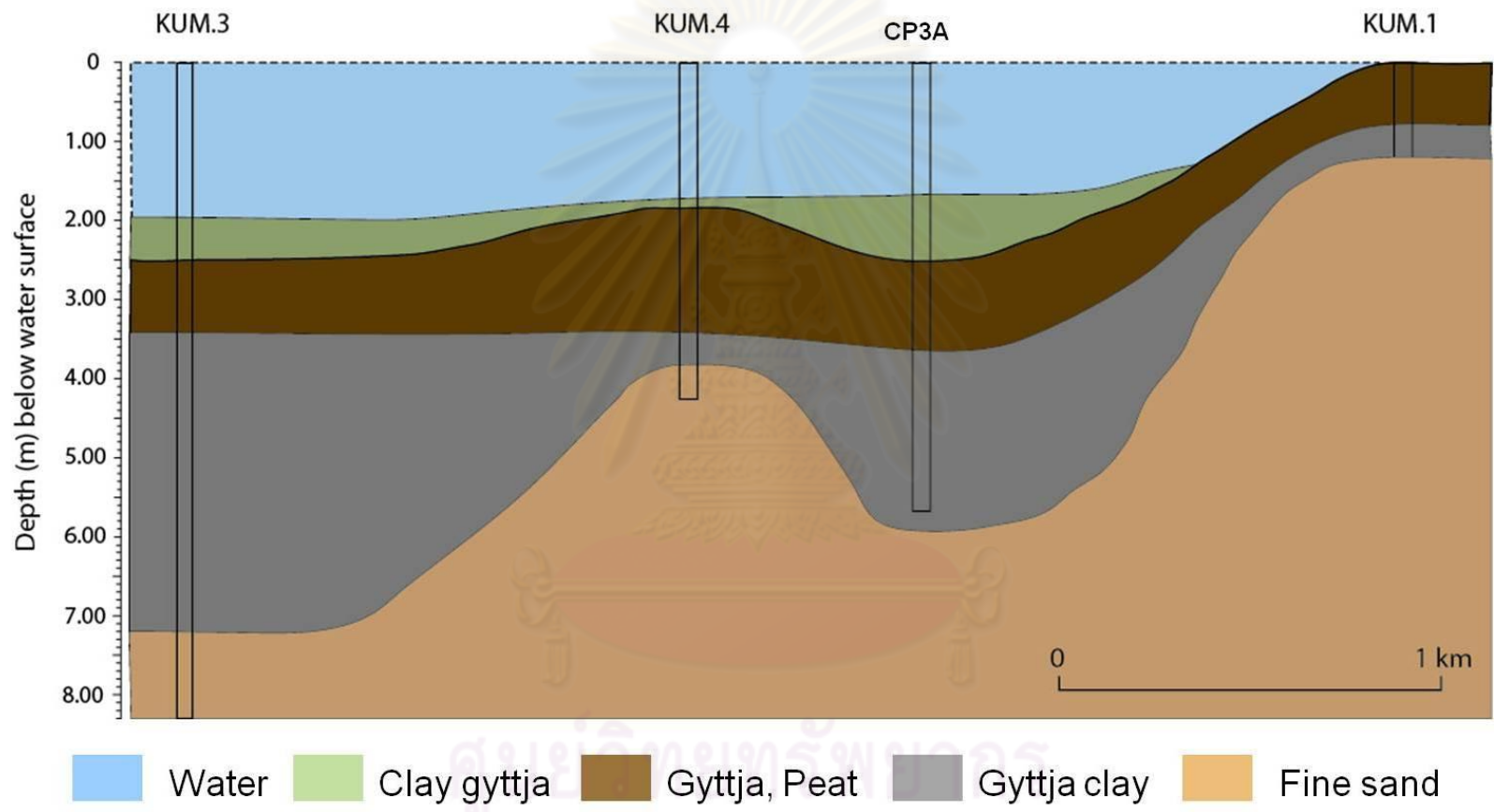


Figure 6-1 Cross section of CP3A coring point and three of Penny's cores.

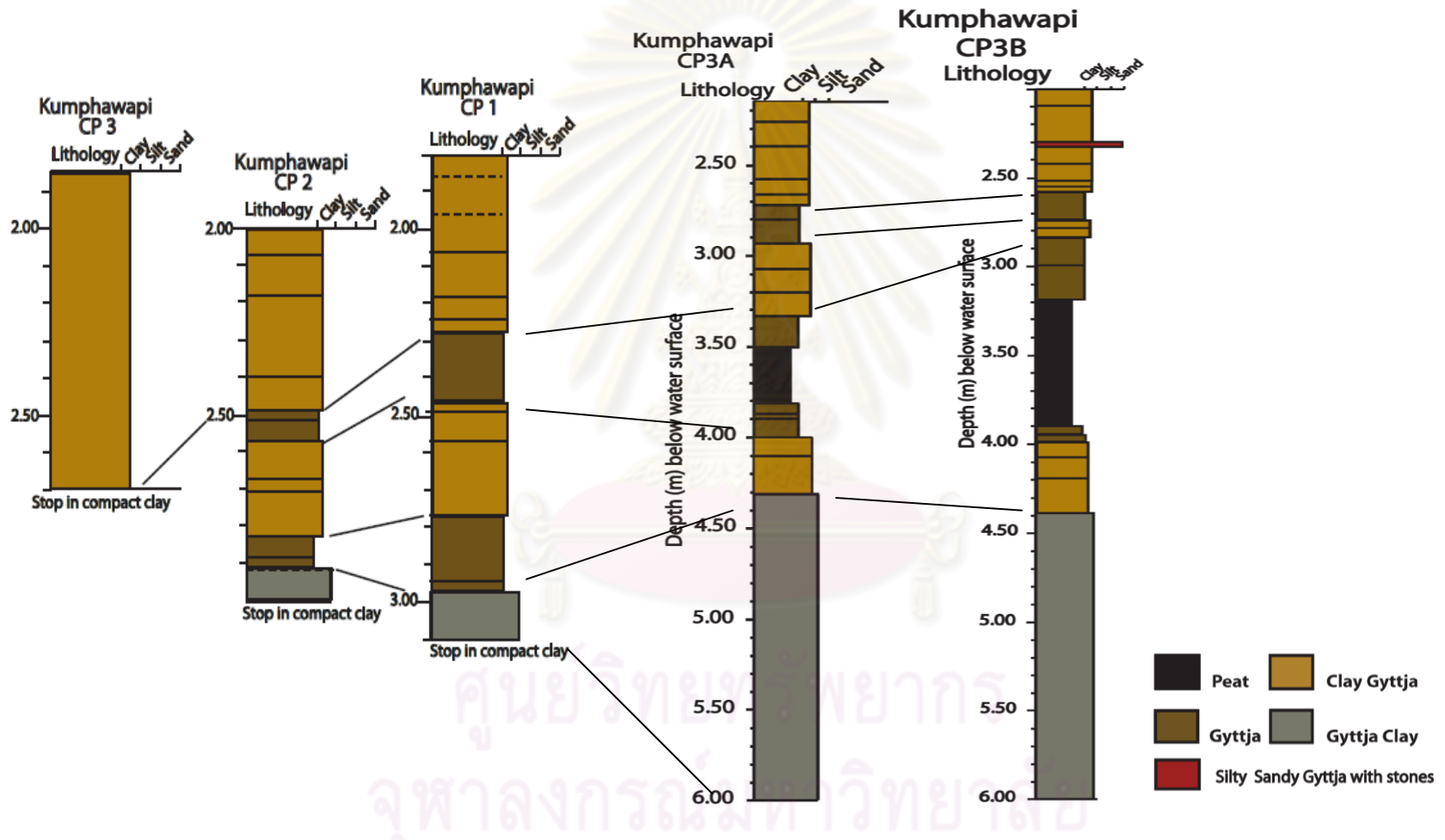


Figure 6-2 Lithostratigraphy correlation of CP1, CP2, CP3, CP3A and CP3B

6.3 Paleoenvironment, paleoclimatic and paleogeographic reconstruction

The bottom sediment of Penny's core have an age of 12,270 \pm 70 B.P. uncal. The pollen data suggest dry climate with low abundance of trees and low total species diversity and phytolith data show burning regime of the ground cover (Kealhofer, 1996, 2002) The conceptual model of paleogeography and paleoenvironment of this period show as below (see Figure 6-3a)

According to the age-depth model, the CP3A sediment sequence can be divided into five time periods (Table 6-1).

> 6000 cal yr B.P.

The sediments and their proxy data may indicate a high lake level, with low productivity and high sediment input from the catchment area. The higher Si, K and Ti counts are possibly related to increasing sediment input. Low values for LOI indicate low organic content of the sediments. The homogenous, gyttja clay accumulated during this time is suggestive of open water condition and gradually infilling of the basin. However, around 7000 cal yr B.P., a decrease in Si, K and Ti counts is observed and possibly relates to decreasing sediment input. This is correlated to higher values of LOI, which indicate higher organic content of the sediments. Moreover, palynological data (Penny, 1999) show that this period may have been substantially more humid than present. The combined data may thus suggest an interval of higher monsoon intensity. The conceptual model of paleogeography and paleoenvironment of this period show as below (see Figure 6-3b)

6000 - 5000 cal yr B.P.

The gyttja clay sequence in the lowermost part changes into peat sequence which corresponds to very high LOI values, low MS values and low K, Ti and Si counts. This may indicated a productive wetland and a low level lake with low minerogenic input.

This change seems to represent not a gradual natural infilling, but an external process. Human activities may cause this abrupt change, but based on archaeological data, there is no evidence of any settlement before ca 5,000 years B.P. Thus, a gradual natural infilling seems more reasonable than human activities. Another cause for the lake level lowering might have been erosion of the outflow. The outflow occurs today however in a broad floodplain with a very low slope. It seems therefore not possible that erosion of the outflow could have caused the rapid lake level lowering. The last possibility could be climate change. From palynological data (Penny, 1999) a decrease in forest pollen taxa is indicated. Moreover, higher charcoal particles during this interval could indicate more frequent or more intense fires. Taken together, the data suggest a dry environment, which may indicate a decrease in monsoon intensity. The conceptual model of paleogeography and paleoenvironment of this period show as below (see Figure 6-3c)

5000 - 2000 cal yr B.P.

The age-depth curve indicates a hiatus around 5000 cal yr B.P., or a very low sedimentation rate. During a period of about 3000 years only around 30 cm of sediment seems to have been deposited. The lake level is low and the lake receives low minerogenic input. This interesting period could have occurred naturally through a decrease in monsoon intensity or could be related to human activities. The Ban Chiang culture phase I-VI occurred during this period. Prehistoric settlements established on the low terrace around the margin of the highest lake level. The conceptual model of paleogeography and paleoenvironment of this period show as below (see Figure 6-3d)

2000 - 400 cal yr B.P.

The sediments during this interval point to a rise in lake level and to wetter conditions. Lower LOI values and higher minerogenic material as indicated by major

elements supports the rise in lake level and could suggest stronger monsoon intensity. The finer grained clay gyttja suggests lower energy inflow as compared to the bottom sediments. In addition, Phase VI of Ban Chiang occurred around this period of time. Ban Muang Phruk (in Nong Han Kumphawapi lake cluster) has a pottery style that is closest to the pottery style of Ban Chiang phase VI. The conceptual model of paleogeography and paleoenvironment of this period show as below (see Figure 6-3e)

400 cal yr B.P. to present

During the early part of this interval, the lake level seems to decrease again, as indicated by lower counts in major elements. However, in the middle part and up to present, the lake level is higher, as is the minerogenic input to the lake. Sometime during this period, Nong Han Kumphawapi probably attained its present status. The conceptual model of paleogeography and paleoenvironment of this period show as below (see Figure 6-3e)

Overall, the sediments and the combined proxy data indicate that Nong Han Kumphawapi underwent several phases with higher/lower lake levels, which potentially could be related to changes in monsoon intensity. The sediment from Nong Han Kumphawapi therefore seems a good archive to reconstruct past monsoon intensity.

6.4 Relationship between archaeological sites and paleogeography

The following map (Figure 6-4) shows the relationship between archaeological sites and paleogeography. Location of prehistoric and historic sites (Figure 6-4) report here after Kijngam and Higham (1983) excavation in 1980-1981. Historic sites occur nearer to the perennial lake than the prehistoric sites. Prehistoric sites are mostly established further around the highest lake level Most of the establishment is on low terrace.

The highest lake level occurs in > 6000 cal yr B.P. with there is no evidence of human interaction during this period of time. The abrupt lowering of lake level occurs during 6000 - 5000 cal yr B.P. while the Ban Chiang cultural started after the end of this period. The first human occupation occurs while the lake is in the transition stage (5000-2000 cal yr. B.P.) of the lower lake level to the lake present status. Prehistoric settlement distribution pattern shows a fairly dense network of sites. The early prehistoric sites occupied the margins of the Kumphawapi flood plain and that later sites occupied the more hazardous terrain nearer to the lake (Figure 6-4). The lake attained its present status during 2000 cal yr B.P. to present correspond to the occurrences of historical sites. The historical sites occupied nearer area to the lake and along the Lam Pao River.

The later settlement (especially, historical sites) shows the close relationship between human activities and the lake. The change of occupation from hunting and gathering to agriculture leads human move closer to water. Thus, the movement of the settlements could reflect a pressure by expanding population and their need for water.

ศูนย์วิทยทรัพยากร
จุฬาลงกรณ์มหาวิทยาลัย

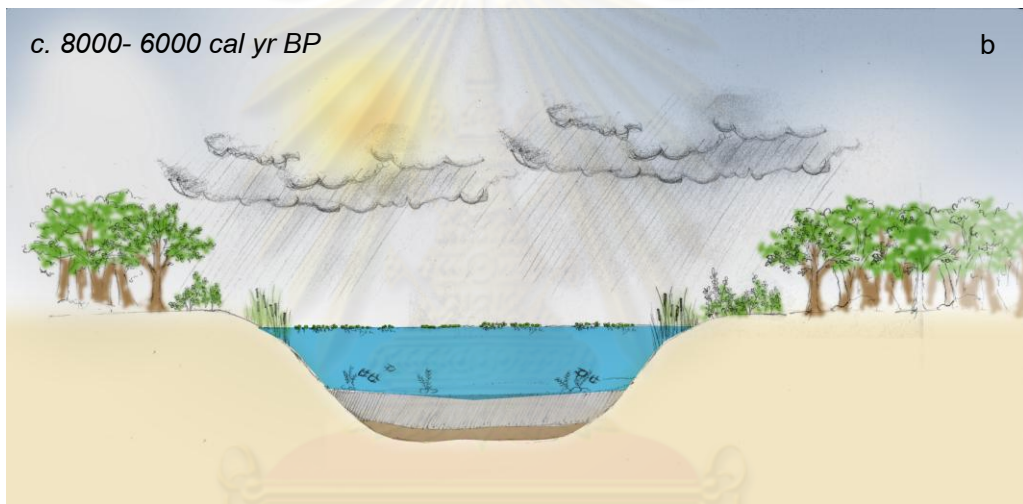
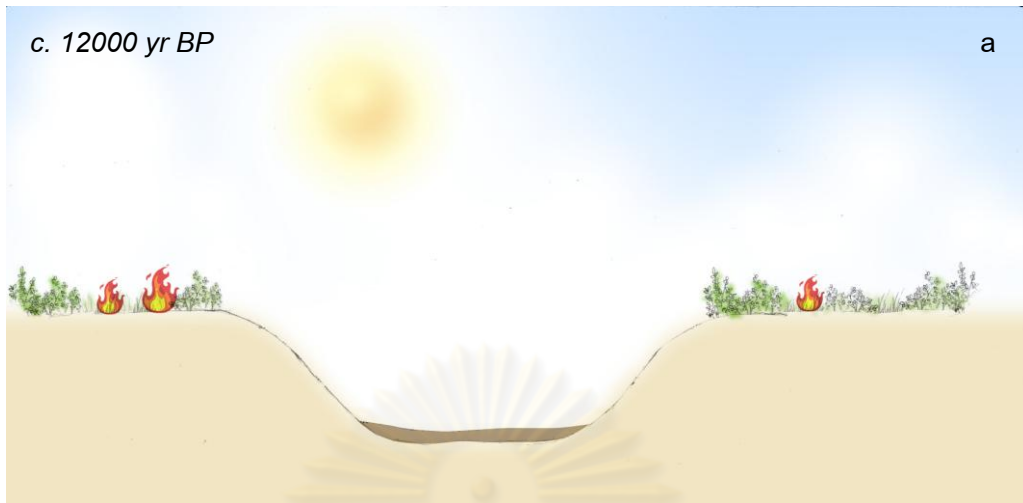
Table 6-1 Paleoenvironment and paleoclimate of Nong Han Kumphawapi

<i>Age cal yr B.P.</i>	<i>Age (B.C.)</i>	Lake characteristic	Indicators	Climate condition	Monsoon intensity
Middle part of interval to present		Higher lake level High minerogenic input Low productivity	MS + XRF+ LOI -	Warm and wet	+
400 cal yr B.P. to present Early part of interval	1550 A.D. to present	Low lake level Low minerogenic input	MS - XRF -	Warm and wet	
2000 - 400 cal yr B.P.	50 B.C.- 1550 A.D.	Rise in lake level High minerogenic input Low productivity	MS + XRF+ LOI -	Warm and wet	+
5000 - 2000 cal yr B.P. (Hiatus)	3050- 50B.C.	Low lake level Low minerogenic input Productive wetland	MS - XRF- LOI +	Cold and dry	-
6000 - 5000 cal yr B.P	4050-3050 B.C.	Low lake level Low minerogenic input Productive wetland	MS - XRF - LOI +	Cold and dry	--
> 6000 cal yr BP	>4050 B.C.	High lake level High minerogenic input Low productivity	MS + XRF + LOI -	Warm and wet	++

Remark*

+ = Strong monsoon intensity ++ = Stronger monsoon intensity

- = Weak monsoon intensity -- = Weaker monsoon intensity



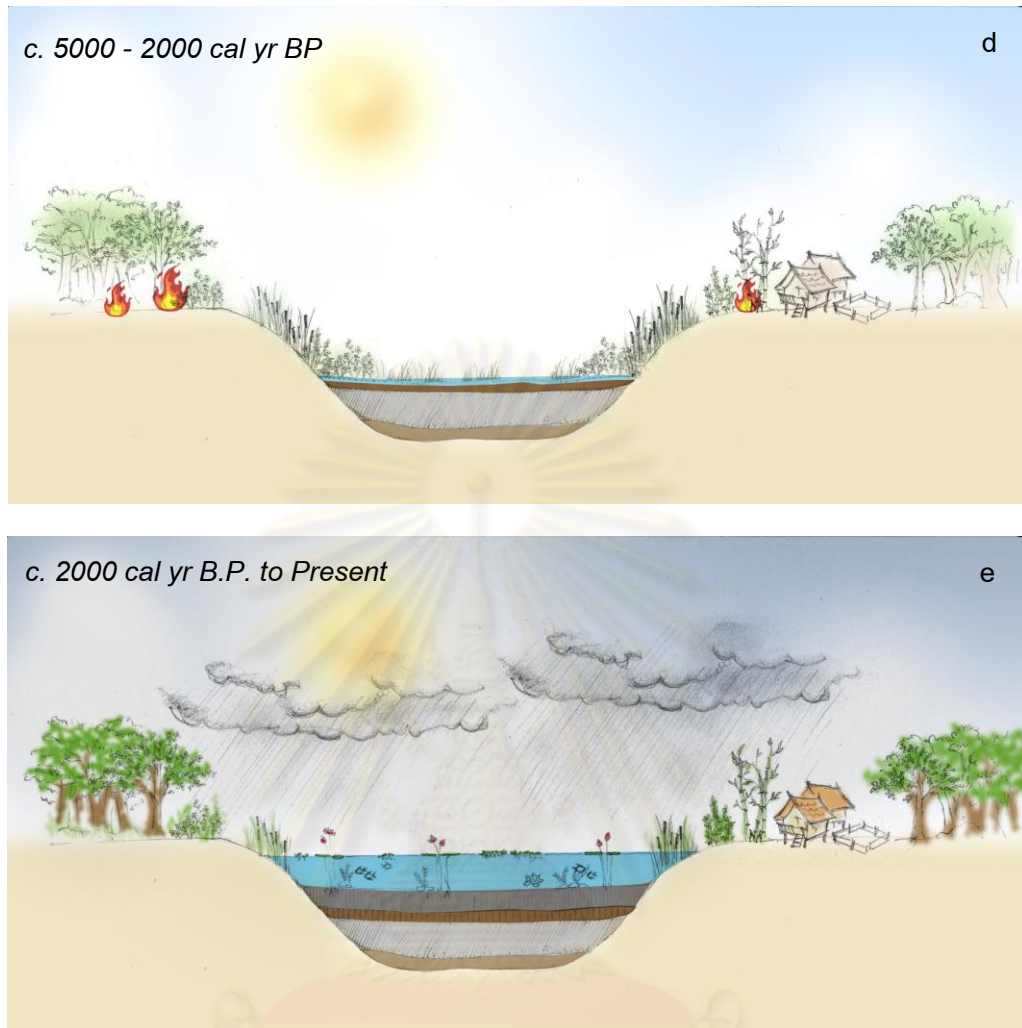


Figure 6-3 a-e Conceptual model suggests five stages of lake level and its paleoenvironment.

ศูนย์วิทยทรัพยากร
จุฬาลงกรณ์มหาวิทยาลัย

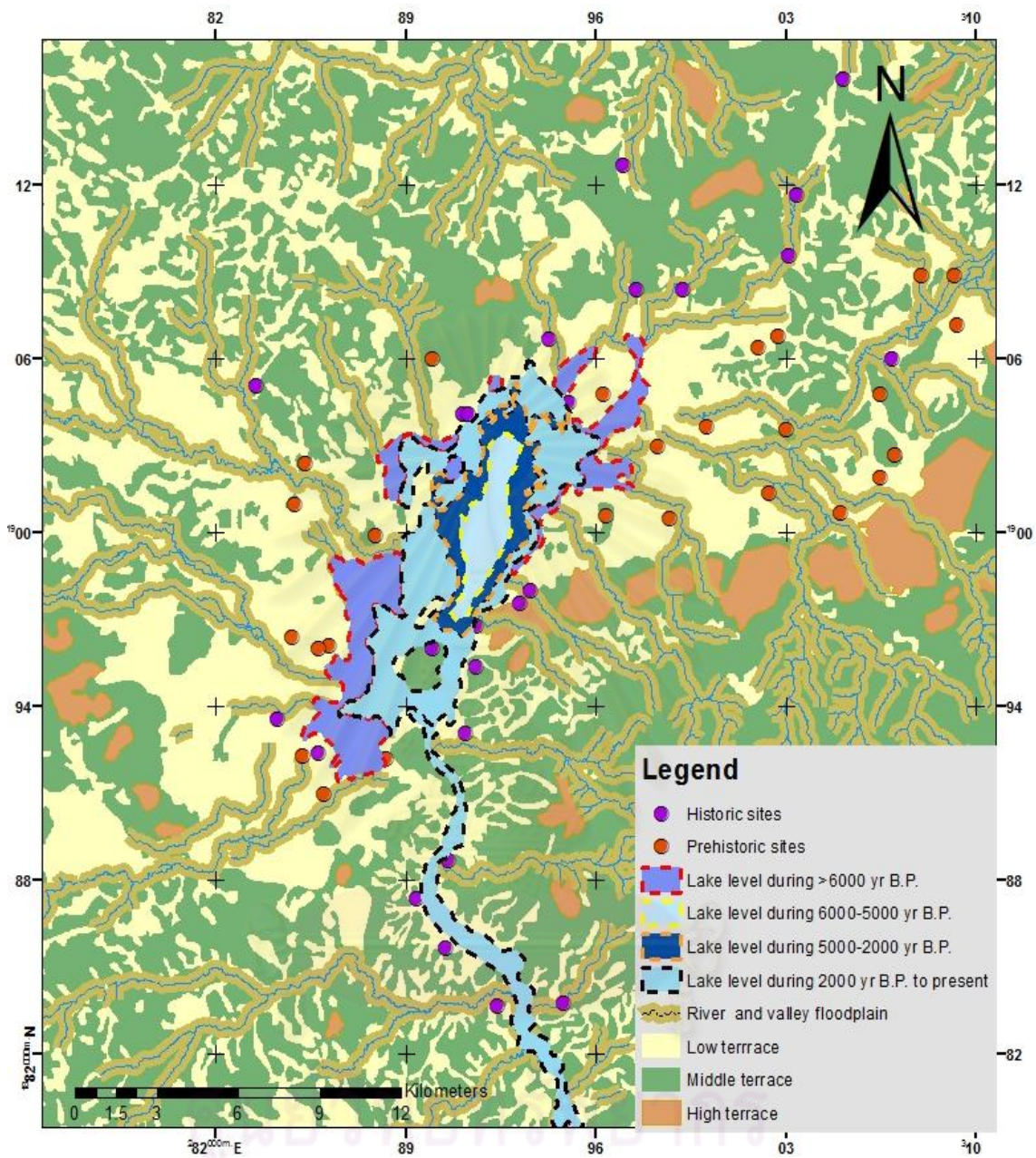


Figure 6-4 Paleogeographic map with archaeological sites of Nong Han Kumphawapi

REFERENCES

- Abram, N. et al., 2007. Seasonal characteristics of the Indian Ocean Dipole during the Holocene epoch. *Nature* 445: 299-302.
- An, Z., 2000. The history and variability of the East Asian paleomonsoon climate. *Quaternary Science Reviews* 19: 171-187.
- An, Z. et al., 2000. Asynchronous Holocene optimum of the East Asian monsoon. *Quaternary Science Reviews* 19: 743-762.
- Bellwood, P., 1997. *Prehistory of the Indo-Malaysian Archipelago*, Revised Edition. University of Hawaii Press, Honolulu.
- Bengtsson L. and Enell M., 1986. Chemical analysis. In: Berglund B.E. (ed.). *Handbook of Holocene Palaeoecology and Palaeohydrology*. 423-454.
- Bird, M.I., Taylor, D., and Hunt, C., 2005. Palaeoenvironments of insular Southeast Asia during the Last Glacial Period: a savanna corridor in Sundaland?. *Quaternary Science Reviews* 24: 2228-2242.
- Birks, H. J. B. and Birks, H. H., 1980. *Quaternary palaeoecology*, Edward Arnold, London.
- Björck, S., Dearing, J.A. and Jonsson A., 1982. Magnetic susceptibility of Late Weichselian deposits in southeastern Sweden. *Boreas* 11: 99-111.
- Björck, S., and Wohlfarth, B. Chapter 10, ¹⁴C chronostratigraphic techniques in paleolimnology. In *Tracking Environmental Change Using Lake Sediments* 1: 205-245.
- Bunopas, S. et al., 1976. Catastrophic Loess, mass mortality and forest fires suggest that a Pleistocene cometary impact in Thailand caused the Australasian Tektite field. *Journal of the Geol. Society of Thailand* 1: 1-17.
- Buckley, B., Palakit, K., Duangsathaporn, K., Sanguantham, P., and Prasomsin, P., 2007, Decadal scale droughts over northwestern Thailand over the past 448 years: links to the tropical Pacific and Indian Ocean sectors: *Climate Dynamics* 29: 63-71.

- Buffetaut E., Ingavat R., 1982. Phytosaur remains (Reptilia, Thecodontia) from the Upper Triassic of north-eastern Thailand. *Geobios* 15: 7–17.
- Croudace I.W., Rindby A. & Rothwell R.G., 2006. ITRAX: description and evaluation of a new multi-function X-ray core scanner. *New techniques in sediment core analysis* 267: 51–63.
- Cruz, F.W. et al., 2005. Insolation-driven changes in atmospheric circulation over the past 116,000 years in subtropical Brazil. *Nature* 434: 63-66.
- Dam, R. A. C., Fluin, J., Suparan, P., and van der Kaars, S., 2001. Palaeoenvironmental developments in the Lake Tondano area (N. Sulawesi, Indonesia) since 33,000 yr B.P. *Palaeogeography, Palaeoclimatology, Palaeoecology* 171: 147-183.
- Dean W. E., 1974. Determination of carbonate and organic matter in calcareous sediments and sedimentary rocks by loss on ignition; comparison with other methods. *Journal of Sedimentary Petrology* 44: 242-248.
- Department of Geosciences, University of Arizona, 2007. *Radiometric and chemical dating techniques*. [Online]. Available from: <http://www.geo.arizona.edu/palynology/geos462/10radiometric.html> [2009, May 1]
- Fleitmann, D. et al., 2007. Holocene ITCZ and Indian monsoon dynamics recorded in stalagmites from Oman and Yemen (Socotra). *Quaternary Science Reviews* 26: 170-188.
- Godwin H., 1962. Half-life of radiocarbon. *Nature* 195: 984.
- Gupta, A.K., Anderson, D.M., and Overpeck, J.T., 2003. Abrupt changes in the Asian southwest monsoon during the Holocene and their links to the North Atlantic Ocean 421: 354-357.
- Hajdas, I., Bonani, G., Moreno, P.I., and Ariztegui, D., 2003. Precise radiocarbon dating of Late-Glacial cooling in mid-latitude South America. *Quaternary Research* 59: 70-78.
- Haile, N. H., 1973. *Note on Triassic fossil pollen from the Nam Pha Formation, Chulaporn (Nam Prom), Thailand*. Geological Society of Thailand.

- Heiri, O., et al, 2001. Loss on ignition as a method for estimating organic and carbonate content in sediments: reproducibility and comparability of results. *Journal of Paleolimnology* 25: 101-110.
- Hellborg, R., and Skog G., 2008. Accelerator mass spectrometry. *Mass Spectrometry Reviews* 27(5): 398-427.
- Herzschuh, U., 2006. Paleo-moisture evolution in monsoonal Central Asia during the last 50,000 years. *Quaternary Science Reviews* 25: 163-178.
- Higham, C., Kijngam, A., 1980. An archaeological site survey in N.E. Thailand, 1980. *Silapakorn* 24(4): 26-30.
- Higham, C.F.W., 1996. *The Bronze Age of Southeast Asia*. Cambridge University Press, Cambridge.
- Hong, Y.T. et al., 2003 Correlation between Indian Ocean summer monsoon and North Atlantic climate during the Holocene. *Earth and Planetary Science Letters* 211: 371-380.
- Hu, Q. et al., 2004. Radiocarbon in tropical tree rings during the Little Ice Age. *Nuclear Instruments and Methods in Physics Research B* 223-224: 489-494.
- Hu, C. et al., 2008. Quantification of Holocene Asian monsoon rainfall from spatially separated cave records. *Earth and Planetary Science Letters* 266: 221-232.
- Hua, Q. et al., 2004. Radiocarbon in tropical tree rings during the Little Ice Age: *Nuclear Instruments and Methods in Physics Research Section B: Beam Interactions with Materials and Atoms* 223-224: 489-494.
- Iwai, J., Asama, K., Veeraburus, M. and Hongnusunthi, A., 1966. Stratigraphy of the so-called Khorat Series and a note on the fossil plants bearing Paleozoic strata in Thailand. *Geology and Paleontology of Southeast Asia* 2: 179-196.
- Kealhofer, L., 1996. Human-Environmental Relationships in Prehistory: An Introduction to Current Research in South and Southeast Asia. *Asian Perspectives* 35: 111-117.
- Kealhofer, L., and Penny, D., 1998. A combined pollen and phytolith record for fourteen thousand years of vegetation change in northeastern Thailand. *Review of Palaeobotany and Palynology* 103: 83-93.

- Khedari, J., Sangprajak, A. and Hirunlabh, J., 2002. Thailand climatic zones. *Renewable Energy* 25: 267-80.
- Kijngam, A., Higham, C., and Wiriyaromp, W., 1980. Prehistoric settlement patterns in Northeast Thailand. *Studies in prehistoric anthropology* 15.
- Kutzbach, J. E., 1981. Monsoon climate of the early Holocene: Climatic experiment using earth's orbital parameters for 9000 Years Ago. *Science* 214: 59-61.
- Liew, P.M., Lee, C.Y., and Kuo, C.M., 2006. Holocene thermal optimal and climate variability of East Asian monsoon inferred from forest reconstruction of a subalpine pollen sequence, Taiwan. *Earth and Planetary Science Letters* 250: 596-605.
- Loßffler, E., Thompson, W.P., and Liengsakul, M., 1984. Quaternary geomorphological development of the lower Mun River Basin, North East Thailand. *CATENA* 11: 321-330.
- Maxwell, A.L., 2001. Holocene Monsoon Changes Inferred from Lake Sediment Pollen and Carbonate Records, Northeastern Cambodia. *Quaternary Research* 56: 390-400.
- Meesook A., Suteethorn, V. and Wongprayoon, T., 1995. Early Cretaceous non-marine bivalves of the Sao Khua Formation, Khorat Group, northeastern Thailand, 3rd symposium. *IGCP* 350: 10-11.
- Moore, E. H., 1988. Notes on two types of moated settlements in North East Thailand. *Journal of the Siam Society* 76: 275-287.
- Morrill, C., Overpeck, J.T., and Cole, J.E., 2003. A synthesis of abrupt changes in the Asian summer monsoon since the last deglaciation. *The Holocene* 13: 465-476.
- Morrill, C. et al., 2006. Holocene variations in the Asian monsoon inferred from the geochemistry of lake sediments in central Tibet. *Quaternary Research* 65: 232-243.
- Nakagawa, T., et al., 2003. Asynchronous climate changes in the North Atlantic and Japan during the last termination. *Science* 299: 688-691.
- O' Sullivan, P. E. & Reynolds, C. S., 2004. The Lakes Handbook Volume 1 limnology and limnetic ecology. 1 st ed. Oxford Blackwell.

- Parry, J.T., 1992. The investigative role of Landsat-TM in the examination of pre- and proto-historic water management sites in Northeast Thailand. *Geocarto International* 4: 5-24
- Partin, J.W. et al., 2007. Millennial-scale trends in west Pacific warm pool hydrology since the Last Glacial Maximum. *Nature* 449: 452-455.
- Penny, D., 1998. Late Quaternary Palaeoenvironments in the Sakon Nakhon Basin, North-east Thailand, Monash University, Victoria, Australia.
- Penny, D., 1999, Palaeoenvironmental analysis of the Sakon Nakhon Basin, northeast Thailand palynological perspectives on climate change and human occupation. *Indo-Pacific Prehistory Association Bulletin* 18: 139-149.
- Penny, D., 2001, A 40,000 year palynological record from north-east Thailand; implications for biogeography and palaeo-environmental reconstruction. *Palaeogeography, Palaeoclimatology, Palaeoecology* 171: 97-128.
- Penny, D., Grindrod, J., and Bishop, P., 1996, Holocene palaeoenvironmental reconstructions based on microfossil analysis of a lake sediment core, Nong Han Kumphawapi, Udon Thani, Northeast Thailand. *Asian Perspectives* 35 (2): 209-228.
- Penny, D., and Kealhofer, L., 2005, Microfossil evidence of land-use intensification in north Thailand. *Journal of Archaeological Science* 32: 69-82.
- Purdue Rare Isotope Measurement Laboratory, Purdue University. *What is AMS?*. [Online]. Available from: <http://www.physics.purdue.edu/primelab/introduction/ams.html> [2009, May 1]
- Rau, J. L., and Supajanya, T., 1985. *Sinking cities of Thailand*, paper presented at Conference on Geology and Mineral Resources Development of the Northeast, Thailand, Khon Kaen University Thailand.
- Rashid, H., Flower, B.P., Poore, R.Z., and Quinn, T.M., 2007. A ~25 ka Indian Ocean monsoon variability record from the Andaman Sea. *Quaternary Science Reviews* 26: 2586-2597.
- Reimer, P. et al., 2004. IntCal04 Terrestrial Radiocarbon Age Calibration, 0-26 cal kyr BP. *Radiocarbon* 46: 1029-1058.

- Sandgren, P. & Snowball, I.F., 2002. Application of mineral magnetic techniques to paleolimnology. In: W.M. Last & J.P. Smol (eds.) *Tracking Environmental Changes in Lake Sediments: Physical and Chemical Techniques. Developments in Paleoenvironmental Research Book Series*, Kluwer Academic Publishers.
- Shakun, J.D. et al., 2007. A high-resolution, absolute-dated deglacial speleothem record of Indian Ocean climate from Socotra Island, Yemen. *Earth and Planetary Science Letters* 259: 442-456.
- Sinsakul, S., Chaimanee, N. and Tiyaipairach, S., 2002, Quaternary geology of Thailand: in Mantajit, M., editor-in-chief, *Proceedings of the Symposium on Geology of Thailand*: Department of Mineral Resources, Bangkok, Thailand.
- Sinsakul, S., Chaimanee, N., and Tiyaipairach, S., 2002. Quaternary Geology of Thailand, *Proceedings of the Symposium on Geology of Thailand 26-31 August 2002, Bangkok, Thailand*: Geological Survey Division, Department of Mineral Resources, Bangkok, Thailand.
- Sirocko, F., Garbe-Schonberg, D., McIntyre, A., and Molino, B., 1996, Teleconnections Between the Subtropical Monsoons and High-Latitude Climates During the Last Deglaciation. *Science* 272: 526-529.
- Stott, L., Timmermann, A., and Thunell, R., 2007. Southern Hemisphere and deep-sea warming led deglacial atmospheric CO₂ rise and tropical warming. *Science* 318: 435-438.
- Thompson, L. et al., 2000. A high-resolution millennial record of the South Asian Monsoon from Himalayan ice cores. *Science* 289: 1916-1919.
- Visser, K., Thunell, R., and Stott, L., 2003. Magnitude and timing of temperature change in the Indo-Pacific warm pool during deglaciation. *Nature* 421: 152-155.
- Von Post, H. 1862, Studier sfver Nutidens koprogena. *Jordbildningar, Gyttja, Dy, lorf, och Mylla. Kgl. Svenska Vatten-skapsakad, Handl.4-1:1-59.*
- Walker, M., 2005, *Quaternary dating methods*. England: John Wiley and Sons Ltd.
- Wang, B., Clemens, S.C., and Liu, P., 2003, Contrasting the Indian and East Asian monsoons: implications on geologic timescales. *Marine Geology* 201: 5-21.

- Wang, P. et al., 2005. Evolution and variability of the Asian monsoon system: state of the art and outstanding issues. *Quaternary Science Reviews* 24: 595-629.
- Wang, S., Lü, H., Liu, J., and Negendank, J., 2007. The early Holocene optimum inferred from a high-resolution pollen record of Huguangyan Maar Lake in southern China. *Chinese Science Bulletin* 52: 2829-2836.
- Wang, Y. et al., 2008. Millennial- and orbital-scale changes in the East Asian monsoon over the past 224,000 years. *Nature* 451: 1090-1093.
- White, J.C., 1986. *A Revision of the Chronology of Ban Chiang and its Implications for the Prehistory of Northeast Thailand*. Unpublished Ph.D. Thesis: University of Pennsylvania, Philadelphia.
- White, J.C., 1995. Modeling the Development of Early Rice Agriculture: Ethnoecological Perspectives from Northeast Thailand. *Asian Perspectives* 34: 37-68.
- White, J.C., 1997. A brief note on new dates for the Ban Chiang cultural tradition. *Bulletin of the Indo-Pacific Prehistory Association* 16: 103-106.
- White, J.C., Penny, D., Kealhofer, L., and Maloney, B., 2004. Vegetation changes from the late Pleistocene through the Holocene from three areas of archaeological significance in Thailand: *Quaternary International* 113: 111-132.
- Wohlfarth, B., Hannon, G., Feurdean, A., Ghergari, L., Onac, B.P., and Possnert, G., 2001. Reconstruction of climatic and environmental changes in NW Romania during the early part of the last deglaciation (~15,000-13,600 cal yr BP). *Quaternary Science Reviews* 20: 1897-1914.
- Wongsawat, S., Dhanesvanich, O., and Panjasutarous, S., 1992. Groundwater resources of Northeastern Thailand. *Proc. of National Conf. on Geologic Resources of Thailand: Potential for Future Development*: DMR, Bangkok, Thailand.
- Wongsomsak, S., 1992. Preliminary investigation on Mekhong terraces in Nakhon Phanom Province: Distribution, Characteristic, age and imbrication. *Proceedings of a National Conference on Geologic Resources of Thailand: Potential for future Development*: Department of Mineral Resources, Bangkok, Thailand.
- Zhao, J., Wang, Y., Collerson, K. D., and Gagan, M. K., 2003. Speleothem U-series of semi-synchronous climate oscillations during the last deglaciation. *Earth and*

Planetary Science Letters 216: 155-161.

Zickfeld, K., Knopf, B., Petoukhov, V., and Schellnhuber, H. J., 2005. Is the Indian summer monsoon stable against global change. *Geophysical Research Letters* 32.



ศูนย์วิทยทรัพยากร
จุฬาลงกรณ์มหาวิทยาลัย



APPENDIX

ศูนย์วิทยทรัพยากร
จุฬาลงกรณ์มหาวิทยาลัย

LOI Data of 379 samples

sample No.	Depth	LOI 550°C %	LOI 950°C %
1	5.975	4.96997	1.865616
2	5.965	5.037067	1.909211
3	5.955	5.221339	1.910055
4	5.945	5.462446	2.058763
5	5.935	5.642715	2.086602
6	5.925	5.459982	2.037718
7	5.915	5.457204	2.085899
8	5.905	5.522811	1.994029
9	5.895	5.563432	1.98475
10	5.885	5.562799	1.999131
11	5.875	5.635236	2.044971
12	5.865	5.603336	2.036561
13	5.855	5.652144	2.059768
14	5.845	5.70486	2.01561
15	5.835	5.891892	2.058559
16	5.825	6.089076	2.072013
17	5.815	5.979855	2.097594
18	5.805	5.864449	2.083423
19	5.795	5.838389	2.17181
20	5.785	5.901474	2.128926
21	5.775	6.001375	2.116688
22	5.765	5.950508	2.097935
23	5.755	6.009701	2.11142
24	5.745	6.006819	2.154582
25	5.735	5.939801	2.220272
26	5.725	5.902598	2.209311
27	5.715	5.847104	2.236547
28	5.705	5.842296	2.26564
29	5.695	5.779468	2.326305
30	5.685	5.655995	2.432517
31	5.675	5.588682	2.596761
32	5.665	5.687989	2.328578
33	5.655	5.698474	2.290793
34	5.645	5.683041	2.308627
35	5.635	5.676885	2.271427
36	5.625	5.647767	2.283614
37	5.615	5.756973	2.306037
38	5.605	5.807677	2.169132
39	5.595	5.639458	2.195374
40	5.585	5.639499	2.183971
41	5.575	5.615052	2.206959
42	5.565	5.66331	2.196391
43	5.555	5.65422	2.194692

sample No.	Depth	LOI 550°C %	LOI 950°C %
44	5.545	5.683189	2.04736
45	5.535	5.622572	2.084973
46	5.525	5.610549	2.151582
47	5.515	5.491904	2.148243
48	5.505	5.503527	2.116057
49	5.495	5.633036	2.153986
50	5.485	5.515695	2.086697
51	5.475	5.555236	2.120253
52	5.465	7.316875	2.861891
53	5.455	5.191848	2.046381
54	5.445	5.884638	2.281997
55	5.435	5.450776	2.203719
56	5.425	5.528859	2.076993
57	5.415	5.485292	2.123064
58	5.405	5.397437	2.123309
59	5.395	5.379833	2.238059
60	5.385	5.338785	2.185619
61	5.375	5.372252	2.163998
62	5.365	5.34545	2.205901
63	5.355	5.244062	2.243779
64	5.345	5.144443	2.290905
65	5.335	5.134565	2.295515
66	5.325	5.093984	2.368576
67	5.315	5.183168	2.352531
68	5.305	6.182074	1.306339
69	5.295	6.141694	1.327208
70	5.285	6.11926	1.266621
71	5.275	6.967985	0.444834
72	5.265	11.15583	-3.68068
73	5.255	6.06674	1.341738
74	5.245	6.087033	1.290568
75	5.235	6.196788	1.234991
76	5.225	6.14945	1.248525
77	5.215	6.135591	1.261768
78	5.205	6.109748	1.203834
79	5.195	6.095135	1.291171
80	5.185	6.144621	1.244399
81	5.175	6.181917	1.17405
82	5.165	7.111192	1.397811
83	5.155	6.208368	1.18347
84	5.145	6.124238	1.195401
85	5.135	6.111715	1.25881
86	5.125	6.166769	1.2395

sample No.	Depth	LOI 550°C %	LOI 950°C %
87	5.115	6.153969	1.248399
88	5.105	6.161192	1.130415
89	5.095	6.307472	1.076885
90	5.085	6.234473	1.141607
91	5.075	6.184413	1.22429
92	5.065	6.15082	1.143607
93	5.055	6.170116	1.213481
94	5.045	5.998152	-30.6947
95	5.035	5.962867	1.159174
96	5.025	5.99562	1.1103
97	5.015	5.958614	1.146846
98	5.005	6.035339	1.102843
99	4.995	6.043625	1.338397
100	4.985	6.063361	1.258829
101	4.975	6.13728	1.320512
102	4.965	6.899681	1.259437
103	4.955	6.420601	1.253219
104	4.945	6.697997	1.363309
105	4.935	6.62798	1.322438
106	4.925	6.553816	1.329488
107	4.915	6.645694	1.367589
108	4.905	6.612756	1.408634
109	4.895	6.554682	1.310936
110	4.885	6.320284	1.311325
111	4.875	6.459442	1.319991
112	4.865	6.567572	1.400475
113	4.855	6.318129	1.338007
114	4.845	5.922728	1.303691
115	4.835	5.872401	1.293282
116	4.825	5.90759	1.317438
117	4.815	6.066726	1.312774
118	4.805	5.642371	1.340014
119	4.795	5.593542	1.34545
120	4.785	5.601039	1.322522
121	4.775	5.551334	1.363836
122	4.765	5.525801	1.477487
123	4.755	5.618661	1.399594
124	4.745	5.558329	1.489433
125	4.735	5.570963	1.581278
126	4.725	5.659532	1.507341
127	4.715	5.643213	1.59204
128	4.705	5.345622	1.754992
129	4.695	5.197824	1.920126
130	4.685	5.575994	1.546917
131	4.675	5.161973	2.019903

sample No.	Depth	LOI 550°C %	LOI 950°C %
132	4.665	4.565588	2.82226
133	4.655	4.9947	2.39135
134	4.645	5.467053	2.032042
135	4.635	4.9001	2.701194
136	4.625	3.853644	3.546172
137	4.615	4.357388	3.230241
138	4.605	3.364035	4.526564
139	4.595	6.086855	1.412709
140	4.585	3.281663	4.116336
141	4.575	6.144949	1.329514
142	4.565	2.848891	4.567037
143	4.555	3.218164	4.649556
144	4.545	4.21203	3.704616
145	4.535	6.510417	1.260965
146	4.525	6.561481	1.198513
147	4.515	6.528159	1.272587
148	4.505	6.578209	1.25471
149	4.495	6.60997	1.275682
150	4.485	6.715431	1.151661
151	4.475	6.712885	1.192739
152	4.465	6.739091	1.235124
153	4.455	6.875235	1.202227
154	4.445	6.986528	1.271092
155	4.435	7.022336	1.220318
156	4.425	7.05915	1.266925
157	4.415	7.18055	1.32119
158	4.405	7.397586	1.330468
159	4.395	7.561826	1.391091
160	4.385	7.626711	1.311934
161	4.375	7.572868	1.298465
162	4.365	7.949438	1.015918
163	4.355	7.971281	0.998711
164	4.345	7.960604	0.98491
165	4.335	7.315492	1.694601
166	4.325	5.804085	3.266732
167	4.315	8.095153	1.133411
168	4.305	8.143727	1.467114
169	4.295	8.712348	1.142031
170	4.285	9.105897	1.090679
171	4.275	9.397678	1.031516
172	4.265	9.078081	1.331138
173	4.255	9.280822	1.125245
174	4.245	9.235229	1.131971
175	4.235	9.210834	0.99172
176	4.225	9.054013	1.007115

sample No.	Depth	LOI 550°C %	LOI 950°C %
177	4.215	8.586055	1.324356
178	4.205	8.89804	0.985196
179	4.195	8.803767	1.083918
180	4.185	8.814445	0.980043
181	4.175	8.775795	0.988822
182	4.165	8.740922	1.047625
183	4.155	8.729148	1.122232
184	4.145	8.311511	1.440282
185	4.135	7.451034	2.3216
186	4.125	5.695469	4.230769
187	4.115	9.014351	1.156069
188	4.105	9.542038	1.280624
189	4.095	9.877905	1.279788
190	4.085	10.21941	1.340009
191	4.075	10.62718	1.316299
192	4.065	10.55056	1.185711
193	4.055	9.82659	2.284613
194	4.045	7.536092	4.821944
195	4.035	11.93913	1.443299
196	4.025	11.38543	1.416917
197	4.015	11.31808	1.132553
198	4.005	9.648749	2.901024
199	3.995	12.09457	3.376192
200	3.985	14.1862	2.802819
201	3.975	20.91284	2.965446
202	3.965	24.8528	2.959405
203	3.955	30.21769	2.544218
204	3.945	43.25748	3.328945
205	3.935	47.51149	2.218669
206	3.925	51.4904	2.075513
207	3.915	59.60603	1.945525
208	3.905	59.98239	2.047105
209	3.895	59.7416	1.963824
210	3.885	55.86541	1.843743
211	3.875	55.4485	1.927047
212	3.865	54.12154	1.835138
213	3.855	52.56277	1.867607
214	3.845	52.62555	1.783085
215	3.835	51.96003	1.985652
216	3.825	53.2229	1.968181
217	3.815	51.50346	2.862196
218	3.805	53.1224	2.081599
219	3.795	52.21012	2.210122
220	3.785	52.59472	1.973894
221	3.775	52.65879	2.049483

sample No.	Depth	LOI 550°C %	LOI 950°C %
222	3.765	54.34963	2.071251
223	3.755	57.96037	1.998633
224	3.745	57.65588	1.953433
225	3.735	50.25601	2.284364
226	3.725	54.79561	2.093719
227	3.715	53.06122	2.082895
228	3.705	49.56537	2.113516
229	3.695	53.32817	1.993034
230	3.685	51.39635	1.969209
231	3.675	51.74094	1.948703
232	3.665	52.50943	2.059762
233	3.655	51.36716	2.671092
234	3.645	52.31375	3.56088
235	3.635	51.59793	2.98161
236	3.625	52.10383	3.035378
237	3.615	53.07214	2.502589
238	3.605	54.30043	1.905579
239	3.595	56.99835	2.126342
240	3.585	50.29294	2.689747
241	3.575	54.7066	2.220864
242	3.565	51.66258	1.942597
243	3.555	53.4969	1.77665
244	3.545	52.62902	2.564103
245	3.535	50.44313	2.240276
246	3.525	49.50069	1.997235
247	3.515	49.1218	2.270456
248	3.505	51.29511	2.182771
249	3.495	54.27221	2.093887
250	3.485	48.55277	2.279713
251	3.475	46.35936	2.47678
252	3.465	6.504961	4.504646
253	3.455	45.06304	2.410489
254	3.445	46.33503	2.255366
255	3.435	46.28223	2.231599
256	3.425	39.04013	2.633336
257	3.415	36.20148	3.354616
258	3.405	33.75178	3.087005
259	3.395	32.51021	2.934339
260	3.385	34.27749	2.701642
261	3.375	30.96961	3.534161
262	3.365	31.30501	2.984048
263	3.355	28.44139	3.005894
264	3.345	27.44182	3.072763
265	3.335	26.50429	3.148949
266	3.325	27.41406	2

sample No.	Depth	LOI 550°C %	LOI 950°C %
267	3.315	25.21572	1.956857
268	3.305	24.35042	1.632725
269	3.295	24.08422	1.694549
270	3.285	22.34556	2.916275
271	3.275	23.27557	1.878144
272	3.265	24.04706	1.619433
273	3.255	25.29334	1.459372
274	3.245	19.00677	5.931238
275	3.235	15.70684	6.994236
276	3.225	13.18695	8.468156
277	3.215	14.27521	7.538428
278	3.205	15.09933	6.610618
279	3.195	18.11205	3.277053
280	3.185	18.13988	3.185646
281	3.175	18.11477	3.172774
282	3.165	18.10374	3.335557
283	3.155	16.89016	3.309558
284	3.145	16.5381	3.314402
285	3.135	16.241	3.162496
286	3.125	17.85114	3.174937
287	3.115	17.59813	3.153973
288	3.105	17.10704	3.055338
289	3.095	16.36879	3.183905
290	3.085	16.86258	3.494336
291	3.075	17.75154	3.19081
292	3.065	17.48236	3.297466
293	3.055	18.05429	3.227646
294	3.045	18.22948	3.491004
295	3.035	21.10825	3.456155
296	3.025	23.86702	3.473371
297	3.015	24.35233	3.494088
298	3.005	23.37521	3.521018
299	2.995	22.77387	3.54423
300	2.985	21.9326	3.369816
301	2.975	21.33384	3.328233
302	2.965	22.77437	3.273127
303	2.955	35.34428	3.176295
304	2.945	44.57286	2.788945
305	2.935	47.03682	2.733026
306	2.925	46.24633	2.564788
307	2.915	43.25945	2.842243
308	2.905	44.14216	2.647059
309	2.895	44.5622	2.876609
310	2.885	46.02649	2.715232
311	2.875	48.61619	2.558747

sample No.	Depth	LOI 550°C %	LOI 950°C %
312	2.865	49.39794	2.496329
313	2.855	48.92332	2.573529
314	2.845	49.1369	2.64881
315	2.835	48.46735	2.55442
316	2.825	45.84298	2.715218
317	2.815	44.76041	2.70936
318	2.805	43.78525	2.932551
319	2.795	43.0692	2.906126
320	2.785	42.97122	3.026927
321	2.775	42.21604	2.998411
322	2.765	40.1469	3.188821
323	2.755	38.80363	3.116192
324	2.745	29.86078	3.680589
325	2.735	27.5278	3.952096
326	2.725	26.6055	3.885591
327	2.715	24.64377	3.824809
328	2.705	20.77313	3.840929
329	2.695	18.42214	3.582311
330	2.685	18.35722	3.572216
331	2.675	19.0542	3.885509
332	2.665	22.26878	3.724395
333	2.655	23.85257	3.741307
334	2.645	23.93913	3.789874
335	2.635	24.2705	3.504709
336	2.625	23.63709	3.540887
337	2.615	22.86791	3.523141
338	2.605	22.78346	3.537937
339	2.595	21.5453	3.602001
340	2.585	19.7433	3.800176
341	2.575	18.27993	3.597527
342	2.565	17.77181	3.540512
343	2.555	17.22253	3.560235
344	2.545	16.14257	3.572605
345	2.535	15.41561	3.608654
346	2.525	14.84991	3.638825
347	2.515	15.70585	3.443973
348	2.505	16.76286	3.495651
349	2.495	17.40111	3.495836
350	2.485	18.31272	3.488597
351	2.475	17.54915	3.484864
352	2.465	17.60677	3.565673
353	2.455	17.54194	3.318745
354	2.445	17.23722	3.52888
355	2.435	17.04169	3.242886
356	2.425	17.10475	3.34891

sample No.	Depth	LOI 550°C %	LOI 950°C %
357	2.415	18.33509	3.352812
358	2.405	20.68573	3.542411
359	2.395	22.70737	3.365445
360	2.385	20.4928	3.671627
361	2.375	22.05244	3.876468
362	2.365	21.51297	3.919308
363	2.355	22.17468	3.953969
364	2.345	20.11494	4.163734
365	2.335	20.88905	3.937593
366	2.325	21.73564	3.990893
367	2.315	21.63765	3.724594
368	2.305	20.97663	3.809614
369	2.295	20.0954	4.085442
370	2.285	16.74826	4.301635
371	2.275	17.43453	4.410317
372	2.265	17.96488	4.663474
373	2.255	18.41303	4.877119
374	2.245	18.95483	5.048716
375	2.235	18.67263	5.409342
376	2.225	19.12601	5.327746
377	2.215	19.66056	4.834096
378	2.205	19.20904	6.282486
379	2.195	18.16472	7.458944

ศูนย์วิจัยทรัพยากร
จุฬาลงกรณ์มหาวิทยาลัย

BIOGRAPHY

Ms. Wichuratree Klubseang was born in Bangkok, Thailand on August 7th, 1984. In 2006 she received a Bachelor of Arts degree in Geography from Department of Geography, Faculty of Arts, Silpakorn University. After then she started as a Master Degree student with a major of Earth Science, Department of Geology, Faculty of Science, Chulalongkorn University in 2007 and completed the program in 2010.



ศูนย์วิทยทรัพยากร
จุฬาลงกรณ์มหาวิทยาลัย